July 2020

Using Optimization Methods for Solving Problems in Sustainable Urban Mobility and Conservation Planning

Zulqarnain Haider
University of South Florida

Using Optimization Methods for Solving Problems in Sustainable Urban Mobility and Conservation Planning

by

Zulqarnain Haider

A dissertation submitted in partial fulfillment
of the requirements for the degree of
Doctor of Philosophy in Industrial Engineering
Department of Industrial and Management Systems Engineering
College of Engineering
University of South Florida

Co-Major Professor: Changhyun Kwon, Ph.D.
Co-Major Professor: Hadi Charkhgard, Ph.D.
Tapas K. Das, Ph.D.
Yujie Hu, Ph.D.
Yu Zhang, Ph.D.

Date of Approval:
June 24, 2020

Keywords: transportation, urban mobility, food deserts, vehicle routing, robust optimization, conservation

Dedication

I dedicate this dissertation to my parents, my wife and my siblings for their love and support.

Acknowledgments

I would like to extend my special gratitude to my major adviser and mentor Dr. Changhyun Kwon for his continued support and help throughout my PhD. His sincerity, guidance, and feedback at crucial junctures of this journey was most valuable for me. I am also grateful to my co-major adviser Dr. Hadi Charkhgard for his motivation, empathy, energy and his guidance throughout this process. I would also like to thank all the members of my committee for their insightful comments and encouragement throughout my research. My special thanks also goes to all my friends and colleagues for being an important part of my PhD journey. Lastly, I truly appreciate my teachers, colleagues, family and my spouse for their patience, kindness and support.

Table of Contents

List of Tables

List of Figures

Abstract

This dissertation considers three separate optimization problems related to sustainable urban and environmental systems. The first problem relates to the nightly relocation and recharging operations for Free-floating electric vehicle sharing (FFEVS) systems. Such operations involve a crew of drivers to move the shared electric vehicles (EVs), and a fleet of shuttles to transport those drivers. Mixed integer programs are used to model the relocation and recharging operations. Two approaches are devised: sequential and synchronized approaches. In the sequential approach, the movement of EVs is first decided, then the routing of shuttles and drivers is determined. In the synchronized approach, all decisions are made simultaneously. To solve large-scale problems, an efficient computational method, called an exchange-based neighborhood-search method, is devised. The synchronized approach saves the total shuttle route up to 15% compared to the sequential approach. Important managerial insights related to operational resource allocation decisions are also presented. The second problem proposes using grocery deliveries to provide healthy foods to the food insecure population. To make the delivery financially viable, the problem considers consolidating customer orders and delivering to a neighborhood convenience store instead of home delivery. An optimization framework involving the minimum cost set covering and the capacitated vehicle routing problems is employed. The experimental studies in three counties in the U.S. suggest that by spatial and temporal consolidation of orders, the deliverer can remove minimum order-size requirements and substantially reduce the delivery costs, depending on various factors, compared to attended home-delivery. The final part of the dissertation considers a robust optimization approach to problems in conservation planning that considers the uncertainty in data. Two of the basic formulations in conservation plan-

ning related to reserve selection and invasive species control are considered. Several novel techniques are developed to compare the results produced by the proposed robust optimization approach and the existing deterministic approach. Some numerical experiments are conducted to demonstrate the efficacy of the proposed approach in finding more applicable conservation planning strategies.

Chapter 1: Introduction

This dissertation consists of three disparate but related problems for improving economic, social and environmental sustainablity using optimiziation methods and algorithms. Sustainability requires firms and governments to focus on the triple bottom line (TBL) of profit, people and planet (Elkington and Rowlands, 1999). Rapid economic growth in the past century has strained the planet's natural resources and the demand for crude oil, wood, metals and agricultural land in developing economies like India and China continues to rise. Global policymakers and business leaders have realized the importance of sustainable development as the threats posed by rapid urbanization, deforestation, global warming and climate change have become increasingly ominous. In this backdrop, using the optimization and operations mangement tools to solve some key problems in sustainability is a worthwhile endeavour.

The first problem in this dissertation relates to the relocation operations of Free-floating electric vehicle sharing (FFEVS) systems. Transportation is a key sector in the drive for global sustainability and is a major source of greenhouse gas (GHG) emissions accounting for one third of the total GHG emissions in the United States (Tang and Zhou, 2012). Climate researchers have shown that anthropogenic GHG emissions contribute significantly to global warming and a reduction of 50 % in global emissions until 2050 is necessary to avoid the worst implications (Wegener, 2013). Currently, most vehicles run on fossil fuels and contribute to urban pollution, environmental degradation and many chronic respiratory and cardiovascular diseases (Khan and Kar, 2009).

Electric vehicles (EVs) are regarded as a solution to reduce the GHG emissions in transportation sector. However, due to various economic, technological and operational

reasons, like high cost of ownership, driving range anxiety or lack of charging infrastructure, electric vehicle adoption has been slow (Egbue et al., 2017). Despite their promise, EVs accounted for only 1.5 % of all new vehicle sales in the United States (Bellan, 2018). Research on decision aspects of electric vehicles has focused on important problems which could resolve some of the aforementioned issues. For instance, researchers have used optimization methods for decisions related to financial, tactical and operational aspects of deployment of charging station infrastructure (Levinson and West, 2018) or battery swapping infrastructure (Tang and Zhou, 2012).

The advances in communication and information technologies in the 21st century has brought the paradigm of shared mobility to the forefront of the debate about future of urban transportation. The most recent model for carsharing, called the free-floating carsharing, eliminates the need for two-way trips and makes vehicles available close to the customers. The confluence of EV technology and shared mobility paradigm has given birth to carsharing business models which rely on electric vehicles. These models bypass some key issues of EV adoption by eliminating the ownership and maintenance costs and resolving the issue of range anxiety by providing customers sufficiently charged vehicles.

Despite the promise of FFEVS systems as environment friendly alternative to car ownership, many challenging operational problems remain unsolved. One such problem is to relocate the vehicles in order to prevent system-wide imbalance and preempt the future demand by relocating close to potential customers. As such, solving the relocation problem for FFEVS systems addresses all three aspects of the tripple bottom line (TBL) paradigm of sustainability, i.e, the economic aspect, the social aspect and the environmental aspect.

FFEVS systems require nightly relocation and recharging operations to better meet the next day's spatial demand with sufficient battery-levels. Such operations involve a crew of drivers to move the shared electric vehicles (EVs), and a fleet of shuttles to transport those drivers. We consider a decision-making problem for routing shuttles and drivers to recharge and relocate EVs in FFEVS systems. Comprehensive studies for relocating EVs and routing

shuttles are limited in the literature, and an optimal mix of shuttles and drivers is unknown. We fill this gap by providing a modeling framework for joint decision making and efficient computational tools.

We formulate mixed integer programs to model the relocation and recharging operations. Two approaches are devised: sequential and synchronized approaches. In the sequential approach, the movement of EVs is first decided, then the routing of shuttles and drivers is determined. In the synchronized approach, all decisions are made simultaneously. To solve large-scale problems, we devise an efficient computational method, called an exchange-based neighborhood-search method. Our computational method can solve real large-scale instances of car2go in Amsterdam within 10 minutes on a generic computer. Our synchronized approach saves the total shuttle route up to 15% compared to the sequential approach. Our extensive numerical experiments show that when the service area is large, increasing the number of shuttles is more cost efficient than increasing the number of drivers. We also find that when the service area is small, the charging infrastructure is scarce, or the recharging requirements are high, increasing the number of drivers can be more beneficial.

In the second problem, we use mixed integer programming models to design a consolidated delivery system for delivery of groceries and fresh produce at neighborhood convenience stores inside the food desert neighborhhods. Food is an essential human need. The production, transportation, access and consumption of fresh and healthy food, its connections with industrialized agriculture and land use, its impact on health and well being of people, and its interactions with built enivronment and socio-economic and political factors make it a major issue for sustainable cities (Caramaschi, 2016). Using the aforementioned TBL paradigm of sustainability, provision of fresh food specifically addresses the people (social) and planet (environmental) aspects of sustainability. Given the proven connections between food insecurity and public health, this problem is also connected with the profit (economic) aspect of sustainability. Providing healthy food can promote a healthier and more livable city, which in turn can engender positive community changes (Caramaschi, 2016).

More recent focus on the problem of food security and food sustainability has sought to move away from the traditional production based approach whereby producing more food was the proposed solution to tackle hunger and food insecurity. Increasingly, the traditional model has become less and less applicable especially in developed economies where production of ample food is no longer a challenge. Instead, the new sustainable paradigm of food insecurity seeks a redesign of food value chain to address social, environmental and economic aspects of food insecurity problem (Lang and Barling, 2012). In fact, food provisioning is both a multiscale and cross-sectorial issue. Therefore, it encompasses more than the three dimensions of social, economic and environmental sustainability (Olsson, 2018). Despite the global importance of the problem, there is scarce operations research literature addressing these various challenges of food insecurity and provision of healthy food to people. Most of the current work focuses on vehicle routing problem related to food rescue operations of food banks and pantries (Nair et al., 2018).

The second problem in the dissertation aims to address the challenge of food insecurity in food desert neighborhoods in the US by consolidating the delivery operations of grocery delivery services at neighborhood convenience stores. For many socioeconomically disadvantaged customers living in food deserts, the high costs and minimum order size requirements make attended grocery deliveries financially non-viable, although it has potential to provide healthy foods to the food insecure population. We propose consolidating customer orders and delivering to a neighborhood convenience store instead of home delivery. We employ an optimization framework involving the minimum cost set covering and the capacitated vehicle routing problems.

Our experimental studies in three counties in the U.S. suggest that by spatial and temporal consolidation of orders, the deliverer can remove minimum order-size requirements and reduce the delivery costs, depending on various factors, compared to attended home-delivery. We find the number and size of time windows for home delivery to be the most important factor in achieving temporal consolidation benefits. Other significant factors in

achieving spatial consolidation include the capacity of delivery vehicles, the number of depots, and the number of customer orders. We also find that the number of partner convenience stores and the walkable distance parameter of the model, have a significant impact on the number of accepted orders, i.e., the service level provided by the deliverer. The findings of this study imply consolidated grocery delivery as a viable solution to improve fresh food access in food deserts. In light of the recent global pandemic, and its exacerbating effects on food insecurity, the innovative solution proposed in this chapter is even more relevant and timely.

The third problem concerns with applying robust optimization techniques to problems in conservation planning in order to find robust conservation strategies. Conservation planning (CP) is the science of preserving biological and ecological diversity. Preservation of biodiversity is crucial for human life on planet Earth (Billionnet, 2013). Anthropogenic processes like desforestation, urbanization and climate change threaten this shared human asset (Parnell et al., 2013; Echeverría et al., 2006). Problems in conservation planning are therefore directly related to the environmental aspect of the TBL paradigm of sustainability. Due to rapid urbanization, conservation managers have to grapple with managing conservation actions in proximity to urban areas and in compeition with other systems for resource allocation. This introduces resource constraints and trade-offs into the decision making process. Due to these tradeoffs and cross sectorial nature of conservation decisions, problems in CP also influence the economic and social aspects of sustainability.

There is a long history of application of operations research methods in conservation planning (Billionnet, 2013). The third part of our dissertation extends the current approaches to address the issue of data scarcity and uncertainty in conservation decisions. In conservation planning, the data related to size, growth and diffusion of populations is sparse, hard to collect and unreliable at best. If and when the data is readily available, it is not of sufficient quantity to construct a probability distribution. In such a scenario, applying deterministic or stochastic approaches to the problems in conservation planning

either ignores the uncertainty completely or assumes a distribution that does not accurately describe the nature of uncertainty.

To overcome these drawbacks, we propose a robust optimization approach to problems in conservation planning that considers the uncertainty in data without making any assumption about its probability distribution. We explore two of the basic formulations in conservation planning related to reserve selection and invasive species control to show the value of the proposed robust optimization. Several novel techniques are developed to compare the results produced by the proposed robust optimization approach and the existing deterministic approach. For the case when the robust optimization approach fails to find a feasible solution, a novel bi-objective optimization technique is developed to handle infeasibility by modifying the level of uncertainty. We conduct numerical experiments to demonstrate the efficacy of our proposed approach in finding more applicable conservation planning strategies.

1.1 Motivation

The following questions motivated the work in this dissertation:

- Question 1: How to optimize the relocation operations of free floating electric car sharing systems by synchronized optimization of EV relocation and shuttle routing decisions as compared to sequential decision making?
- Question 2: What is the optimal resource allocation of personnel to carry out the relocation operations in FFEVS systems?
- Question 3: Can last-mile grocery delivery be used to resolve the problem of food insecurity in food desert neighborhoods?
- Question 4: What are the consolidation benefits of delivering groceries to neighborhood convenience stores rather than customer homes?

- Question 5: How to apply robust optimization algorithms to address the issue of uncertainty in conservation planning problems and design robust conservation planning strategies?

1.2 Related Publications and Preprints

In answering the aforementioned questions, following papers were published or submitted:

- Haider, Z., Charkhgard, H., Kim, S. & Kwon, C. Optimizing the Relocation Operations of Free-Floating Electric Vehicle Sharing Systems. *Production and Operations Management*, Under review.
  Available at SSRN.

- Haider, Z., Hu, Y., Charkhgard, H., Himmelgreen, D. & Kwon, C. Creating Grocery Delivery Hubs for Food Deserts at Local Convenience Stores via Spatial and Temporal Consolidation. *Socio-Economic Planning Sciences Journal*, Under review.
  Available at SSRN.

- Haider, Z., Charkhgard, H., & Kwon, C. (2018). A robust optimization approach for solving problems in conservation planning. *Ecological modelling*.
  https://doi.org/10.1016/j.ecolmodel.2017.12.006.

1.3 Outline of the Thesis

The remaining content of this thesis is organized as follows:

- In Chapter 2, we propose an exchange based neighborhood search algorithm for solving nightly static relocation problem with charging in FFEVS systems. We also deliver important operational insights for FFEVS system managers.

- Chapter 3 quantifies the consolidation benefits of grocery delivery at neighborhood convenience stores or pickup points rather than customer homes. The practicality and applicability of this approach in addressing the food insecurity problem in certain food desert neighborhoods is also discussed.

- In Chapter 4, we solve conservation planning problems using robust optimization approaches. We also compare the deterministic and robust approaches and show that latter provide robust conservation strategies for conservation managers.

- Chapter 5 concludes the dissertation by summarizing the three problems, solution methods and key managerial insights while also providing future directions for further research.

Chapter 2: Optimizing the Relocation Operations of Free-Floating Electric Vehicle Sharing Systems

2.1 Introduction

An important goal in the development of smart cities is improving efficiency and flexibility in resource utilization. In transportation sector, with the rapid advancements of mobile technologies and devices, on-demand vehicle sharing platforms have emerged as a viable alternative to the notion of car ownership, potentially leading to an efficient utilization of vehicles and urban land. Currently, several key players, such as car2go and DriveNow, are gaining traction with their on-demand, free-floating car sharing (FFCS) services, leading fast expansion of the industry. As of 2019, car2go, the largest car sharing company in the world, operates in 31 cities across North America and Europe with over four million registered members and a total fleet of over 20,000 vehicles. It is forecast that such free-floating mobility services would serve 15 million users worldwide with expected annual total revenue of 3.7–5.6 billion euros by 2020 (Bert et al., 2016; MonitorDeloitte., 2017).

Unlike station-based car sharing models like ZipCar, FFCS systems let users pick an available car and drop it off at any legally permissible parking location within a large designated service area. As a result, users can make customized one-way trips in conjunction with other mobility options, directly addressing the first-mile last-mile problem in urban mobility.[1] For this reason, FFCS systems have the potential to be a true alternative to private car ownership, with much higher adoption than traditional car sharing (Formentin et al., 2015). In North America, for example, it is estimated that a single car sharing vehicle

[1]It refers to the problem of unavailability of public transit for the first and last mile of commute, forcing commuters to opt for private modes of transit over public ones.

can potentially reduce the need for 6 to 23 cars, substantially reducing the total number of vehicles held by households (Shaheen and Cohen, 2007; Martin et al., 2010). Moreover, FFCS systems can also facilitate more efficient use of urban infrastructure and land by reducing the need for perennially occupied or "locked" parking spots in the city centers with 36–84 m^2 of public spaces freed-up per vehicle (Loose, 2010).

Car sharing systems with electric vehicle (EV) fleets are also projected to play a crucial role in making urban transportation systems more sustainable (Firnkorn and Müller, 2011; Le Vine and Polak, 2017). Although EVs are often proposed as one of the most promising solutions to curbing green house gas emissions from the transportation sector, their mass adoption has yet to come. In particular, their short driving range and high fixed costs create psychological concerns to the potential drivers, known as range anxiety and resale anxiety, imposing barriers to the adoption (Lim et al., 2015). In 2017, EVs make up only 1.15% of total U.S. car sales (Bellan, 2018). By relieving the burden of car ownership, free-floating EV sharing (FFEVS) systems can effectively mitigate these psychological adoption barriers: With EVs owned by the service provider rather than the individuals, FFEVS systems relieve the drivers' concerns about technological risks, future resale value, as well as maintenance (He et al., 2017). In fact, car2go has already deployed full EV fleets in four major cities in Europe with more than 2,000 EVs, and DriveNow operates mixed fleets of EVs and combustion engine cars in over ten European cities.

Despite these potential social benefits, FFEVS systems also engender multiple operational challenges. First, the vehicles should be available in the right place at the right time. Research into users' booking behavior has shown that distance to an available vehicle is an important determining factor in a booking decision (Herrmann et al., 2014), and users are only willing to walk up to 500 meters to the available vehicle (Weikl and Bogenberger, 2015). Customers' rental activities may place the vehicles at less favorable locations and cause a spatial mismatch between supply and demand the following day. Hence, repositioning vehicles to ensure availability under imbalanced demand is the key to a successful operation

of the service. Second, EVs need to be relocated with sufficient battery level. Studies show users in FFEVS also exhibit range anxiety: they feel uncomfortable booking an EV if their trip length is 75% or more of the remaining range of the EV (Weikl and Bogenberger, 2015). In addition, there is a strong evidence that demand for FFEVS service is sensitive to the vehicles' battery levels (Kim et al., 2019). Indeed, vehicle unavailability and range anxiety were cited as main reasons when car2go had to close its EV operations in San Diego (Garrick, 2016).

In the presence of these operational challenges, developing an efficient decision support tool for the relocation operations for FFEVS systems is essential for their successful implementation and expansion. Indeed, such a decision tool could be of great academic and practical significance because of the following reasons. First, EV relocation operation can be very costly. Unlike other shared mobility services such as bikes or scooters, vehicle relocation operation in FFCS systems cannot be done by moving multiple vehicles at a time, making it complex and costly—the cost of relocation can be as much as 15 euros per movement (Chianese et al., 2017). Second, vehicle relocation problem in FFEVS systems is computationally hard. The simplest relocation in a FFCS system would require a service vehicle, or a shuttle, to take a driver to a car and the driver to relocate the car to the target location, and then the driver to be picked up by the shuttle again. Then, the additional layer of recharging the EVs, which requires available charging stations nearby and at least a few hours of charging time, drastically increases the complexity of the relocation problem. Third, there are many important yet unanswered operational questions for FFEVS systems. For example, how would operational resource allocation decisions impact the efficiency of EV relocation operations in FFEVS systems? More specifically, with a given number of available drivers, which would be a better operational strategy: running more shuttles or having more drivers available for relocation? Although FFEVS systems have already been operated in many cities for years, comprehensive studies for the EV relocation problem, and the actual relocation operation, are limited in the literature. This has motivated this work: we aim to

provide an efficient computational tool for the integrated EV relocation and shuttle routing problems in FFEVS systems.

The relocation operation in FFEVS systems consists of two levels of decisions: i) EV relocation decision; and ii) Service shuttle routing decision. The EV relocation decision is to determine which EV should be moved to where and how it should be recharged. The shuttle routing is to determine how shuttles should move and pickup/dropoff drivers to fulfill such an EV relocation decision. Ideally, it would be desirable to develop a framework where the two decisions are made jointly and synchronously. This approach, which we call a *synchronized approach*, is rarely studied in the vehicle relocation literature—instead, most of the existing studies approach the two decision problems separately and sequentially.

In practice, different FFEVS systems use service shuttles of different size and type to carry out the relocation operation. Therefore, we use service shuttle or "shuttle" as an all encompassing term which could describe a van with a large capacity, or a car with relatively limited capacity, or even single person mobility options like scooters and foldable bicycles which can be loaded into an EVs trunk (Weikl and Bogenberger, 2015). Our flexible modeling approach works for shuttles of various types and capacities by varying the maximum number of drivers allowed on board each shuttle.

In this chapter, we develop a comprehensive modeling and computational framework applicable to the joint optimization of relocation/recharging operations and shuttle routing. Then, based on the computational framework, we conduct a case study using actual data to address important operational questions regarding the relocation operations of FFEVS systems. Our contributions can be summarized as follows.

- We present a combined MIP formulation for the problem of EV relocation for given demand and charging level considerations and the subsequent shuttle routing problem to carry out the recommended relocation. The MIP formulation can be directly applied to small-scale problems and solved by optimization solvers such as CPLEX and Gurobi. Our formulation makes the following important methodological contributions.

1. Our path-based formulation for relocation problem models each EV route as a separate variable and improves the computability of the EV relocation problem significantly, whereas the existing link-based formulations for EV relocation problem have suffered from increasing complexity as the problem size increases.

2. This work is the first in the literature that formulates a synchronized EV routing and shuttle routing problem. Our extensive numerical study using real FFEVS data shows that the synchronized decision making improves the total shuttle route length up to 15% relative to the sequential approach.[2] When accumulated over time, this improvement can be a significant benefit for the operation.

- We develop an efficient heuristic algorithm for large-scale problems that can obtain a quality synchronized solution in a few minutes. To derive synchronized decisions, our heuristic algorithm integrates the path-based EV relocation problem with the shuttle routing problem, which is a unique variant of dial-a-ride-problem (DARP) (Psaraftis, 1983) involving charging stops for EVs. The heuristic algorithm, which we call an exchange-based neighborhood-search method (EBNSM), draws upon clustering, exchange based neighborhood search, and a customized exchange algorithm for multiple precedence-constrained DARP.

- We conduct a case study using real data from car2go service in Amsterdam, the Netherlands. Our findings from extensive full-scale numerical experiments, summarized below, inform several important operational decisions.

    1. Our results suggest that, in most cases, increasing the number of shuttles is more cost effective than increasing the number of drivers on each shuttle. In particular, it is especially the case when the service area is large or when the charging requirements are low (e.g., the initial battery levels are high). In many cases, we

[2]This is the result when both the sequential and synchronized approaches use our efficient path-based formulation. Therefore, it is expected the performance gap could be higher if compared with a sequential approach using other computationally less efficient formulation such as link-based ones.

find that pairing a separate shuttle with each driver and have the shuttle only to support that driver's movement, is optimal.

2. Our results also show that reducing the number of shuttles, and therefore, increasing the number of drivers per each shuttle can be beneficial when the service area is small, and the charging requirement is high. In particular, when the charging requirement is high (e.g., the initial battery levels are low), adding more shuttles may not be cost effective as it can only increase each shuttle's wait time to pick up the drivers.

The remainder of the chapter is organized as follows. In Section 2.2, we review the related literature. In Section 2.3, we develop and present MIP formulations for synchronized approach and sequential approach for the problem of electric vehicle relocation for given demand and charging level considerations and shuttle routing problem to carry out the recommended relocation. In Section 2.4, we develop heuristic methods including an exchange-based neighborhood-search method (EBNSM) for synchronized approach. In Section 2.5, we set up computational experiments using the exact and heuristic approaches, show the efficacy of our algorithms for full sized instances of the problem, and compare the results with the sequential approach. In Section 2.6, we present managerial insights.

2.2 Literature Review

In this section, we focus mainly on reviewing the literature on operational aspects of the relocation problem in vehicle-sharing systems to highlight our contributions. We refer the reader to Laporte et al. (2015) for a more comprehensive review of other relevant operational problems.

The problem of relocation has been well recognized in one-way car sharing and bike sharing systems. The current vehicle relocation strategies fall into two broad categories. The user-based relocation strategies include incentives, pricing mechanisms and policy inter-

ventions to influence user behavior (Weikl and Bogenberger, 2013). In one-way car sharing systems, repositioning can be carried out either through operator intervention, e.g., using relocation personnel (Kek et al., 2009; Jian et al., 2016; Bruglieri et al., 2014) and using a trip choice mechanism (de Almeida Correia and Antunes, 2012) or through customers by controlling their actions, e.g., through incentives (Pfrommer et al., 2014). Similarly, in case of bike sharing systems, the problem of system-wide imbalance is further compounded by the two-sided demand for bicycles to rent and empty racks to return. The focus of repositioning is to achieve certain desirable inventory levels either through manual rebalancing using trucks (Raviv et al., 2013) or through incentive mechanisms designed to influence customer behavior (Fricker and Gast, 2016; Haider et al., 2018).

In an initial conceptual paper, Weikl and Bogenberger (2013) present and evaluate several user-based and operator-based relocation strategies for FFCS systems. In a subsequent paper, Weikl and Bogenberger (2015) propose a practice ready six step relocation model for a mixed FFCS system with traditional and electric vehicles. Based on historical data, the area is categorized into macro zones and an optimization model is used to achieve desired macro level relocation. Rule based methods are used for making intra zone micro-level relocation and refueling/recharging decisions. A similar model for demand-based relocation in FFCS systems is presented by Schulte and Voß (2015) and Herrmann et al. (2014). Caggiani et al. (2017) propose dynamic clustering method to identify the size and number of flexible zones in which to perform repositioning operations. He et al. (2019a) study robust repositioning strategies in dynamic environments.

Only a few papers, however, have considered a unique and critical component of EV relocation operations: shuttle routing. Gambella et al. (2018) present a time-space-network-based formulation for relocating the vehicles in car sharing systems given some demand and battery considerations, but they only consider *station-based* car sharing systems. In their work, the relocation is carried out by the so called relocators (drivers) who are on board the vehicle itself when traveling between a pair of stations. Kypriadis et al. (2018) propose a

minimum-walking car repositioning problem for FFEVS systems. In their model, the drivers *walk* between the relocation assignments as opposed to travelling on board a shuttle. The problem of shuttle routing to carry out the recommended relocation for FFCS systems is also underserved. Maintaining a dedicated fleet of shuttles and drivers can be expensive and minimizing the cost of relocation operation is one of the key system objectives. For an FFCS system, Santos et al. (2017) consider the problem of shuttle routing given a fleet of shuttles and drivers and provided a set of pre-determined relocation assignments; hence their approach is sequential, rather than joint or synchronized.

Closely related to our work, Folkestad et al. (2020) consider joint decision making for EV relocation and shuttle routing. The modeling approach, formulation, and algorithms in this chapter, however, are distinct. In Folkestad et al. (2020), EVs are moved to charging stations rather than close to actual demand points, assuming a situation with ubiquitous charging infrastructure whereby a charging station can be blocked indefinitely. In case of non-availability of charging stations, postponement of charging is considered. This makes their relocation model similar to the one for station-based systems rather than free-floating systems, especially when charging infrastructure is scarce. Many cities and FFCS systems can have saturated charging infrastructure and station blocking may not be an option. Considering access to limited charging infrastructure in recharging planning is a key factor for success of FFEVS systems (He et al., 2019b). Our work models the charging process more explicitly and flexibly. Specifically, our model can handle partial recharging, and therefore the operator can achieve different charging levels in different service zones, to better respond to battery level sensitive customers. The operator can also choose to partially charge all fleet vehicles up to desired charging levels as opposed to charging only a subset of vehicles fully while postponing the charging operation for others. We also note that Folkestad et al. (2020) only relocate EVs with battery levels below a certain threshold whereas our model is flexible to different charging / relocation requirements: Our model can handle purely demand based relocation (i.e., a fully charged EV may need to be relocated to fulfill demand requirements)

or a purely recharging based relocation (i.e., a low charged EV needs charging but must stay in its current neighborhood). Also, whereas a hybrid genetic algorithm is proposed in Folkestad et al. (2020), we employ an exchange-based neighborhood search method to address computational challenges in joint decision making. Lastly, our case study provides important managerial insights for running the relocation operation more efficiently.

2.3 The Model

In this section, we present a MIP formulation for our problem. Our MIP formulation is divided into three distinct, but related, sub-problems; namely, the EV relocation and recharging problem, the shuttle routing problem, and the synchronization problem. These sub-problems are put together in a single model in Section 2.3.5.

2.3.1 Modeling Demand and Charging Satisfaction for Each Neighborhood

The relationship between location and demand is incorporated into our model to ensure the optimal placement of the EV fleet across the study area. To incorporate the demand information into our relocation decision, we divide the service area into small neighborhoods $h \in \mathcal{H}$. The size of the neighborhoods is small enough—less than $250.000\,\mathrm{m}^2$—so that assumptions of demand uniformity and similarity of demand characteristics throughout the neighborhood hold reasonably well. We find the neighborhood level status data at 12 am at night to find the initial inventory levels, I_h^0. The average values of historical demand data from 6 am to 9 am the subsequent day are calculated for the neighborhood specific desired inventory levels, I_h^d.

Besides the requirements for demand fulfillment, we also consider the relationship between charging levels and the location of a vehicle. We posit that neighborhoods located in different areas of a town may have different charging level requirements for the vehicles located therein. For example, users in downtown could be more sensitive to the vehicles battery levels than those in the suburbs possibly because of the uncertainty in road traffic

conditions. The system manager can thus have neighborhood specific charging requirements. The initial battery level of EVs, denoted by c^0, can be found using system status data. We use historical trip data and average the battery levels at the beginning of all trips originating in a neighborhood h to find the desired charging level c^f for all nodes located in the neighborhood. The system manager can, however, update the desired charging level for any neighborhood or decide to charge all vehicles fully. Later, these charging levels are used in determining crucial parameters for our path based electric vehicle relocation and recharging problem.

Let us consider a set of permissible parking spots in the service area. We associate two boolean characteristics with every node in the original network: the occupancy of the node (occupied or unoccupied) and the availability of charging infrastructure at the node (Yes or No). An occupied node without charging infrastructure, called *Type 1* node, is designated as a *supplier* node and represents current EV locations. An unoccupied node without charging infrastructure, called *Type 2* node, is designated as a *demander* node. An unoccupied node with charging infrastructure, called *Type 3* node, is designated as a *charger* node. In the special case where an occupied node may also be a charging node, called *Type 4* node, we create two nodes at the same location; a supplier node for the occupancy and a charger node for the charging station. A demand relocation happens when an EV moves from one of the occupied spots, a *supplier* to one of the empty spots, or *demander*. In case the EV needs to be charged, the EV must first visit a charging node. Since the charging process takes time, we create a dummy node for each charging node called a *dummy charger* node. The EV movement between a charger and its sister dummy charger represents the charging process. In Figure 2.1, we show the process of conversion to an extended network.

In the extended network, the nodes are designated as *supplier*, *demander*, *charger* or *dummy charger* based on their functions. Let us call the initial sets of these nodes $\hat{\mathcal{S}}_h$, $\hat{\mathcal{D}}_h$, $\hat{\mathcal{C}}_h$ and $\hat{\mathcal{C}}_h^d$ for each neighborhood h and $\hat{\mathcal{S}}$, $\hat{\mathcal{D}}$, $\hat{\mathcal{C}}$ and $\hat{\mathcal{C}}^d$ for the whole network, respectively. The supplier nodes correspond to the initial location of electric vehicles in each neighborhood, i.e., $|\hat{\mathcal{S}}| = \sum_{h \in \mathcal{H}} I_h^0$. Since street level parking spots are very close and

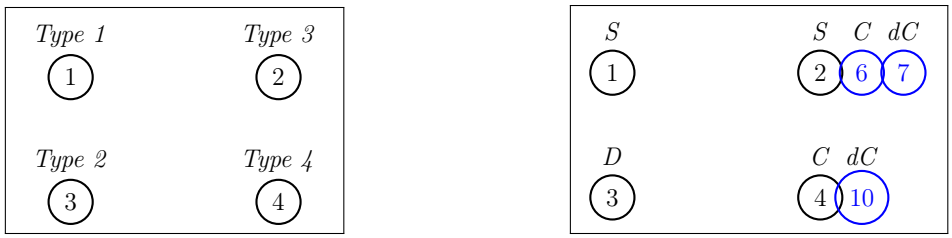

(a) Original Network (b) Extended Network

Figure 2.1 – Conversion of an original network to an extended network with dummy nodes shown in blue. In the extended network, nodes are shown with their respective designations as supplier, demander and charger nodes

virtually indistinguishable, we use the central measure of all the spots in a neighborhood and create as many demander nodes in a neighborhood as the size of desired inventory in each neighborhood, i.e., $|\hat{\mathcal{D}}| = \sum_{h \in \mathcal{H}} I_h^d$. It is worth noting that since we model the nighty static relocation, we assume that no new demand arrives during the night. This ensures that the current EV locations and the desired inventory in each neighborhood stay unchanged throughout the relocation operation. This assumption is justified since many FFEVS systems close their operations at night. Even when a system stays operational, the demand levels are insignificant. For instance, in the case study we consider, the demand is only 6% of the peak demand levels. Finally, each neighborhood can also have dozens of closely located charging stations. If the number of charging stations is greater than $\max\left(|\hat{\mathcal{S}}_h|, |\hat{\mathcal{D}}_h|\right)$, we use central measure of all charging stations to create as many charging nodes as the larger of the number of demanders or the number of suppliers in a neighborhood, i.e., $|\hat{\mathcal{C}}_h| = \max\left(|\hat{\mathcal{S}}_h|, |\hat{\mathcal{D}}_h|\right)$. In case the number of these charging stations is less than $\max\left(|\hat{\mathcal{S}}_h|, |\hat{\mathcal{D}}_h|\right)$, number of charging nodes created is equal to the number of charging stations for each neighborhood.

We can further reduce the size of this network by deleting certain nodes depending on neighborhood-level desired inventory and desired charging level using Algorithm 1. In all neighborhoods, only suppliers with initial battery level greater than the desired charging level can be removed, since the rest requires charging. For neighborhoods where $I_h^0 \leq I_h^d$, suppliers that do not require charging can be removed. An equal number of chargers and

demanders can also be removed, while the rest are kept for suppliers which require charging and suppliers incoming from other neighborhoods to satisfy the leftover demand. On the other hand, for neighborhoods where $I_h^0 > I_h^d$, $I_h^0 - I_h^d$ suppliers are retained to satisfy demand in other neighborhoods. Out of I_h^d suppliers left, those that require charging are retained, while the rest are removed. An equal number of chargers and demanders are also removed while the rest are kept for suppliers that require charging.

Algorithm 1: Procedure for removing nodes from the network

Input: $\hat{\mathcal{S}}$, $\hat{\mathcal{C}}$, $\hat{\mathcal{C}}^d$, $\hat{\mathcal{D}}$, I_h^0, I_h^d,
Output: $\mathcal{S}$, $\mathcal{C}$, $\mathcal{C}^d$, $\mathcal{D}$

for $h \in \mathcal{H}$ **do**
  $\texttt{removeCount}_h = 0$;
  for $i \in \hat{\mathcal{S}}_h$ **do**
    if $c_i^0 > c_h^f$ **then**
      $\texttt{removeCount}_h = \texttt{removeCount}_h + 1$;
  if $I_h^0 \leq I_h^d$ **then**
    $\mathcal{S}_h^r = \{i \in \hat{\mathcal{S}}_h \mid c_i^0 > c_h^f\}$;
    for $k \leftarrow 1$ **to** $\texttt{removeCount}_h$ **do**
      $\hat{\mathcal{S}}_h \leftarrow \hat{\mathcal{S}}_h \setminus \mathcal{S}_h^r[k]$, $\hat{\mathcal{C}}_h \leftarrow \hat{\mathcal{C}}_h \setminus \hat{\mathcal{C}}_h[1]$, $\hat{\mathcal{D}}_h \leftarrow \hat{\mathcal{D}}_h \setminus \hat{\mathcal{D}}_h[1]$;
  if $I_h^0 > I_h^d$ **then**
    $\mathcal{S}_h^r = \{i \in \hat{\mathcal{S}}_h : c_i^0 > c_h^f\}$;
    for $k \leftarrow 1$ **to** $\min\{\texttt{removeCount}_h, I_h^d\}$ **do**
      $\hat{\mathcal{S}}_h \leftarrow \hat{\mathcal{S}}_h \setminus \mathcal{S}_h^r[k]$, $\hat{\mathcal{C}}_h \leftarrow \hat{\mathcal{C}}_h \setminus \hat{\mathcal{C}}_h[1]$, $\hat{\mathcal{D}}_h \leftarrow \hat{\mathcal{D}}_h \setminus \hat{\mathcal{D}}_h[1]$;
$\mathcal{S} \leftarrow \bigcup_{h \in \mathcal{H}} \hat{\mathcal{S}}_h$, $\mathcal{D} \leftarrow \bigcup_{h \in \mathcal{H}} \hat{\mathcal{D}}_h$;
$\mathcal{C} \leftarrow \bigcup_{h \in \mathcal{H}} \hat{\mathcal{C}}_h$;

2.3.2 Modeling the EV Relocation and Recharging (EVRR) Problem

In second part of our modeling approach, we describe the relocation and recharging decision for electric vehicles (EVs). We call this problem the EV relocation and recharging (EVRR) problem. The traditional relocation problem in car sharing and bike sharing systems involves the decision to relocate vehicles from current node i to a future node j to cater to

(a) A traditional Relocation Decision

(b) An EV Relocation and Recharging Decision

Figure 2.2 – In a traditional demand-based relocation problem, a single relocation operation involves movement between two nodes. In a demand and recharging based relocation model, a single relocation operation can involve a charging stopover at a pair of intermediate charger-dummy charger nodes

shifting demand needs as shown in Figure 2.2a. In case of electric cars, node j can be a charging station. The relocation scenario we consider is decidedly different than traditional setting. In our model, a vehicle can visit up to four nodes during its journey as shown in Figure 2.2b. From its current node i, a supplier node, it can go to a pair of charger-dummy charger nodes k and l, one each for receiving and dispatching the vehicle, and once recharged to the required level, it can move to a demander node j. Dummy charger nodes are introduced to allow for two shuttle visits to the charging station since the driver does not wait while the vehicle is being charged. Finally, a vehicle may also choose to stay put at its current node if it is sufficiently charged and does not have to fulfill a demand-based relocation. Our model only specifies the neighborhood a vehicle needs to be relocated to and the required charging level. Our model, therefore, chooses an optimal route for an EV, not only deciding the terminal node j, if any, of its journey but also deciding which pair of charger nodes, if any, it should visit for recharging purposes.

Let $\mathcal{N}$ be the set of permissible parking spots in the reduced network, i.e., $\mathcal{N} = \mathcal{S} \cup \mathcal{D} \cup \mathcal{C}$. Let $\mathcal{N}'$ be the network with addition of dummy nodes, $\mathcal{C}^d$. The notation for EVRR problem is given in Table 2.1. Given $\mathcal{S}$, $\mathcal{C}$, $\mathcal{C}^d$, and $\mathcal{D}$, We can enumerate all the possible EV paths and associate a binary decision variable x_p with each path $p \in \hat{\mathcal{P}}$. The path variable is 1 if an electric vehicle moves on path p and 0, otherwise. An EV may or may not require charging. In the former case, the number of possible paths is equal to $|\mathcal{S}| \times |\mathcal{D}|$.

In case of charging, the number of possible EV paths is $|\mathcal{S}| \times |\mathcal{C}| \times |\mathcal{D}|$. The total number of paths $|\hat{\mathcal{P}}|$ is equal to $|\mathcal{S}| \times |\mathcal{D}|\,(1 + |\mathcal{C}|)$.

We reduce the size of $\hat{\mathcal{P}}$ by removing infeasible or unnecessary paths. Associated with each path p are parameters c_p^0, c_p^f, and w_p representing initial battery level at the supplier, desired charging level at demander, and the charging time required to achieve c_p^f, respectively. Since we have already enumerated all the paths, then for a path $i \to k \to l \to j$, knowing the initial battery level at the supplier, the final charging level at the demander and the discharging on arcs (i, k) and (l, j), one can determine path dependent charging time w_p on charging arc (k, l) as follows:

$$w_p = \frac{1}{\beta_2}\left(c_p^f - c_p^0 + \beta_1 \sum_{(i,j)\in\mathcal{A}^t(p)} t_{ij}\right) \qquad \forall p \in \hat{\mathcal{P}}. \tag{2.1}$$

In essence, w_p represents the service time at a charging station. Our model for charging process assumes that charging time has a linear relationship with charging levels. Others have considered non-linear charging process and used piece-wise linearization to model different charging speeds (Pelletier et al., 2018). However, a linear charging process sufficiently models the reailty for our case when the focus is on operational problem and the total time spent on recharging rather than the non linearities of the charging process itself. If $w_p \leq 0$ for a path, charging stop is not needed and hence the corresponding path $p : i \to k \to l \to j$ is removed and only direct path $p : i \to j$ is kept. Conversely, if $w_p > 0$, direct path $p : i \to j$ is removed since a charging station must be visited. The path set $\hat{\mathcal{P}}$ is reduced to $\mathcal{P}$:

$$\begin{aligned}\mathcal{P} = \hat{\mathcal{P}} \setminus \{p = i \to k \to l \to j : i \in \mathcal{S}, j \in \mathcal{D}, k \in \mathcal{C}, w_p \leq 0\} \\ \setminus \{p = i \to j : i \in \mathcal{S}, j \in \mathcal{D}, w_p > 0\}.\end{aligned} \tag{2.2}$$

The full enumeration of paths and the subsequent reduction of path set ensures that all paths p will fulfill charging requirements at their respective demander node because of

charging time w_p associated with them. Furthermore, for each path $p \in \mathcal{P}$, the total path time l_p can be calculated as $l_p = t_{ik} + w_p + t_{lj}$.

Table 2.1 – Mathematical Notation for EVRR

Sets	
$\mathcal{N}$	Set of permissible parking spots
$\mathcal{N}'$	Set of permissible parking spots plus the dummy nodes
$\mathcal{C}$	Set of charger nodes
$\mathcal{D}$	Set of demander nodes
$\mathcal{S}$	Set of supplier nodes
$\mathcal{C}^d$	Set of dummy charger nodes
$\mathcal{H}$	Set of demand neighborhoods indexed by $h \in \mathcal{H}$
$\mathcal{P}$	Set of all feasible paths indexed by $p \in \mathcal{P}$ where each path $p = (i_0, i_1, \ldots, i_s)$
$\mathcal{A}$	Set of all possible arcs indexed by $a \in \mathcal{A}$ where each arc $a = (i, j)$
$\mathcal{A}(p)$	Set of arcs in path p, where $\mathcal{A}(p) = \mathcal{A}^c(p) \cup \mathcal{A}^t(p)$, i.e., charging and travelling arcs on path p
$\mathcal{N}(p)$	Set of nodes in EV path p, where $\mathcal{N}(p) = \{\mathcal{S}(p), \mathcal{C}(p), \mathcal{C}^d(p), \mathcal{D}(p)\}$, i.e., supplier, charger, dummy charger and demander nodes of a particular path p
$\phi(i)$	Set of paths p that contain node i, i.e., $\{p \in \mathcal{P} : i \in p\}$
Variables	
x_p	Binary variable; 1 when a vehicle is to be relocated along a path p, 0 otherwise
Parameters	
t_{ij}	travel time alongside a travel arc (i, j)
w_p	charging time between charger and dummy charger nodes for path p
c_p^0	initial battery level at supplier node for path p
c_p^f	desired charging level at demander node for path p
β_1	rate of depletion; the decrease in battery level of a vehicle per unit of travel time
β_2	rate of charging; the increase in battery level of a vehicle per unit of time

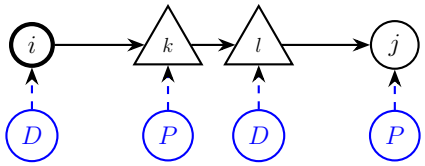

Figure 2.3 – Drop off (D) and pickup of (P) of drivers by shuttle at different nodes for a particular EV path p. Drivers do not wait at the charging station. The shuttle must visit the Charger node k to pick a driver and Dummy Charger node l to drop a driver

Given the notation in Table 2.1, we can write the EVRR feasibility problem as follows:

$$\text{(EVRR)} \quad \sum_{p \in \phi(i)} x_p \leq 1 \qquad \forall i \in \mathcal{N}, \tag{2.3}$$

$$\sum_{p \in \mathcal{P}} x_p = \min\{|\mathcal{S}|, |\mathcal{D}|\}, \tag{2.4}$$

$$x_p \in \{0, 1\} \qquad \forall p \in \mathcal{P}. \tag{2.5}$$

In the feasibility problem described above, the objective is to find a path for every electric vehicle. Constraint (2.3) makes sure that each node can only be visited once by an EV while it treads a path p. Constraint (2.4) ensures that the total number of paths chosen must be equal to total number of EV movements. In case $|\mathcal{S}| \geq |\mathcal{D}|$, the number of EV paths must be equal to $|\mathcal{D}|$. Conversely, if $|\mathcal{D}| \geq |\mathcal{S}|$, the number of EV paths should equal $|\mathcal{S}|$.

2.3.3 Modeling the Shuttle Routing (SR) Problem

The second part of our combined operational problem is a shuttle routing (SR) problem. The network for SR, $\mathcal{N}_0'$, is same as the extended network of Section 2.3.2, with two dummy nodes for depot for beginning and termination of shuttle route added. Let z_{ij} be 1 if a shuttle travels between nodes i and j as part of its route and 0, otherwise. Similarly, let y_i be the number of drivers on a shuttle while it is leaving node i.

Table 2.2 – Mathematical Notation for SR Problem

Sets	
$\mathcal{N}'$	Set of permissible parking spots plus the dummy nodes
$\mathcal{N}'_0$	Set of permissible parking spots, the dummy nodes and the depots
$\delta^-(j)$	set of shuttle arcs entering node j
$\delta^+(j)$	Set of shuttle arcs leaving node j
Variables	
z_{ij}	Binary variable which equals one if a shuttle travels directly from node i to node j, and zero otherwise
y_i	Number of drivers carried on a shuttle when it leaves node i.
τ_i	Continuous variable representing the arrival time for shuttle at node i.
τ^k_{N+1}	Continuous variable representing the arrival time for shuttle k at depot node $N+1$.
Parameters	
K	The number of shuttles available
q	The maximum number of drivers available for each shuttle

The detailed notation for SR feasibility problem is given in Table 2.2 while the problem itself is described henceforth:

$$\text{(SR)} \quad \sum_{j\in\delta^+(0)} z_{0,j} \le K, \tag{2.6}$$

$$\sum_{i\in\delta^-(N+1)} z_{i,N+1} \le K, \tag{2.7}$$

$$\sum_{i\in\delta^-(j)} z_{ij} \le 1 \qquad \forall j \in \mathcal{N}', \tag{2.8}$$

$$\sum_{i\in\delta^-(j)} z_{ij} - \sum_{i\in\delta^+(j)} z_{ji} = 0 \qquad \forall j \in \mathcal{N}', \tag{2.9}$$

$$z_{ij} = 1 \implies \tau_j \ge \tau_i + t_{ij} \qquad \forall j \in \mathcal{N}',\ i \in \delta^-(j), \tag{2.10}$$

$$z_{i,N+1} = 1 \implies \tau^k_{N+1} \ge \tau_i + t_{i,N+1} \qquad \forall\ i \in \delta^-(N+1), \forall\ k \in \mathcal{K} \tag{2.11}$$

$$z_{ij} = 1 \implies y_j = y_i - 1 \qquad \forall j \in S \cup C',\ i \in \delta^-(j), \tag{2.12}$$

$$z_{ij} = 1 \implies y_j = y_i + 1 \qquad \forall j \in C \cup D,\ i \in \delta^-(j), \tag{2.13}$$

$$0 \le y_i \le q \qquad \forall i \in \mathcal{N}', \tag{2.14}$$

$$z_{ij} \in \{0,1\} \qquad \forall (i,j) \in A. \tag{2.15}$$

The SR feasibility problem (2.6)–(2.15) is then to ensure that every shuttle route begins at the starting dummy node (0) and ends at the terminal dummy node $(N+1)$. Constraints (2.6)–(2.7) ensure that total arcs leaving depot node (0) or entering depot node $(N+1)$ must be less than or equal to the total shuttles K. All the other nodes must only be visited once by one of the shuttles (2.8). Constraint (2.9) is flow conservation constraint. Constraint (2.10) updates the arrival time of a shuttle at a node j when it visits arc (i,j) while constraint (2.11) finds arrival times at terminal depot node $N+1$ for multiple shuttles. Constraints (2.12) and (2.13) update the number of drivers on the shuttle as it drops off and picks up the drivers at node j. As shown in Figure 2.3, a driver is dropped off at supplier and dummy charger nodes while one is picked up at charger and demander nodes. Finally, constraint (2.14) ensures the number of drivers on each shuttle must not exceed shuttle capacity q. In the SR feasibility problem described in this section, a feasible shuttle route is any route that begins at a depot, ends at a depot while visiting any number of intermediary nodes and loading and unloading an indeterminate number of drivers. Next section synchronizes the feasibility problems described in Sections 2.3.2 and 2.3.3.

2.3.4 Synchronizing EVRR and SR Decision Models

A feasible synchronized EV and shuttle routing problem (f-SYNC) admits only those shuttle routes that include visits to the nodes supplied by the EVRR problem, as opposed to any number of nodes in a feasible SR. Similarly, an f-SYNC solution makes sure that drivers are available to drive the electric vehicles on the routes supplied by the EVRR problem, as opposed to an indeterminate number of drivers loaded and unloaded in a feasible SR solution. Finally, an f-SYNC solution only admits those shuttle routes that respect the time windows E_i of EV routes for the EVRR problem. The following constraints (2.16)–(2.19) serve the purpose of synchronizing τ_j and z_{ij} variables, representing the shuttle route, with

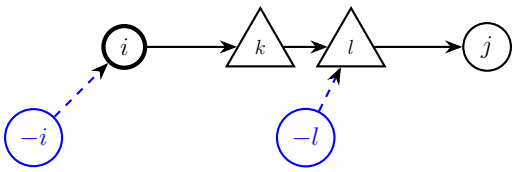

Figure 2.4 – The arrival times of EV at each node i on a path p depend only on shuttle arrival times at Supplier node i (driver drop-off) and Dummy Charger node l (driver drop-off) for a particular path p

E_j and x_p variables, representing the EV paths.

$$\sum_{i \in \delta^{-}(j)} z_{ij} = \sum_{p \in \phi(j)} x_p \qquad \forall j \in \mathcal{N}', \tag{2.16}$$

$$x_p = 1 \implies \tau_j \geq \tau_i + l_p \qquad \forall p \in \mathcal{P}, i = \mathcal{S}(p), j = \mathcal{D}(p), \tag{2.17}$$

$$x_p = 1 \implies \tau_j \geq \tau_i + t_{ij} \qquad \forall p \in \mathcal{P},\ (i,j) \in A(p), \tag{2.18}$$

$$z_{ij} \in \{0,1\} \qquad \forall (i,j) \in \mathcal{A}, \tag{2.19}$$

where $l_p = t_{ik} + w_p + t_{lj}$ is the length of path $i \to k \to l \to j$. Figure 2.4 illustrates such a path.

Consider a path $p = i \to k \to l \to j$ where $i = \mathcal{S}(p), k = \mathcal{C}(p), l = \mathcal{C}^d(p)$ and $j = \mathcal{D}(p)$. The electric vehicle arrival time at nodes belonging to path p can be uniquely determined as follows:

$$E_i = \tau_i, \tag{2.20}$$

$$E_k = \tau_i + t_{ik}, \tag{2.21}$$

$$E_l = \tau_i + t_{ik} + w_p, \tag{2.22}$$

$$E_j = \max\left(\tau_i + t_{ik} + w_p + t_{lj}, \tau_l + t_{lj}\right). \tag{2.23}$$

For a direct path $p = i \to j$ where $i = \mathcal{S}(p)$ and $j = \mathcal{D}(p)$:

$$E_i = \tau_i, \tag{2.24}$$

$$E_j = \tau_i + t_{ij}. \tag{2.25}$$

The set of equations can be used to determine the path dependent arrival times of each electric vehicle once the arrival times of shuttle at node i and node l are known. As a repositioning shuttle completes its tour, it drops and picks the drivers, who in turn relocate the EVs between nodes. Given a shuttle route, at different nodes, we may have a shuttle, an EV or a driver waiting for some time. Equation (2.20) states that arrival of EV at supplier node i only occurs after a driver is dropped off by the shuttle at time τ_i. Therefore, the EV wait time is simply equal to the arrival time of the shuttle at the node, i.e., $EV_{\text{wait}} = E_i$. Given τ_i, the charging process for EV begins at $\tau_i + t_{ik}$ and ends at $\tau_i + t_{ik} + w_p$. At charger node k, a driver may wait for a shuttle after dropping the EV, i.e., $D_{\text{wait}} = \tau_k - E_k$. The charging process for EV begins at $\tau_i + t_{ik}$, therefore, it does not wait on the node. EV arrival on dummy charger node l occurs at the end of charging process at time $\tau_i + t_{ik} + w_p$. At each dummy charger node, if the charging process is over before shuttle arrives, the EV must wait for the driver, i.e, $EV_{\text{wait}} = \tau_l - E_l$. In this case, EV arrival time at demander j is $\tau_l + t_{lj}$. Conversely, if the charging process is not over when the shuttle arrives, the driver must wait for the EV, i.e., $D_{\text{wait}} = E_l - \tau_l$. the EV arrival at demander j occurs at $E_l + t_{lj}$. At demander node j, if the driver has already dropped the EV before shuttle's arrival, the driver must wait, i.e., $D_{\text{wait}} = \tau_j - E_j$. In some cases, however, a shuttle may arrive at a demander before the driver brings the EV, i.e., $SH_{\text{wait}} = E_j - \tau_j$; hence, the shuttle must wait for driver's arrival.

2.3.5 Final Formulation for the Synchronized Approach

Thus far, we have presented three disjoint feasibility problems. The EVRR problem finds feasible EV routes and only admits the EV routes that fulfill the demand and charging requirements of the system. Similarly, the SR problem finds feasible shuttle routes, and the f-SYNC admits only those feasible shuttle routes that are synchronized with the requirements outlined in the EVRR problem. In this section, we connect all three disjoint feasibility problems into a combined MIP formulation with an overarching objective function.

$$\begin{aligned} \text{(SYNC)} \quad \min \quad & \sum_{k \in K} \tau_{N+1}^{k}, && (2.26) \\ \text{s.t.} \quad & (2.3)\text{–}(2.5), && \text{[EV Relocation and Recharging (EVRR)]} \\ & (2.6)\text{–}(2.15), && \text{[Shuttle Routing (SR)]} \\ & (2.16)\text{–}(2.19). && \text{[Synchronizing EV and Shuttle Routing (f-SYNC)]} \end{aligned}$$

The objective function (2.26) of the combined problem minimizes the travel time or makespan of shuttle routes. Thus the combined MIP problem makes sure that only those electric vehicle relocations are carried out that are promising for the overall system objective of minimizing the physical cost of carrying out that relocation using shuttles and drivers.

2.3.6 Formulation for the Standalone EVRR Problem

EVRR feasibility problem in Section 2.3.2 describes a relocation problem complete with demand and charging requirements. This relocation model can be used in a standalone manner by the decision makers, interested in relocation alone, using an appropriate objective function.

$$\text{(P1)} \quad \min \quad \sum_{p \in \mathcal{P}} l_p x_p, \tag{2.27}$$

$$\text{(P2)} \quad \min \quad \max_{p \in \mathcal{P}} (l_p x_p) \tag{2.28}$$

We recommend two different objective functions for relocation problem as given by (2.27) and (2.28). The former minimizes the total length of the paths selected for EVs while the latter minimizes the maximum length of paths selected. The second objective can be linearized by introducing an auxiliary variable m and adding an extra constraint.

$$\text{(P3)} \quad \min \quad m \tag{2.29}$$

$$\text{s.t.} \quad m \geq l_p x_p \qquad \forall p \in \mathcal{P} \tag{2.30}$$

It is easy to show that (P3) with constraint (2.30) is equivalent to (P2). The relocation problem gives a set of EV routes $\bar{x}$ as an optimal solution. On its own, the solution of EVRR problem for the full city-wide network provides decision makers with optimal relocation decision. The problem will also be used in the heuristic approaches for solving the synchronized EV relocation and shuttle routing problem.

2.3.7 Formulation for the Sequential Approach

We can use the standalone relocation model presented in Section 2.3.6 and a subsequent shuttle routing model to formulate the sequential approach.

$$\text{(SEQ-A)} \quad \min \quad \sum_{p \in \mathcal{P}} l_p x_p, \tag{2.31}$$

$$\text{s.t.} \quad \text{(2.3)–(2.5).} \qquad \text{[EV Relocation and Recharging (EVRR)]}$$

Let $\bar{x}$ be an optimal solution for (SEQ-A). Given $\bar{x}$, solve (SEQ-B).

$$\text{(SEQ-B)} \quad \min \quad \sum_{k \in K} \tau_{N+1}^{k}, \tag{2.32}$$

$$\text{s.t.} \quad (2.6)\text{–}(2.15), \qquad \text{[Shuttle Routing (SR)]}$$

$$(2.16)\text{–}(2.19). \qquad \text{[Synchronizing EV and Shuttle Routing (f-SYNC)]}$$

The sequential approach uses same modeling components as synchronized approach. It is easy to see that the sequential approach gives us solutions which are feasible for synchronized approach but are sub-optimal. Therefore, solutions for sequential approach can be used as initial solutions for synchronized approach.

2.4 Computational Methods

Owing to large size of our problems for the full city-wide network, we devise heuristic approaches to solve the sequential (SEQ) and the synchronized (SYNC) problems. The heuristic approaches for SEQ and SYNC rely on cluster-relocate-route approach to solve the EV relocation and shuttle routing problems. The algorithmic components for the two approaches are described in this section. In Section 2.4.1, we describe the heuristic approach for solving the sequential problem. The best solution from sequential approach serves as an initial solution for our main algorithm, the Exchange-Based Neigborhood-Search Method (EBNSM), for solving the SYNC problem as described in Section 2.4.2.

2.4.1 Setting the Benchmark: the Sequential Approach

To show the system wide benefits of the synchronized (SYNC) approach to EV relocation and shuttle routing problem, we compare it with the sequental (SEQ) approach. Since we want to compare the two approaches in terms of their relocation decisions, we use a similar cluster-relocate-route approach for the SEQ problem. The steps to solve the SEQ problem are described as Algorithm 2.

Algorithm 2: The Sequential Approach

Input: $\mathcal{N}_0', K, q$

Output: Best EV paths: $\mathcal{X}_k$, Best shuttle route: $\mathbf{z}$

Given number of shuttles K, find K-centers in the network using greedy approximation approach mentioned in Section 2.4.1.1;

Solve the MIP problem (NCA) described in Section 2.4.1.2 for creating K clusters of nodes from K-centers. Put the objective coefficient $d_{ik} = t_{ik}, \forall i \in \mathcal{N}, k \in \mathcal{K}$. Let $\mathcal{N}_k, \mathcal{S}_k, \mathcal{C}_k, \mathcal{D}_k,$ and $\mathcal{P}_k$ be the sets of nodes, suppliers, chargers, demanders and paths for each cluster k, respectively;

foreach $1 \leq k \leq K$ **do**

    Given $\mathcal{N}_k, \mathcal{S}_k, \mathcal{C}_k, \mathcal{D}_k,$ and $\mathcal{P}_k$, solve (SEQ-A). Let $\mathcal{X}_k$ be the set of best EV paths;

    Given $\mathcal{X}_k$, obtain an initial route r_k for the shuttle using greedy approach;

    Given an initial shuttle route (r_k), run the customized 2-interchange algorithm to get the best shuttle route. Let $\text{ub}^k \leftarrow$ obj(2-int);

bestSoln $\leftarrow \sum_{k \in \mathcal{K}} \text{ub}^k$;

bestRoutes $\leftarrow \bigcup_{k \in \mathcal{K}} r_k$;

The clusters for the SEQ approach are formed using minimum cost assignment problem NCA with objective coefficient $d_{ik} = t_{ik}$ while the relocation decision is achieved by solving minimum path cost EV relocation and recharging problem (SEQ-A). The MIP formulation SEQ-B can be used to get optimal shuttle routes for moderate sized instances but fails for large instances owing to precedence constraints and loose time windows. Therefore, we use a greedy algorithm to construct an initial shuttle route from optimal EV path set and use the customized 2-interchange algorithm to improve the route.

2.4.1.1 Finding K-centers

As first step for sequential method, we solve a K-center problem to find K centers in the network. The K-center problem is a well known NP-hard problem (Megiddo and Supowit, 1984). We use a 2-opt greedy approximation algorithm (Plesník, 1987) to solve the problem. We let t_{ij} be the traversal time between nodes i and j and assume the time matrix to be symmetric.

2.4.1.2 Creating K Clusters

Once K-centers have been found, we can assign to each center k a set of nodes which form the k-th cluster. The assignment must fulfill certain high level requirements.

1. The number of nodes within each cluster should be approximately equal to form evenly sized clusters.

2. For each cluster, the number of demanders and chargers in the cluster should be greater than or equal to the minimum of the number of suppliers and demanders in the cluster to ensure that each electric vehicle has an available path within the cluster.

Given K clusters, these requirements are equivalent to fulfilling the following conditions: $|\mathcal{S}_k| \geq \min\left\{\frac{|\mathcal{S}|}{K}, \frac{|\mathcal{D}|}{K}\right\}$, $|\mathcal{D}_k| \geq |\mathcal{S}_k|$, $|\mathcal{C}_k| \geq |\mathcal{S}_k|$. The assignment of nodes to clusters is done using an assignment problem that minimizes the total *distance* from all nodes to the assigned center. Let r_{ik} be a binary variable which is 1 if node i is assigned to center k and 0, otherwise. Similarly let $d_{ik} = t_{ik}$ be the measure of *distance* from node i to center k. The node to center assignment problems (NCA) can be written as follows:

$$\text{(NCA)} \quad \min \quad \sum_{i\in\mathcal{N}}\sum_{k\in\mathcal{K}} d_{ik}r_{ik}, \tag{2.33}$$

$$\text{s.t.} \quad \sum_{k\in\mathcal{K}} r_{ik} = 1 \qquad \forall i \in \mathcal{N} \tag{2.34}$$

$$\sum_{i\in\mathcal{S}} r_{ik} \geq \min\left\{\frac{|\mathcal{S}|}{K}, \frac{|\mathcal{D}|}{K}\right\} \qquad \forall k \in \mathcal{K}, \tag{2.35}$$

$$\sum_{i\in\mathcal{D}} r_{ik} \geq \sum_{i\in\mathcal{S}} r_{ik} \qquad \forall k \in \mathcal{K}, \tag{2.36}$$

$$\sum_{i\in\mathcal{C}} r_{ik} \geq \sum_{i\in\mathcal{S}} r_{ik} \qquad \forall k \in \mathcal{K}, \tag{2.37}$$

$$r_{ik} \in \{0,1\} \qquad \forall i \in \mathcal{N}, k \in \mathcal{K}. \tag{2.38}$$

2.4.1.3 Finding Optimal EV Routes

Once K clusters have been formed, optimal EV paths in each cluster can be found by simply solving the minimum path cost EV relocation and recharging problem (SEQ-A). The output of the problem is an optimal set of paths for each cluster. The set of paths is subsequently used to find best shuttle routes for each cluster.

2.4.1.4 Finding Optimal Shuttle Routes

We present a customised 2-interchange algorithm which draws from a 2-interchange procedure for Dial-A-Ride Problem (DARP) presented in Psaraftis (1983). A DARP involves a vehicle picking up and dropping off multiple customers. In our problem, the EVs are equivalent to customers in DARP.

Contrary to a customer in DARP, each EV moves multiple times through the nodes on its route. Therefore, a shuttle must satisfy multiple precedence constraints for each EV. However, given a set of EV paths, a shuttle route r can be constructed trivially using a greedy procedure whereby the suppliers are visited first, followed by chargers, dummy chargers and demanders, in this order, while maintaining capacity feasibility for drivers. Given r, a new route r_{new} can be constructed by swapping two arcs $(i, i+1)$ and $(j, j+1)$ with two new arcs (i, j) and $(i+1, j+1)$. Since direction of segment $(i+1 \to \cdots \to j)$ is now reversed, it is necessary to check precedence feasibility and ensure driver availability on the shuttle. The proposed 2-interchange procedure is presented as Algorithm 4 in Section 5.3 in the e-companion. The feasibility and improvement checks are customised for our problem and their algorithmic descriptions are also presented, in relative detail, in Section 5.3 in the e-companion.

2.4.2 Solving the SYNC Problem Using EBNSM

In this section, we describe in relative details the steps of EBNSM procedure for finding solutions to synchronized EV relocation and shuttle routing problem (SYNC). EBNSM

is an iterative procedure, described as Algorithm 3, for solving EV relocation and shuttle routing problem synchronously. It relies on solution for SEQ method and improves it by iteratively adding neighborhood paths and updating the shuttle routes. Here, we expand on the individual steps.

EBNSM improves the solution obtained from sequential method by iteratively adding new EV paths and updating the shuttle route. The exchange procedures, `ExchangeSuppliers()`and `ExchangeChargers()`, are used to replace a pair of old paths in path set $\mathcal{X}$ with a pair of new paths by exchanging their supplier and charger/dummy charger nodes, respectively. No new nodes are added in the process. However, the visiting order of exchanged nodes must be changed in the shuttle route to ensure that precedence feasibility is maintained. The route update step in EBNSM, `UpdateRoutes()`, swaps the positions of the pair of exchanged nodes in the shuttle route according to the updated path set $\bar{\mathcal{X}}_k$. In doing so, since a supplier is swapped with a supplier, and a charger with a charger, the capacity feasibility of shuttle route is also maintained. Finally, the route improvement check for the new route r_{new} is done using the same procedure `RouteImprovement()` as used in Algorithm 4 and described in Section 5.3.

2.5 Case Study: car2go in Amsterdam

We apply our framework to a fully operational system of car2go in Amsterdam, the Netherlands, where the FFEVS service is provided using more than 300 EVs. From the actual data, we take the initial and target locations of EVs that need to be relocated and test the performance of our computational method. We use actual municipal boundaries of smallest size as neighborhoods as shown in Figure 2.5a. For the computaional experiment, we first construct a full network containing 339 neighborhoods, 829 nodes, 332 dummy nodes and 2 nodes representing the depot. We use rules in Section 2.3.1 to reduce the size of the network. Final network has 155 suppliers, 270 chargers, 270 dummy chargers and 155 demanders. The total number of possible EV paths is $|\mathcal{P}| = 6,267,580$ out of which, 155 paths need to be

Algorithm 3: Exchange-Based Neighborhood-Search Method (EBNSM)

Input: $\mathcal{N}_0', \mathcal{S}, \mathcal{C}, \mathcal{C}^d, \mathcal{D}$, K = Number of Shuttles = Number of Clusters, q = Number of Drivers per Shuttle, SNSIt: Number of iterations for Small Neighborhood Search

Output: Best shuttle routes: $\mathbf{z}$

Given number of shuttles K, use Algorithm 2 to find initial paths $\mathcal{X}_k$ and initial shuttle routes r_k for each cluster k ;
for $k \leftarrow 1$ **to** K **do**
  for it $\leftarrow 1$ **to** SNSIt **do**
    $\Delta \leftarrow 0$;
    for $i \leftarrow 1$ **to** $|\mathcal{X}_k|$ **do**
      for $j \leftarrow i+1$ **to** $|\mathcal{X}_k|$ **do**
        $\bar{\mathcal{X}}_k^i, \bar{\mathcal{X}}_k^j \leftarrow$ `ExchangeSuppliers(`$\mathcal{X}_k^i, \mathcal{X}_k^j$`)` ; `//` $\bar{\mathcal{X}}_k$ `is the updated path set`
        $r_{\text{new}}^k \leftarrow$ `UpdateRoutes(`$\bar{\mathcal{X}}_k$`)` ;
        $\Delta_{ij} \leftarrow$ `RouteImprovement(`r^k, r_{new}^k`)` ;
        if $\Delta_{ij} > \Delta$ **then**
          $\Delta \leftarrow \Delta_{ij}$;
    if $\Delta = 0$ **then**
      break ;
    $r^k \leftarrow r_{\text{new}}^k$, $\mathcal{X}_k \leftarrow \bar{\mathcal{X}}_k$;
  for it $\leftarrow 1$ **to** SNSIt **do**
    $\Delta \leftarrow 0$;
    for $i \leftarrow 1$ **to** $|\mathcal{X}_k|$ **do**
      for $j \leftarrow i+1$ **to** $|\mathcal{X}_k|$ **do**
        $\bar{\mathcal{X}}_k^i, \bar{\mathcal{X}}_k^j \leftarrow$ `ExchangeChargers(`$\mathcal{X}_k^i, \mathcal{X}_k^j$`)` ; `//` $\bar{\mathcal{X}}_k$ `is the updated path set`
        $r_{\text{new}}^k \leftarrow$ `UpdateRoutes(`$\bar{\mathcal{X}}_k, r^k$`)` ;
        $\Delta_{ij} \leftarrow$ `RouteImprovement(`r^k, r_{new}^k`)` ;
        if $\Delta_{ij} > \Delta$ **then**
          $\Delta \leftarrow \Delta_{ij}$;
    if $\Delta = 0$ **then**
      break ;
    $r^k \leftarrow r_{\text{new}}^k$, $\mathcal{X}_k \leftarrow \bar{\mathcal{X}}_k$;
  $\text{ub}^k = \text{length}(r^k)$
Given route r^k, generate a vector $\mathbf{z}_k$;
$\text{ub} \leftarrow \sum_{k \in K} \text{ub}^k$;
bestSoln $\leftarrow$ ub, bestRoutes $\leftarrow \mathbf{z}_k$;

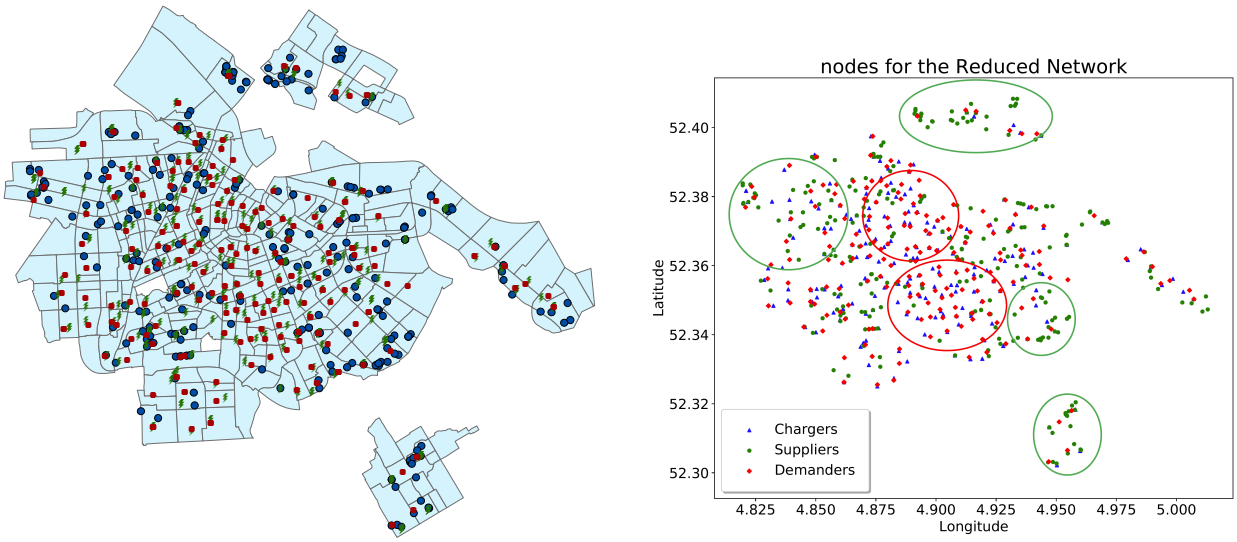

(a) Map for the Neighborhoods

(b) All Nodes for Reduced Network

Figure 2.5 – Left: Map for the Neighborhoods together with Suppliers (blue circle), Demanders (red square) and Chargers (green bolt sign), Right: All Nodes for Reduced Network

selected to relocate the 155 EVs. The nodes are depicted in Figure 2.5b, which clearly shows that the current EV locations (suppliers) and the desired locations (demanders) are concentrated in different areas, hence necessitating relocation operations.

2.5.1 Dataset and Parameters

In our numerical experiments, we use both neighborhood level and spot level data. Based on the two boolean characteristics, i.e., occupancy and availability of charging infrastructure at a node, each node can belong to either of the four node types described in Section 2.3.2. Each node is also located in a certain neighborhood. All the neighborhoods and the nodes therein have locations described through their coordinates. The locations are used to generate their inter node distances and travel times. We calculate Euclidean distances, and multiply them with a detour index of 1.4 to estimate driving distances (Boscoe et al., 2012). We use city speeds of 30 miles per hour to estimate travel times in minutes. The parameter value of β_1, the vehicle's charge depletion rate, is set to 2.5 minutes per unit of charge depletion. Similarly, β_2 representing a vehicle's charging rate and given in percentage gain in

charging per minute is set at 0.4. The values for β_1 and β_2 were derived from actual system data. Barring a major technological shift, these values will likely stay fixed over the medium term. The starting battery level for all vehicles parked at the supplier nodes given by c^0 is found from the system status data at 11:59 am on May 8th, 2016. The desired charging level c^f for all nodes located in a particular neighborhood is found as an average of the initial battery levels for all the trips originating in that neighborhood. In our experiments, we allow for full recharging whereby all the EVs are recharged to 100%.

2.5.2 The Exact Approach

In this Section, we present the results for solving the standalone EV relocation and recharging problem (Section 2.3.6), sequential EV relocation and shuttle routing problem (Section 2.3.7) and synchronized EV relocation and shuttle routing problem (Section 2.3.5) using exact solution approaches. All the experiments were done on a machine with 3.6 GHz CPU clock speed, 16 GB RAM and 64-bit Windows 8 operating system using Java API of CPLEX 12.9.0.

For sequential approach, the relocation and recharging problem (SEQ-A) was solved to optimality for the full network with 829 nodes within 118 seconds. However, the subsequent shuttle routing problem (SEQ-B) is a DARP variant with each EV (customer) being served up to four times by a repositioning shuttle. The problem also involves multiple precedence constraints and loose time windows which depend on shuttle arrivals at the preceding nodes. CPLEX was only successful in solving SEQ-B exactly for up to 10 EVs and 50 nodes. For synchronized EV relocation and shuttle routing problem described in Section 2.3.5, CPLEX failed to solve the MIP model for the system sized instance discussed in this chapter. For this instance, we could not even get a feasible solution for the model. In general, CPLEX was successful in solving the MIP model exactly when the problem size was limited to 15 neighborhoods and 50 total nodes.

Table 2.3 – Value of Objective Function for Different Network Sizes with a) Exact Method for SYNC b) EBNSM c) Exact Method for SEQ and d) Heuristic Approach for SEQ for the 15, 25, and 45 Node Networks

$\lvert\mathcal{N}'\rvert$	$\lvert\mathcal{H}\rvert$	$\lvert\mathcal{X}\rvert$	Value	SYNC-CPLEX	SYNC-EBNSM	SEQ-CPLEX	SEQ-Heuristic
15	6	2	Objective	123.8	123.8	123.8	123.8
			CPU Time	10.65	2.23	1.80	2.07
25	10	4	Objective	156.7	155.3	155.3	155.3
			CPU Time	3600	2.45	470.40	2.28
45	15	9	Objective	184.6	184.8	184.8	184.8
			CPU Time	3600	2.76	3600	2.69

Solution time was another important consideration. The operational nature of the problem necessitates solution methods which provide "reasonably good" solutions within a few minutes. In some cases, customized decomposition-based approaches have previously been used for similar integrated models in other industries. However, the instances solved were either small (Luo et al., 2019) or took many hours to achieve sufficient convergence (Cordeau et al., 2001). The structure of our problem combined with large size of our instances and the need for quick solutions makes our problem less suitable for decomposition based approaches. Therefore, we used heursitic approaches to solve the real-life instances of our problem.

The results comparing the exact approaches with the heuristic approaches for solving SEQ and SYNC problems for small instances are provided in Table 2.3. Generally, for the smaller sized problems, the difference between synchronized and sequential approaches was not substantial owing to the fact that even in sequential approach, the relocation objective is to minimize the total EV path length of all EVs. In smaller networks, this is a good proxy for minimizing the total shuttle route. The results obtained using heuristic approaches were comparable to those with exact approaches for small instances while taking considerably smaller time. Therefore, for solving the system sized instance of the sequential and synchronized problems, we use the heuristic approaches presented in Section 2.4.

2.5.3 Computational Performance of EBNSM

We run EBNSM for instances of the SYNC problem for various numbers of shuttles K and number of drivers q. Each shuttle services one cluster. We solve SEQ-A to get an initial path set $\mathcal{X}_k$ and use the 2-interchange procedure to get shuttle route r_k. Since we do not have a lower bound for the shuttle route length, we use number of iterations to be the termination criterion. Moreover, if K is small, each shuttle will have larger route length. Therefore, the number of 2-interchange iterations are inversely proportional to K. We use $1000/K$. The numbers are empirically chosen as when the 2-interchange procedure has stopped improving the objective. Given the size of the instances, we also want to limit the run time of the algorithm to 20 minutes. Since the size of clusters varies in inverse proportion to number of shuttles/clusters K, we run $500/K$ iterations of the neighborhood procedure for finding the "best" EV relocation decision. We use a depth-first strategy and for each iteration select the exchange with highest improvement. For each iteration of the neighborhood search, we update the shuttle route while maintaining precedence and capacity feasibility to get the best shuttle route given the EV paths selected. When the iterations have stopped giving improvement, we terminate the exchange procedure. Each instance of EBNSM for SYNC problem takes less than 10 minutes to terminate. Moreover, the number of iterations can be modified according to the size of the problem.

2.5.4 Value of the SYNC Approach

We compare the results by the SYNC and SEQ approaches. The purpose of comparing sequential and syncrhonized approaches is not to claim equivalance between the two problems. Similar integrated models have been presented before to show the benefits of integration. For instance, the two aspects of location and routing have been "simultaneously" considered in location-routing literature. The combined problem, although more complex, offers the "promise of more effective and economical decisions" (Balakrishnan et al., 1987).

Given values of K and q, the output of each instance of algorithms is in terms of total route length in minutes denoted as L. We can also calculate following parameters: total number of personnel ($P = Kq + K$) and average route time per shuttle in hours ($T = \frac{L}{60 \times K}$). We also calculate total wait times for shuttles (SH_{wait}), EVs (EV_{wait}) and drivers (D_{wait}) for the best route. We compare the peformance of SYNC and SEQ approaches for 100% recharging situation. For full recharging, the SYNC approach outperforms the SEQ approach in terms of total route length for all instrances of the problem. On average, the route length for SYNC approach is 15% shorter as compared to the SEQ approach. The difference in objective function value varies considerably, in 5–28% range, across instances. Generally, the difference grows larger when the number of drivers on board each shuttle increases as can be seen in Figure 2.6. However. if the number of drivers is increased so much that some drivers are not utilized at all, the difference between the two approaches shrinks. As with the exact approach, when service area is very small, i.e., when the number of clusters/ shuttles is very large, the difference between the SYNC and SEQ approaches decreases.

We also compare the cumulative wait times for all EVs (155), all shuttles (K) and all drivers ($K \times q$) for SYNC and SEQ approaches. The SYNC approach outperforms the SEQ approach in terms of EV wait times. On average, the average improvement for full recharging is 21%. The improvement for driver wait times is also 24% on average. However, the difference decreases as number of drivers per shuttle increases. In case of shuttles, the wait times are negligibly small for small K values. As K increases, the wait times oscillate and SEQ approach has, on average, smaller shuttle wait times in case of full recharging.

2.6 Resource Allocation and Operational Efficiency

An important managerial decision in the operation of EV relocation for FFEVS systems is how operational resource allocation decisions impact the efficiency of operation. In this section, we study the relationship between the operational cost of EV relocation and the size of the shuttles and number of drivers. Specifically, using our computational method

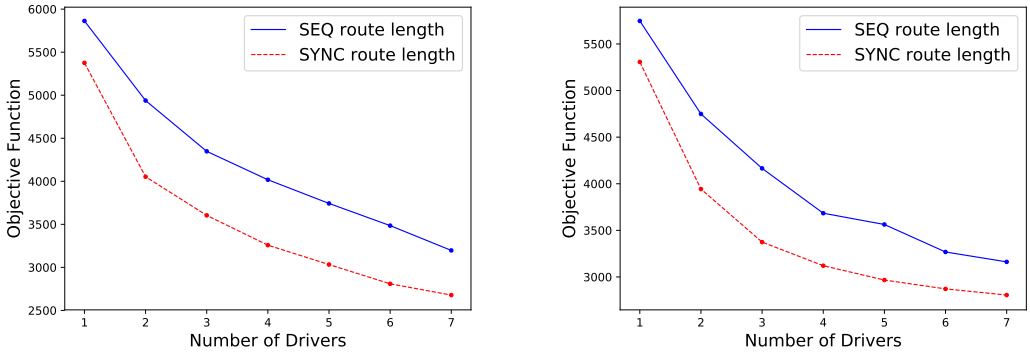

(a) $K = 4$ (b) $K = 5$

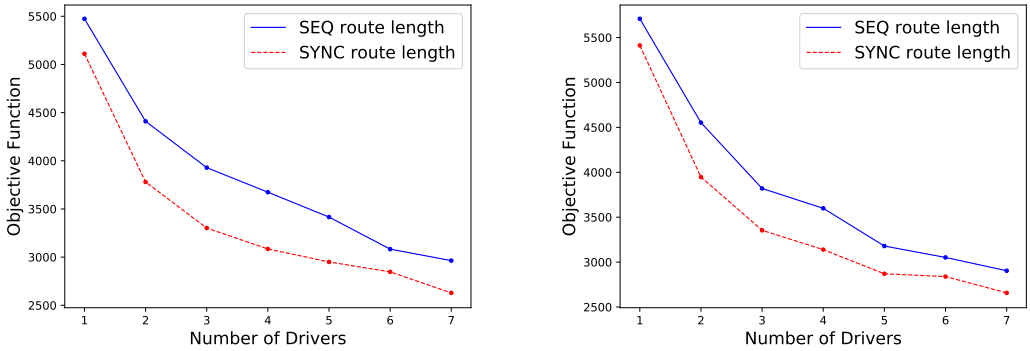

(c) $K = 6$ (d) $K = 7$

Figure 2.6 – The difference in objective function values for SYNC and SEQ approaches for different values of K and q.

and car2go data, we conduct an extensive numerical experiment by calculating the relocation cost for different number of shuttles (clusters) and number of drivers on board each shuttle. We find that besides the per unit shuttle and personnel costs, the size of service area and the initial battery levels of EV fleet are important determining factors for an efficient operation of EV relocation in FFEVS systems.

2.6.1 Cost Parameters

Let Γ_{D} and Γ_{SH} be the hourly costs for personnel and shuttles, respectively. The total cost of relocation operation can be calculated as $C = P \times T \times \Gamma_{\mathrm{D}} + K \times T \times \Gamma_{\mathrm{SH}}$. It is the sum of personnel cost and the shuttle operating cost. In our experiments, we assume the labor cost to be \$40/hr, and the per hour operating cost for a shuttle to be \$24. We also

limit the available time for relocation operation to 7 hours. Therefore, we only consider the instances which achieve the relocation operation within the time limit.

2.6.2 Sensitivity Analysis for the Number of Shuttles and Size of Shuttles

We consider the sensitivity to the number of repositioning shuttles K and the maximum number of drivers on board each shuttle q. The parameter q is also a proxy for the size and type of shuttle being used by the system. As mentioned earlier, different FFEVS systems may use a van, a car, or single-person mobility options like scooters and foldable bicycles to carry out the relocation. It is worthwhile to know which of these options is most cost effective for system operators and also results in least wait times for personnel.

To carry out the sensitivity analysis, we vary the value of K from 1 to 30 and q from 1 to 12. By varying K and q, we not only vary the extent of clustering, but also find out the best way to distribute manpower and shuttle resources to carry out system-wide relocation of EVs. Given a number of total personnel P, a manager may be interested in the best resource allocation in terms of shuttles and drivers. For instance if $P = 6$, the possible resource allocation combinations could be $(K, q) = \{(1, 5), (2, 2), (3, 1)\}$, since each shuttle also requires a driver. In Figure 2.7, we map the cost of all such combinations for P ranging from 2 to 50 with K ranging from 1 to 30 and q ranging from 1 to 12 when 155 EVs are to be relocated. We observe that in most cases the combination (K, q) with larger number of shuttles is also more cost effective. However, as shown in boxes in Figure 2.7, in some cases, for given P, increasing K actually increases the cost of operation and combinations with smaller number of shuttles and larger number of drivers per shuttle are more cost effective. When we repeat the same experiment with a smaller network of 10 EVs varying K from 1 to 5 and q from 1 to 12, we obtain similar results, shown in Figure 2.8, where choosing the highest K is not the best option. Details of the instances for which (K, q) combinations with smaller number of shuttles are more cost effective are given in Table 2.4.

Therefore, it is important for a decision maker to understand when it is advantageous to increase drivers as opposed to shuttles and vice versa, for given number of available personnel. Systems with relatively high labor cost should consider single person mobility options like foldable bicycles or scooters so a cluster of EVs could be assigned to an individual driver without any cars or vans moving him/her around. Changing the per unit cost parameters may also impact these results and the optimal strategy may shift to two drivers per shuttle rather than one driver. However, increasing the number of drivers per shuttle beyond two drivers invariably gives diminishing returns due to large driver wait times on the shuttle. This suggests that for most systems with high hourly personnel costs, using large vans may not be a cost effective option.

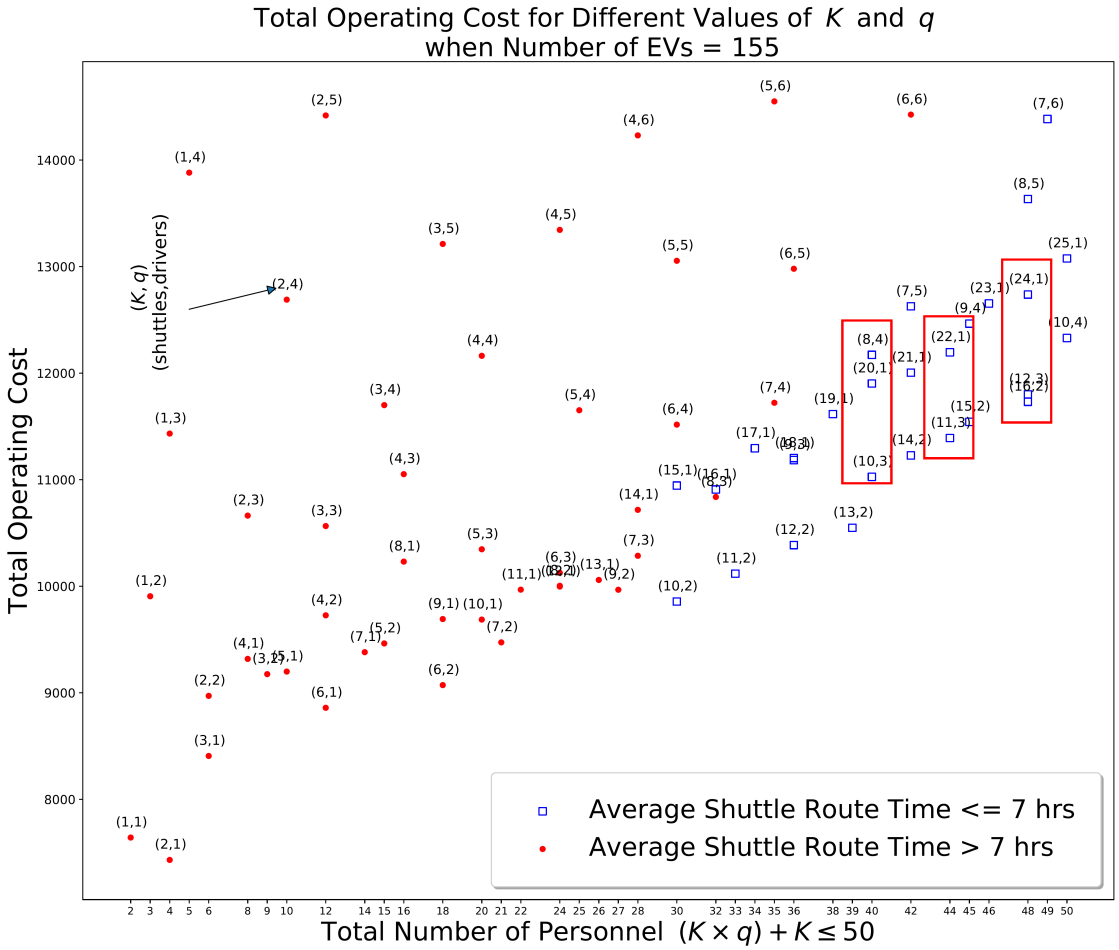

Figure 2.7 – For a Large Network with 155 EVs and given a certain number of personnel and per unit costs, it is advantageous to cluster more and increase the number of shuttles

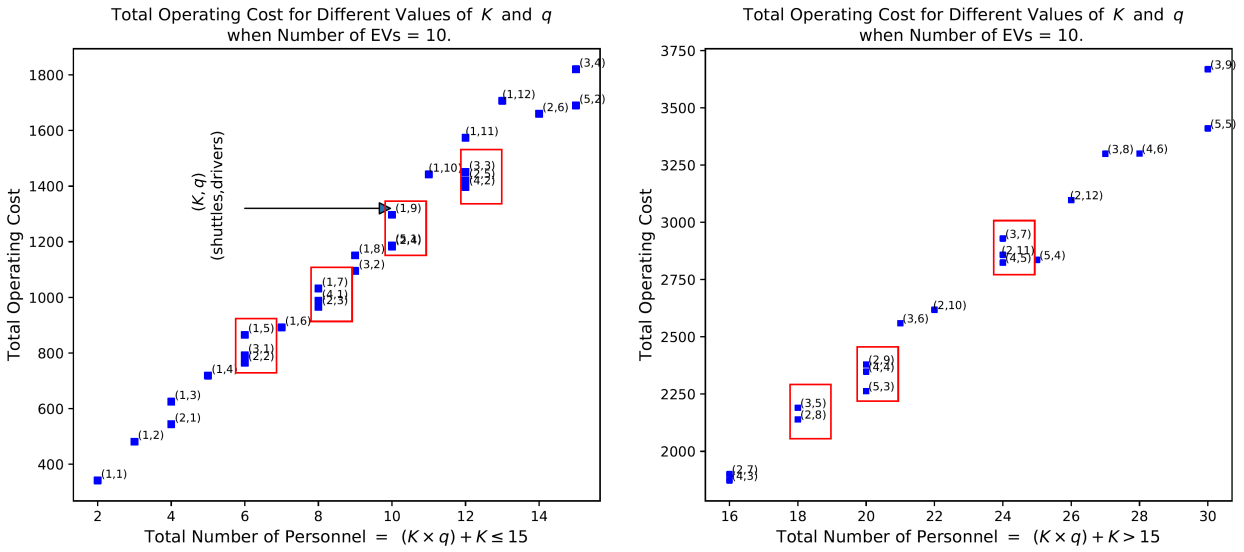

Figure 2.8 – For a Small Network with 10 EVs and given a certain number of personnel and per unit costs, it is advantageous to increase the number of drivers

2.6.3 Analyzing the Shuttle, EV, and Driver Wait Times

For given Γ_D and Γ_{SH}, the average route time per shuttle given by T also impacts the total cost of operation. T is in turn inlfuenced by shuttle wait times. As K is increased, each shuttle is responsible for relocating smaller number of EVs. For $K = 1$, a shuttle must relocate all 155 EVs and for $K = 14$, the number drops to less than 12 EVs. As the number of EVs per shuttle decreases, the corresponding shuttle wait times start increasing as can be seen in Figures 2.9 and 2.10.

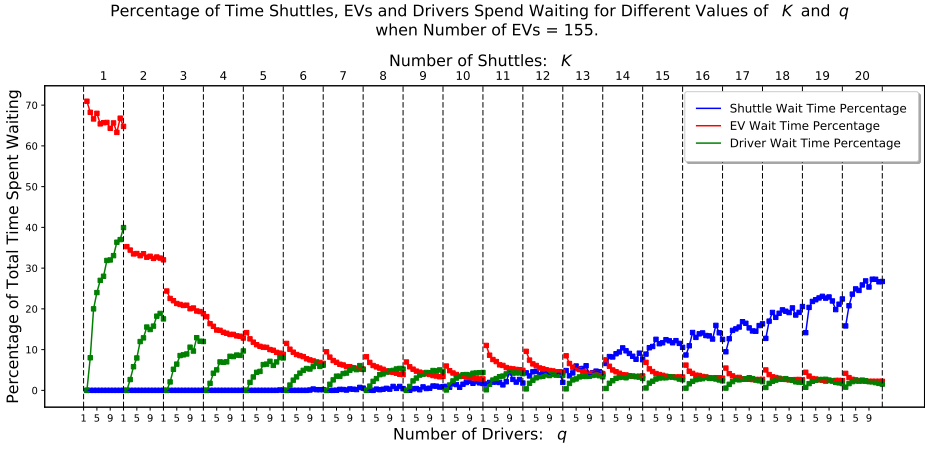

Figure 2.9 – Shuttle wait times increase as the number of shuttles increases

Table 2.4 – Comparison of Shuttle Route Length and Operating Costs for For Various (K, q) Combinations Given Number of Personnel for a Small Network when Number of EVs = 10. The Instances in the Table, Marked Red in Figure 2.8, Correspond to Situations when Increasing the Number of Drivers is Advantageous

P	(K, q)	Average Hours per Shuttle	Total Operating Cost	Shuttle Wait Time	EV Wait Time	Driver Wait Time
6	(1,5)	3.7	972	4	716	589
	(2,2)	3.3	948	146	505	498
	(3,1)	3.5	1,092	328	738	331
8	(1,7)	3.3	1,122	8	500	681
	(2,3)	3.1	1,132	128	383	578
	(4,1)	3.2	1,345	488	647	489
10	(1,9)	3.3	1,388	0	502	676
	(2,4)	3.0	1,341	136	292	791
	(5,1)	3.1	1,603	611	499	614
12	(1,11)	3.3	1,667	3	451	746
	(2,5)	3.0	1,580	137	241	686
	(3,3)	3.1	1,700	295	196	869
	(4,2)	3.0	1,713	426	172	773
24	(2,11)	3.0	3,017	124	235	658
	(3,7)	3.1	3,179	300	179	944
	(4,5)	3.0	3,140	406	161	745

This is owing to the fact that for smaller number of EVs, shuttles must wait for EVs to get recharged before picking up the final batch of drivers from the demander nodes. Therefore, after some point, adding more shuttles only increases the wait times of the shuttles, and it becomes beneficial to increase the number of drivers instead, as shown for a small instance in Figure 2.11.

2.6.4 Analyzing the Impact of Initial Battery Levels and Charging Speed

The difference between initial battery levels and desired charging levels is also an important factor in relocation operations. A larger difference signifies longer recharging processes and larger wait times for shuttles and drivers. This impact is considerable especially for small-scale networks where an EV's charging process may delay the trip completion. For

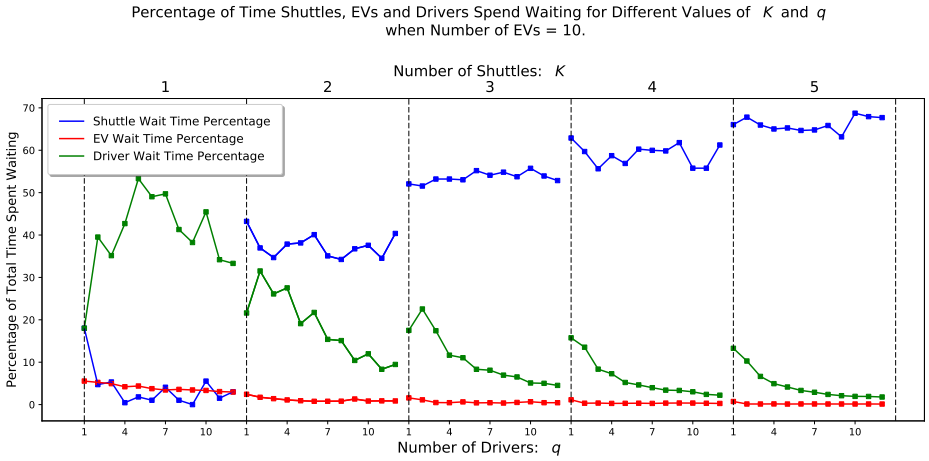

Figure 2.10 – Shuttle wait times increase as the number of shuttles increases

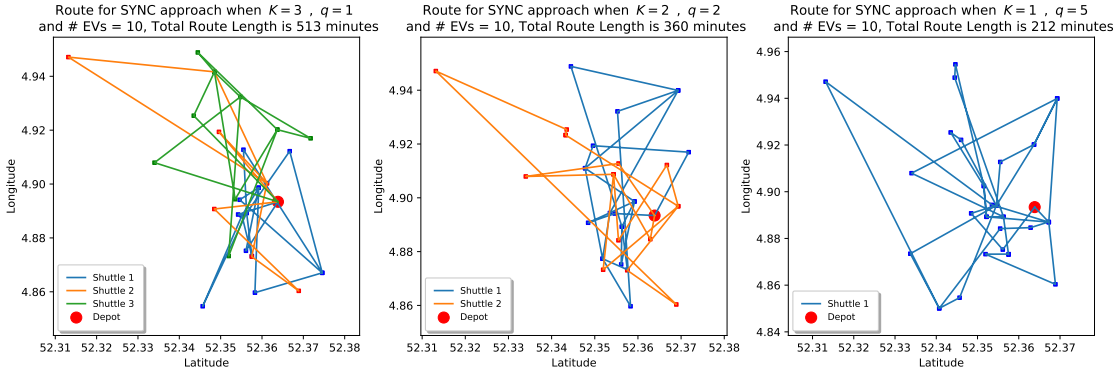

Figure 2.11 – Possible relocation operation alternatives when number of personnel = 6, number of EVs = 10. For $(K, q) = (3, 1)$, shuttles wait 52% of the time; for $(K, q) = (2, 2)$, shuttles wait 37% of the time; for $(K, q) = (1, 5)$ shuttles wait 1.8% of the time.

low initial battery levels, the charging process takes longer and adding extra shuttles only contributes to shuttle wait times. However, if the initial battery levels get higher (so the charging requirements become lower), increasing the number of shuttles can still be beneficial. As shown in Figure 2.12, we increase the initial battery levels from c^0 to αc^0 uniformly. As α increases, the charging requirement decreases, and the cost of operation with larger number of shuttles (green asterisks) becomes more favorable.

It should be noted that, as shown in equation (2.1), increasing the initial charging levels c^0 decreases w_p, i.e., the time spent charging on the charging station. A similar effect will occur as we vary the charging speed, i.e., parameter β_2. As charging speeds become

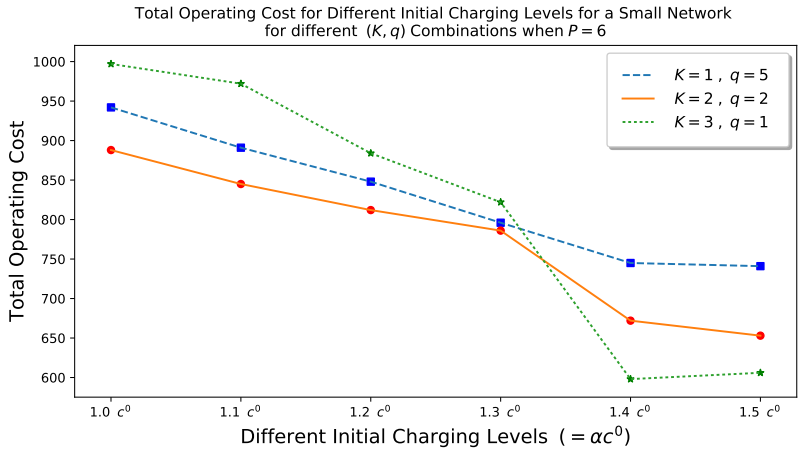

Figure 2.12 – As initial battery levels increase, it becomes beneficial to increase the number of shuttles

faster, due to technological advancement, it will result in a decrease in w_p. Therefore, the sensitivity analysis with different initial battery levels is a good proxy for varying the charging speed. As technology advances, and charging speed becomes faster, increasing the number of shuttles, i.e., using a larger number of smaller shuttles to carry out the relocation operation becomes beneficial.

Chapter 3: Creating Grocery Delivery Hubs for Food Deserts at Local Convenience Stores via Spatial and Temporal Consolidation

3.1 Introduction

The term food deserts is used to describe neighborhoods and communities where access to affordable and nutritious foods is limited due to issues of income and access (Council, 2009). Various qualitative and quantitative definitions have been proposed and used to categorize certain neighborhoods as food deserts. The United States Department of Agriculture (USDA) uses locations of supermarkets and grocery stores and the census tract level demographic, income and vehicle access data to classify census tracts as food deserts. Different criteria are used for rural and urban census tracts (USDA, 2019). A tract is designated as a food desert if the tract's poverty rate is 20 percent or greater and a significant number (at least 500 people) or share (at least 33 percent) of the population is greater than 0.5 miles (alternately 1 mile) from the nearest supermarket, supercenter, or large grocery store for an urban area or greater than 10 miles (alternately, 20 miles) for a rural area (USDA, 2019). Food deserts are neighborhoods marked by lack of access to affordable, nutritious and healthy foods with measurably adverse impacts on individual and community health. Food insecurity as a health risk is linked to costly and preventable chronic diseases, including high blood pressure, coronary heart disease, hepatitis, cancer, arthritis, and chronic obstructive pulmonary disease (Bhatt, 2020). On one hand, the distance to supermarket and food prices is positively correlated with obesity (Ghosh-Dastidar et al., 2014) and lack of access to supermarkets is associated with lower expenditures on healthy foods (Ver Ploeg et al., 2012). On the other hand, better access to convenience stores, often the only available food location, causes an increased risk of obesity (Ver Ploeg et al., 2012). Convenience stores

offer food choices with the lowest nutritional value among all store types (Cannuscio et al., 2013).

Food insecurity has a close, intuitive link to not only poverty and food prices, but also spatial access to healthy foods, which is the focus of this chapter. The lack of healthy food options in many neighborhoods represents a market failure. Supermarkets are unwilling to locate in such neighborhoods, while the small convenience stores either do not offer healthy food options or offer them at higher cost and low quality. The efforts for incentivizing supermarkets to relocate through tax rebates and rezoning have not worked. Many households in these neighborhoods also lack access to personal or public means of transportation. Public transit in many cities is perennially under-resourced and even modern shared mobility mechanisms like car-sharing and bike-sharing disproportionately serve advantaged neighborhoods. This chapter quantifies the potential of consolidated last-mile food delivery for converting convenience stores within food deserts from sources of unhealthy food to hubs of healthy foods. This research ultimately aims to contribute to improve the quality of foods accessible to people living in food deserts and promote food security.

The proposed solution involves modern last-mile delivery services specialized in food, such as Instacart, Walmart Same-Day Grocery Delivery, and Amazon Prime Now. The grocery delivery orders are usually in small quantities and deliverers need to make multiple stops. Since the delivery vehicle is not equipped with refrigeration, there is a limit on the amount of fresh produce that can be delivered at once. The attended home delivery requirements for fresh produce can also cause missed deliveries, and narrow delivery time windows. While last-mile delivery options can certainly provide access to healthy foods to people in food deserts, the aforementioned factors pose a significant challenge of high delivery cost. For many socioeconomically disadvantaged customers living in food deserts, the costs associated with attended home delivery of groceries and the minimum order size requirements make grocery deliveries financially non-viable. To reduce the delivery cost, this chapter proposes consolidating customer orders and delivering to a convenience store

in the neighborhood, instead of delivering directly to the customer's home locations. The convenience store will serve as a pickup point.

This proposed solution has several advantages. First, by consolidating orders, the deliverer can enjoy the economy of scale to not only lower the delivery cost but also enable small-quantity orders from customers in food deserts. For store delivery, fewer delivery points are visited by delivery vehicles. We call this *spatial consolidation*, i.e., when there are no time windows on both store delivery and home delivery. Second, the deliverer does not need to deliver to attended homes, and therefore they need not consider time windows to ensure customers are present at home. Moreover, since most convenience stores are equipped with refrigerated spaces, the delivery of fresh produce can occur at any time within a day. Therefore, delivering to convenience stores not only achieves spatial consolidation but also *temporal consolidation*. Third, this proposal significantly improves the access to healthy foods for customers living in food deserts. The total delivery costs are reduced and customers can walk within a reasonable distance to obtain healthy foods. The improved access can in turn lead to better health outcomes for people utilizing the delivery service. This approach can also moderate the adverse impacts of disruptions caused by Covid-19 pandemic on grocery access, which predominantly affect food deserts, by delivering healthy foods directly to the most affected neighborhoods.

This chapter also makes a crucial contribution to the literature of last mile urban delivery, beyond the current application for food insecurity problem. No other study has quantified both spatial and temporal aspects of consolidation at neighborhood pickup points for last mile urban delivery. Achieving such consolidation for grocery delivery requires special arrangement with attended convenience stores because of refrigeration requirements. For package delivery, however, a larger number of locations can be selected as pickup points. In fact, such partnerships between shipping companies and partner locations to install lockers are already in practice in North America and in Europe where kiosks, florists, subway stations and all manner of small retail locations can serve as pickup points.

In this chapter, we focus on quantifying the consolidation benefits, both spatial and temporal, from delivery of fresh foods and groceries at convenience stores closest to the underserved customers. The following specific research aims can help fill crucial parts of this puzzle:

- To quantify the consolidation benefits to grocery delivery services achieved by delivering groceries to neighborhood convenience stores compared with direct-to-home delivery;
- To identify the ideal number, density, and location of partner convenience stores to achieve "sufficient" consolidation and service level; and
- To evaluate how urban form and certain model parameters, including size of delivery time windows, delivery vehicle capacity, number of depots, and number of customers affect the extent of consolidation and the service level.

To address the first research question, we employ an optimization framework involving minimum cost set covering problem (Garfinkel and Nemhauser, 1969) and a customized version of capacitated vehicle routing problem (CVRP) (Toth and Vigo, 2002) with multiple depots and time windows, i.e., MDCVRP-TW. The customer orders are randomly generated and only orders within a walkable distance to one of the convenience stores are accepted for fulfillment. The set cover problem minimizes the number of convenience stores that can service (cover) the accepted customers. To quantify the impact of consolidation on order delivery costs, MDCVRP-TW is run twice; first time to fulfill the orders without consolidation at each customer's location and second time to fulfill the orders at consolidation points selected by the set cover model. The second research question is addressed by varying the number of available convenience store locations as a model sensitivity parameter in the optimization framework. We are interested in determining the number of locations necessary to achieve sufficient levels of consolidation as well as accepted customer orders (service level) to justify the deliverer-store partnership. The final research question involves determining

the circumstances, including urban form and other model parameters, which impact the extent of consolidation and the service level.

Our experimental set up consists of data from three counties with marked differences in urban form and population densities. For each county, we create eight instances of varying sizes, depending on the number of depot locations (low, high), number of partner convenience stores (low, high) and number of customer orders (low, high). For comparison across instances, we calculate delivery cost per order and the percentage of accepted orders (service level). Following are the key findings of this chapter:

- The results show that only spatial consolidation, measured in terms of reduction in delivery costs per order, although substantial, is not sufficient to justify the store delivery;
- Our results also show that benefits of temporal consolidation in terms of total delivery cost far outweigh those of only spatial consolidation. For our instances, temporal consolidation due to store delivery can accrue delivery cost benefits of ten times and more when narrow customer time windows are considered.
- The capacity of delivery vehicles is an important factor in determining the extent of consolidation. The difference in delivery costs between two schemes is larger for larger capacity vehicles due to in-vehicle pooling.
- Number of available partner stores positively impacts the service level, while a higher number of depot locations and customer orders reduce the cost of delivery.
- The consolidated delivery using only chain stores in rural and less dense urban neighborhoods provides insufficient service level and a wider set of partner locations may need to be explored.

The rest of the chapter is organized as follows: in Section 3.2, we present an extensive literature review of food desert related transportation problems and the last mile of grocery

logistics. We also review work related to benefits of consolidation in urban logistics. In Section 3.3, we present mixed integer programming models for the underlying set cover and routing problems and the algorithms used to solve these models. Section 3.4 details the experimental setup, including data collection and the case studies used in this chapter. Section 3.5 summarizes the key findings and results of the model including sensitivity analysis of key model parameters.

3.2 Literature Review

We identify two research streams relevant to our study: research at the confluence of transportation and food insecurity and online grocery delivery research. Each stream is discussed in turn.

3.2.1 Food Deserts

The term food deserts is used to describe neighborhoods and communities where access to affordable and nutritious foods is limited due to issues of income and access (Council, 2009). USDA uses a poverty level of more than 20 percent and a distance to the closest supermarket of 0.5 miles (alternately 1 mile) for urban areas and 10 miles (alternately, 20 miles) for rural areas, to designate a tract as food desert (USDA, 2019). Others have suggested the inclusion of non spatial characteristics like income, time use and household characteristics (Widener, 2018). Efforts have been made to use localized studies to collect data on a neighborhood food environment including details about local households and available food options. However, the extensive data collection effort and budget constraints make it difficult to replicate such studies on national level. Following USDA's definition, Figure 3.1 shows the food desert tracts in continental US, using low income and a distance to supermarket of 1 mile and 10 miles for urban and rural areas, respectively.

The current efforts to combat food insecurity have addressed the three dimensions of 1) income, 2) location, 3) and mobility using various non-governmental and governmental

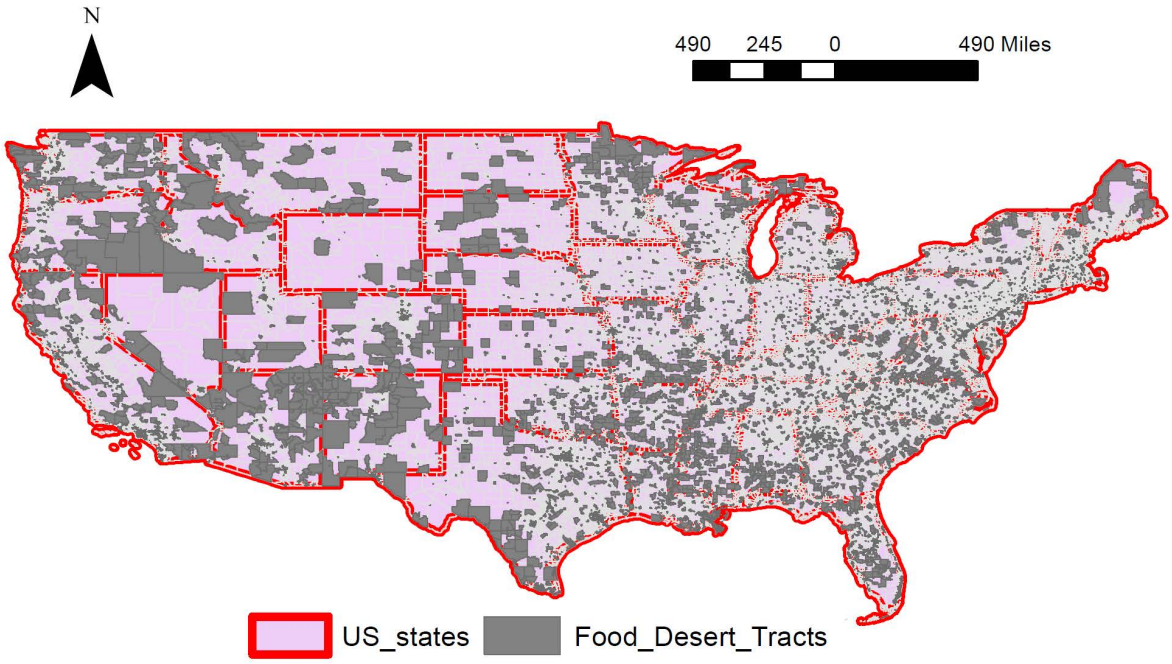

Figure 3.1 – Tracts designated as food deserts in the continental US shown in Grey

policy interventions. There is a large body of evidence supporting an inverse causal link between low income and food insecurity; and consequent nutritional deprivation; in disadvantaged households (Mark et al., 2012; De Marco and Thorburn, 2009). There are also federal and state run programs to promote consumption of healthy foods through grants and tax breaks (Aussenberg, 2014; National Center for Chronic Disease Prevention and Health Promotion, 2011). These initiatives, along with community kitchens, community farms, food pantries, food banks, fruit and vegetable box delivery schemes, and other community initiatives, although structurally inadequate, serve to moderate the effect of low income on food insecurity (Tarasuk and Reynolds, 1999; Akobundu et al., 2004; Bhattarai et al., 2005; Daponte, 2000; Zorbas et al., 2018).

The location dimension explores the proximity of households to supermarkets, grocery stores and other sources of healthful foods. Lack of access to supermarkets causes greater prevalence of health challenges, like diabetes, heart disease and cancer, with diet as a major risk factor (Walker et al., 2010). The disparities in access to supermarkets overwhelmingly affect low-income and minority communities (Walker et al., 2010; Dai and Wang, 2011). The

Let's Move! program launched in 2010 by the then first lady, Michelle Obama, envisaged building or expanding 1,500 stores to sell fresh food in underserved communities across the United States (Obama, 2012). Despite efforts made by all levels of government, and by some industry organizations (Kalkanci et al., 2019), it is impracticle to locate supermarkets in all low-income neighborhoods (Varney, 2019). Moreover, building more supermarkets is hardly a panacea for food insecurity and their impact on dietary habits is unclear (Ghosh-Dastidar et al., 2017; Cummins et al., 2014; PBS, 2014). Because online grocery delivery services provide access to a wider variety of foods and do so digitally, their offerings and suggestions can be tailored to increase positive behaviors (Dillahunt et al., 2019) and promote the consumption of healthy foods.

Efforts to combat the mobility dimension of food insecurity have taken a variety of forms. For many residing in socioeconomically disadvantaged neighborhoods, lack of mobility can hamper access to healthy foods, education, healthcare and employment opportunities (Syed et al., 2013; Gottlieb and Fisher, 1996; Kodransky and Lewenstein, 2014). Modern mobility options, like bike-sharing and car-sharing can complement the under-resourced public transit systems and improve urban mobility and help households overcome the 'tyranny of distance'. However many social, financial, and cultural barriers to their widespread use remain in place (Kodransky and Lewenstein, 2014; Pendall et al., 2016), and mobility benefits of these systems appear to accrue disproportionately to advantaged populations (Tyndall, 2017; Prieto et al., 2017). Moreover, apart from some small-scale pilots using carshare for grocery delivery (Lyft, 2019), their potential for improving access to healthy foods remains unexplored.

Our proposed solution to use consolidated delivery services makes fresh food accessible to underserved communities by addressing all three dimensions of food insecurity. For socioeconomically disadvantaged communities, the proposal reduces the cost of delivery and makes it easier for deliverers to deliver small quantity orders. From location perspective, the proposal seeks to convert convenience stores, which are sources of unhealthy food in

the communities, to hubs of healthy food. In terms of mobility, the solution removes the need for grocery trips by providing customers access to fresh food within their communities. Initial research on grocery-delivery solutions has found that an affordable online grocery delivery model could serve as a feasible solution for improving access to healthy foods in transportation-scarce and low-income contexts (Dillahunt et al., 2019). However, there is currently no research on how an "affordable" grocery-delivery transportation model could work in practice in low-income contexts. This research is also timely because of the unprecedented strains imposed on all three dimensions of food insecurity by the Covid-19 pandemic (Southey, 2020; Rockett, 2020; Adams, 2020), and the growing popularity of food delivery as a cheaper, healthier and safer method of accessing fresh food (Hobbs, 2020).

3.2.2 Logistics of Food Recycling

Most operations research literature for addressing food insecurity have focused on the problem of food recycling. There is a rich literature on using vehicle routing problems to collect and distribute food through food banks or pantries. The food is picked up from pickup nodes (providers) and dropped at one or multiple delivery nodes. The problem is defined as an Unpaired Pickup and Delivery Vehicle Routing Problem (UPDVRP) (Nair et al., 2017). What makes food recycling problems unique is their focus on fairness and equity considerations where unsatisfied demand for all food recipients, the latest arrival time and the total response time is minimized (Nair et al., 2017). The perishability of food items, however, makes time of service completion a critical factor to consider. Various exact and heuristic approaches have been proposed to solve the single period vs multi period, and capacitated vs uncapacitated versions of the problem (Nair et al., 2018). Davis et al. (2014) propose a solution similar to that presented in this chapter for food banks to deliver food to satellite locations called food delivery points (FDPs) rather than directly to charitable agencies. They solve a set covering model to determine the assignment of food receiving agencies to FDPs,

and a periodic vehicle pick-up and delivery model with backhauls (PVRPB) for delivering food to FDPs.

3.2.3 Last Mile Grocery Logistics

Research in last mile logistics has focused in most part on solving vehicle routing problems with or without time windows (Toth and Vigo, 2002; Desaulniers et al., 2014; Voccia et al., 2019; Emeç et al., 2016). More recently, the advent of modern delivery options, such as cargo-bikes, tricycles, electric vehicles, autonomous vehicles, drones and crowd-sourced delivery has initiated research on these new models and systems of delivery (Dayarian et al., 2020; Sanchez, 2016; Castillo et al., 2018). The last mile of grocery supply chain is a complex but important problem area with research work needed to understand the connections between conventional supply chain solutions, like consolidation, and last-mile realities (Starr and Van Wassenhove, 2014).

Current research in same day delivery (SDD) space is focused on optimizing order acceptance and order fulfillment to address the high degree of information dynamism arising in SDD (Klapp et al., 2019). An important problem in SDD is designing mechanisms for accepting or rejecting arriving customer orders (Campbell and Savelsbergh, 2005; Ehmke and Campbell, 2014). One stream of research focuses on approximation of delivery costs and their incorporation into booking process for acceptance of arriving orders (Köhler and Haferkamp, 2019). Another stream focuses on evaluating arriving customer requests to create optimal or maximal time window offer sets (Agatz et al., 2011; Köhler et al., 2020; Hungerländer et al., 2017). Another well-studied problem involves design of pricing mechanisms including differentiated slot pricing (Klein et al., 2019), incentive schemes (Campbell and Savelsbergh, 2006), and dynamic pricing for time slots for management of arriving demand (Asdemir et al., 2009; Yang et al., 2016).

This chapter proposes to use the well-established last mile logistics channel to address the access and mobility dimensions of food insecurity. This solution is made possible by

confluence of a variety of enabling factors. The direct to consumer (D2C) delivery market, driven by rapid growth in e-commerce, has seen an annual growth of 7%–10% in mature markets like the United States (Dayarian et al., 2020). The value of the US online grocery market, led by Walmart, Instacart, and Amazon Prime Now, has grown from $12 billion in 2016 to a projected $47 billion in 2020, which is 7% of the total grocery market (Magana, 2020). Recently, USDA launched an online purchasing pilot in many US states, allowing Supplemental Nutritional Assistance Program (SNAP) dollars to be spent on online food purchases (USDA, 2020). Last-mile logistics driven by the instant meal delivery and the same-day grocery delivery has seen huge investment from major competitors in capacity expansion, technology, and delivery systems. Recently, the Covid-19 pandemic has created a sudden expansion in online grocery orders, as more consumers comply with stay-at-home and social distancing orders (Hobbs, 2020).

Despite these positive developments, the 'last mile' of grocery logistics can be costly and ineffective due to the lack of economies of scale and issues of attended home delivery, like difficult to find addresses, narrow time windows and missed deliveries (Deutsch and Golany, 2018). For groceries, especially fresh produce, the need for refrigerated storage further complicates the last-mile logistics. The resulting high cost of delivery has been a major impediment in market growth and customers have shown resistance to delivery charges (Netzer et al., 2017). Most delivery services charge $6–$9 per order for delivering orders including fresh produce. However, some deliverers have started offering annual subscription based services including for fresh produce and other similar items (Thomas, 2019). This cost is a big barrier for residents in food insecure neighborhoods. Furthermore, due to very thin margins in grocery retailing, demand side factors like number of expected customers and supply side factors like location of delivery depots can bypass low income localities with predominantly minority populations (Kalkanci et al., 2019; Carman, 2018) . The solution we propose consolidates delivery at neighborhood pickup points, therefore eliminating most cost-inducing factors mentioned above.

Recently, major e-commerce players have explored the concepts of locker-boxes to allay some issues in attended home delivery. Although popular in Europe, these intermediate consolidation points have only recently gained traction in the US. Online retailers like Walmart and Amazon have started pilot partnerships with convenience stores and apartment complexes to install lockers for unattended parcel delivery. However, no such partnership currently exists for grocery deliveries. Very little research in the US is focused on design of network of alternate delivery points as a means for consolidation in the last-mile of grocery logistics.

3.2.4 Benefits of Consolidation

Many parcel delivery services have recently experimented with a network of hyperlocal pickup points to achieve last mile consolidation (Deutsch and Golany, 2018; Faugere and Montreuil, 2016). Pickup points are locations where customers can pick up their orders. They can be unattended, e.g. locker boxes, or attended, e.g. fuel stations and local convenience stores. Pickup point networks also have economic benefits as they increase the number of successful first-time deliveries and allow more effective optimization of delivery routes (due to reduced location and time uncertainty) (Morganti et al., 2014b; Savelsbergh and Van Woensel, 2016). Such networks have recently proliferated in Europe with large number of pickup locations in France, UK, Germany and other countries. Most research on pickup points has focused on the network design problem and location problem for pickup points (Deutsch and Golany, 2018; Morganti et al., 2014a; Wang et al., 2017). Most systems use current locations like convenience stores, commuter stations or other attended locations like florists or kiosks as potential locations in the network (Morganti et al., 2014a). The current models do not take into account walkable-distance considerations when designing the pickup point networks.

The benefits of freight consolidation in long haul transportation and global supply chains are well-known. In the context of urban logistics, researchers have studied urban

consolidation centers (UCC) as terminals outside urban centers where incoming urban freight from multiple carriers could be consolidated and dispatched for delivery on smaller, energy efficient vehicles (Lin et al., 2013; Simoni et al., 2018). In the US, Conway et al. (2012) study the design and impacts of urban micro-consolidation centers (UMC) aided by last-mile tricycle deliveries in New York City. However, there is little work, if any, on small scale consolidation in the context of urban last-mile delivery services. Moreover, very few studies quantify the cost-benefits from spatial consolidation achieved by the delivery services due to pickup points and no other study explores the temporal dimension of consolidation. Durand et al. (2013) is the only other chapter which quantifies the benefits from spatial logistic pooling but only for non-food items.

3.3 Methodology

We envisage spatial and temporal consolidation of order delivery at pickup points or neighborhood convenience stores. The stores work as pooling locations for multiple customers (orders). Information about all customer orders is assumed to be available at the beginning of planning horizon and the orders must be delivered on the same day. A coalition of customers is assigned to each pick up store. Pick up points can have limited capacity, especially if they are a standalone kiosk. However, we assume these points to have unlimited capacity to serve customer orders since we only consider convenience stores with refrigerated storage. A customer is assigned a pick up store which is within walkable distance to their home. Our model therefore cannot service all customers and only those within a walkable distance are accepted for service. We also assume the depot locations to have unlimited capacity. Similarly, the delivery routes available are also assumed to be unlimited in number since we must deliver all the accepted orders. The delivery vehicles are assumed to be homogenous and are assumed not to have a refrigerated compartment for delivery of refrigerated/frozen groceries. The size of delivery time windows is also assumed to be the same for all customers.

This scheme helps achieve aggregation, removes last mile delivery costs for the retailer, and helps in order consolidation. Most retailers currently require a minimum order of \$30–\$35 to deliver at homes. Order consolidation can help retailers waive the minimum cost requirements and deliver smaller orders to the pickup points. The customers end up paying smaller delivery costs and get the flexibility of making smaller orders. Our proposed methodology involves solving a minimum set cover problem and a multi depot capacitated vehicle routing problem with time windows. In this section, we describe the two problems and the solution methods employed for solving them.

3.3.1 Set Cover Problem

A set cover model is solved to assign customer orders to neighborhood convenience stores which are also referred interchangably as stores. All stores within a walkable distance can serve the customer orders. The set cover model minimizes the number of stores required to serve the customer orders by aggregating the orders in minimal number of stores. The "walkable" distance ω is varied as a model parameter. In our experiments, we use 600 meters and 1000 meters. Customers without a convenience store within the walkable distance are not served. Although stores may have limited storage capacity or refrigerated space, we do not put any upper limit on the number of customers which can be served by a single store. However, due to limits on vehicle capacity, we allow multiple vehicle visits to a store.

Given the notation in Table 3.1, we can write the minimum cost set cover problem (SCP) as follows:

$$\text{(SCP)} \quad \min \quad \sum_{q \in \mathcal{Q}} y_q, \tag{3.1}$$

$$\text{s.t.} \sum_{q \in \Phi(o)} x_{oq} = 1 \qquad \forall o \in \mathcal{O}, \tag{3.2}$$

$$x_{oq} \leq y_q \qquad \forall a = (o, q) \in \mathcal{A}, \tag{3.3}$$

$$x_{cq}, y_q \in \{0, 1\} \qquad \forall c \in \mathcal{C}, \forall q \in \mathcal{Q}. \tag{3.4}$$

Table 3.1 – Mathematical Notation for SCP

Sets	
$\mathcal{C}$	Set of all customer orders in a planning period indexed by $c \in \mathcal{C}$
$\mathcal{Q}$	Set of neighborhood convenience stores (stores) within 1 mile of food desert tracts indexed by $q \in \mathcal{Q}$
$\Phi(c)$	Set of stores q within walkable distance ω to a customer c, i.e., $\{q \in \mathcal{Q} : d_{cq} \leq \omega\}$
$\mathcal{R}$	Set of stores which are within walkable distance to one or more customer orders and can service one or more customer orders, i.e., $\mathcal{R} = \bigcap_{c \in \mathcal{C}} \Phi(c)$
$\mathcal{O}$	Set of accepted customer orders indexed by $o \in \mathcal{O}$, where $\mathcal{O} = \{c \in \mathcal{C} : \Phi(c) \neq \emptyset\}$
$\mathcal{A}$	Set of all possible arcs indexed by $a \in \mathcal{A}$ where each arc $\mathcal{A} = \{(o, q) : q \in \Phi(o), \forall o \in \mathcal{O}\}$
$\mathcal{S}$	Optimal set of stores selected by the set cover model, i.e., $\mathcal{S} = \{q \in \mathcal{Q} : y_q = 1\}$
$\bar{\mathcal{S}}$	Set of all store vertices to be visited to deliver customer orders. The set includes the set of original store nodes $\mathcal{S}$ and the dummy nodes, created to allow multiple vehicle visits to a single store due to capacity limitations
Variables	
x_{oq}	Binary variable; 1 when a a customer order o is assigned for delivery at store location q, 0 otherwise
y_q	Binary variable; 1 when a store location q is selected as a pickup point, 0 otherwise
Parameters	
d_{oq}	travel distance alongside a travel arc (o, q)
P	capacity of delivery vehicles in terms of number of orders
ω	Parameter representing walkable distance

In the set cover problem described above, the objective is to find the minimum number of stores required to service all the customers. Constraint (3.2) makes sure that each accepted order is covered by (assigned to) a neighborhood store q. Constraint (3.3) ensures that customers can only be serviced by a store q if the store is selected as a pickup point. The output of the set cover model is the set of stores selected ($y_q = 1$) and the respective customers serviced by each store ($x_{oq} = 1$). The total demand at a store vertex q, denoted as d_q is given as $d_q = \sum_{o \in \mathcal{O}} x_{oq}, \forall q \in \mathcal{S}$. Since vehicles have limited capacity P, a store location may need multiple vehicle visits if $d_q > P$. Therefore, we create dummy store locations for each subsequent vehicle visit. Let β_q be the number of such dummy nodes created for each store q, given as:

$$\beta_q = \left\lfloor \frac{\sum_{o \in \mathcal{O}} x_{oq}}{P} \right\rfloor, \qquad \forall q \in \mathcal{S}. \tag{3.5}$$

Given P and β_q, the updated demand value at each original and dummy node can also be calculated. For example, let us consider three stores with demands $d_1 = 12, d_2 = 4, d_3 = 8$, and the vehicle capacity limited to 5. The number of dummy nodes created to accommodate the extra trips to the stores can be given as $\beta_1 = 2, \beta_2 = 0$ and $\beta_3 = 1$. Accordingly, for store 1, the demand for original node is updated from 12 to 5 while the demands for two dummy trips are 5 and 2, respectively. The outputs of set cover model, after the post processing, include the set of all store vertices ($\bar{\mathcal{S}}$), demand at all store vertices ($d_i,\ \forall i \in \bar{\mathcal{S}}$) and set of accepted orders ($\mathcal{O}$). These serve as inputs for the subsequent vehicle routing problem.

3.3.2 Multi Depot Capacitated Vehicle Routing Problem with Time Windows

The second part of our methodological framework is a multi-depot capacitated vehicle routing problem with time windows (MDCVRP-TW). MDCVRP-TW can be formally described as follows. Let $\mathcal{G} = (\mathcal{V}, \mathcal{E})$ be a graph, where $\mathcal{V}$ is the set of vertices and $\mathcal{E}$ is the set of eges or arcs connecting each pair of vertices. The set $\mathcal{V}$ consists of delivery locations

and depot locations. The two subsets are described as: $\mathcal{V}_c = \{v_1, v_2, \ldots, v_N\}$ which is the set of delivery locations to be served; and $\mathcal{V}_d = \{v_{N+1}, v_{N+2}, \ldots, v_M\}$ which is the set of depots. Each vertex $v_i \in \mathcal{V}$ has several non-negative weights associated with it. These include a nonnegative demand d_i representing the number of orders to be delivered at the vertex, a nonnegative waiting time w_i and a delivery time window $[e_i, l_i]$, where, e_i is an earliest start time and l_i is a latest start time for the delivery. Let $r_i = l_i - e_i$ br the size of the time window for delivery vertex i. If T is the total time available for delivery, let $q = \frac{T}{r}$ be the number of equally sized, non-overlapping, time windows available for delivery. In this chapter, we choose T and r such that T is divisible by r and q is an integer. Further, for the depot vertices $v_i \in \mathcal{V}_d$, there is no demand and wait times, i.e. $d_i = w_i = 0$. The set of edges $\mathcal{E} = \{(v_i, v_j) | v_i, v_j \in \mathcal{V}, i \neq j\}$ is defined for all vertex pairs. Each arc belonging to the set $\mathcal{E}$ has an associated cost, given by the travel time t_{ij}. A total of K homogenous vehicles are available. Each vehicle has the capacity P. Feasible solutions exist only if

$$e_d = E_d \leq \min_{i \in \mathcal{V}_c} \{l_i - t_{di}\}, \qquad \forall d \in \mathcal{V}_d, \tag{3.6}$$

$$l_d = L_d \geq \min_{i \in \mathcal{V}_c} \{e_i + w_i + t_{id}\}, \qquad \forall d \in \mathcal{V}_d. \tag{3.7}$$

Note also that an arc $(i, j) \in \mathcal{E}$ can be eliminated due to temporal considerations, if $e_i + w_i + t_{ij} > l_j$, or capacity limitations, if $d_i + d_j > P$, or by other factors.

With the notation in Table 3.2, MDCVRP-TW consists of determining a set of vehicle routes in such a way that:

- Each vehicle route starts at a depot and ends at the same depot.
- The number of vehicles used at each depot cannot exceed the fleet size.
- Each delivery vertex is serviced exactly once by a vehicle route.

Table 3.2 – Mathematical Notation for MDCVRP-TW

Sets	
$\mathcal{V}$	Set of vertices consisting of two subsets: a set of delivery locations $\mathcal{V}_c$ and depot locations $\mathcal{V}_d$
$\mathcal{E}$	Set of edges or arcs connecting each pair of vertices, i.e., $\mathcal{E} = \{(v_i, v_j) \mid v_i, v_j \in \mathcal{V}, i \neq j\}$
$\mathcal{K}$	Set of vehicles available for order delivery at all depots. For each depot, set $\mathcal{K}_d$ of vehicles is available
Variables	
x_{ijk}	Binary variable; 1 when a vehicle k traverses arc $(i, j) \in \mathcal{E}$, 0 otherwise
τ_{ik}	Integer time variables specifying the arrival of vehicle k at vertex i
Parameters	
d_i	Demand at vertex $i \in \mathcal{V}$ representing the number of orders to be delivered at that vertex
w_i	A nonnegative waiting time w_i at vertex $i \in \mathcal{V}$
$[e_i, l_i]$	Delivery time window for vertex $i \in \mathcal{V}$ where e_i is an earliest start time and l_i is a latest start time for the delivery
t_{ij}	The travel time for arc $(i, j) \in \mathcal{E}$ representing the traversal cost
T	Total time available for delivery
q	The number of equally sized (with size r in minutes), non-overlapping, time windows available for delivery given as $q = \frac{T}{r}$
P	capacity of delivery vehicles in terms of number of orders

- The total demand (number of orders) served by each vehicle route is bounded by the vehicle capacity P while the total route duration (the sum of travel time and wait time) must not exceed maximum route length T.
- Orders must be delivered during the delivery time window $[e_i, l_i]$ for each delivery vertex. If a vehicle arrives at a vertex i earlier than time e_i, it must wait.
- The objective is to minimize the total cost of delivery.

The mathematical formulation for MDCVRP-TW can be defined using two types of decision variables: binary decision variables related to flow, notated as $x_{ijk}, (i,j) \in \mathcal{E}, k \in \mathcal{K}$, equal to 1 if the pair of vertices i and j are in the route of vehicle k, and 0 otherwise; and time variables $\tau_{ik}, i \in \mathcal{V}, k \in \mathcal{K}$, specifying the arrival of vehicle k at vertex i.

The formulation for MDCVRP-TW is given as follows:

(MDCVRP-TW)

$$\min \sum_{\substack{k\in\mathcal{K}\\(i,j)\in\mathcal{E}}} t_{ij}x_{ijk}, \tag{3.8}$$

$$\text{s.t.} \sum_{k\in\mathcal{K}} \sum_{j\in\delta^+(d)} x_{djk} \le |\mathcal{K}_d|, \qquad \forall d \in \mathcal{V}_d, \tag{3.9}$$

$$\sum_{k\in\mathcal{K}} \sum_{j\in\delta^+(i)} x_{ijk} = 1, \qquad \forall i \in \mathcal{V}_c \tag{3.10}$$

$$\sum_{d\in\mathcal{V}_d} \sum_{j\in\delta^+(d)} x_{djk} \le 1, \qquad \forall k \in \mathcal{K} \tag{3.11}$$

$$\sum_{d\in\mathcal{V}_d} \sum_{i\in\delta^-(d)} x_{idk} \le 1, \qquad \forall k \in \mathcal{K} \tag{3.12}$$

$$\sum_{i\in\delta^-(j)} x_{ijk} - \sum_{i\in\delta^+(j)} x_{jik} = 0, \qquad \forall k \in \mathcal{K}, \forall j \in \mathcal{V} \tag{3.13}$$

$$x_{ijk}\left(\tau_{ik} + w_i + t_{ij} - \tau_{jk}\right) \le 0, \qquad \forall k \in \mathcal{K}, \forall\, (i,j) \in \mathcal{E} \tag{3.14}$$

$$e_i \left(\sum_{j\in\delta^+(i)} x_{ijk} \right) \le \tau_{ik} \le l_i \left(\sum_{j\in\delta^+(i)} x_{ijk} \right), \qquad \forall k \in \mathcal{K}, \forall i \in \mathcal{V}_c \tag{3.15}$$

$$E_d \leq \tau_{ik} \leq L_d, \qquad \forall k \in \mathcal{K}, \forall d \in \mathcal{V}_d \tag{3.16}$$

$$\sum_{i \in \mathcal{V}_c} d_i \sum_{j \in \delta^+(i)} x_{ijk} \leq P, \qquad \forall k \in \mathcal{K} \tag{3.17}$$

$$\sum_{i \in \mathcal{V}_c} x_{idk} \left(\tau_{ik} + w_i + t_{id}\right) - \sum_{i \in \mathcal{V}_c} x_{dik} \left(\tau_{ik} - t_{id}\right) \leq T, \qquad \forall k \in \mathcal{K}, d \in \mathcal{V}_d \tag{3.18}$$

$$x_{ijk} \geq 0, \qquad \forall k \in \mathcal{K}, \forall \left(i,j\right) \in \mathcal{E} \tag{3.19}$$

$$x_{ijk} \in \{0,1\}, \qquad \forall k \in \mathcal{K}, \forall \left(i,j\right) \in \mathcal{E}. \tag{3.20}$$

MDCVRP-TW (3.8)–(3.20) is then to determine a minimal cost set of routes required to complete all deliveries while fulfilling constraints related to capacity, total time and delivery time windows. All routes must originate at one of the depots, and end at the same depot. Constraint (3.9) ensures that the number of vehicle routes originating at a depot is not more than total number of vehicles available at the depot. Constraint (3.10) ensures that each delivery vertex must be visited exactly once by exactly one vehicle. Constraints (3.11)–(3.12) represent that each vehicle route used in the model must start from a depot, and end at a depot, respectively. Constraint (3.13) is flow conservation constraint. Constraint (3.14) updates the arrival time of a vehicle at a vertex j when it visits arc (i, j). Additionally, constraints (3.15)–(3.18) guarantee schedule feasibility with respect to time windows, capacity and total route time aspects, respectively. Note that for a given k, constraints (3.15) force $\tau_{ik} = 0$ whenever vertex i is not visited by vehicle k. Constraints (3.19) denote the range of flow decision variable.

A small example of the aforementioned routing problem is shown in Figure 3.2. The problem determines the optimal routes for delivery of all orders while satisfying the delivery time windows. The optimal origin depot for all orders is also determined. The number of available vehicles (or routes) is assumed to be unlimited.

To evaluate the benefits of consolidation in store delivery, we compare the routing costs of the two scenarios by running the vehicle routing problem twice: once for store deliveries and once for direct to customer deliveries. In the former instance of the problem,

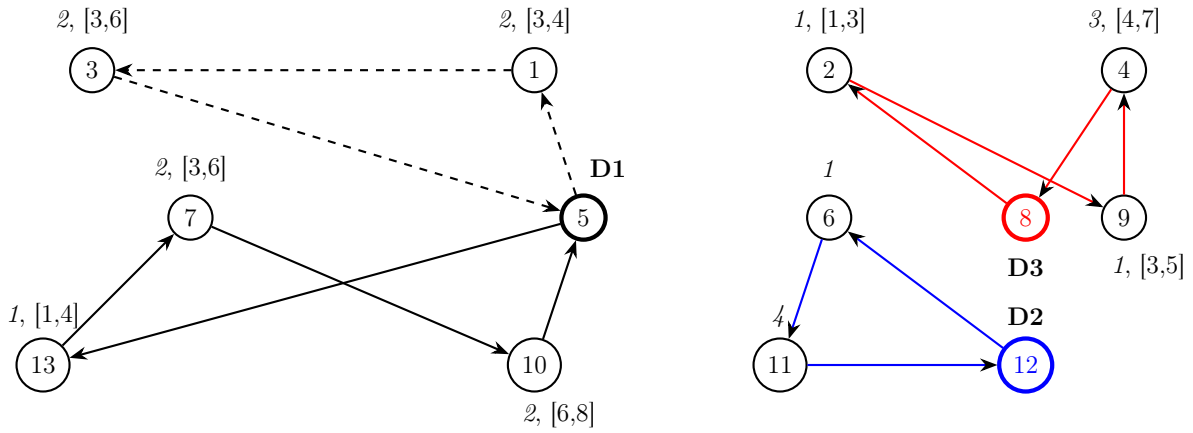

Figure 3.2 – A small example of a multi-depot capacitated vehicle routing problem with time windows (MDCVRP-TW)

$\mathcal{V} = \bar{\mathcal{S}}$ while for the latter case, $\mathcal{V} = \mathcal{O}$. For store deliveries, the set cover problem furnishes the demand at each vertex while for direct-to-home delivery, we assume unit demand. Total available time, length and number of time windows, and vehicle capacity are varied as model parameters in our experiments.

All the experiments were done on a machine with 3.6 GHz CPU clock speed, 16 GB RAM and 64-bit Windows 8 operating system. To solve the set cover problem, we used Python API of CPLEX 12.9.0. The routing problem for our model can involve multiple depots, hundreds of customers, time windows and scores of vehicles. Therefore, to solve MDCVRP-TW instances, we use vehicle routing library of Google OR-Tools 7.5 which is Google's software suite for combinatorial optimization (Perron and Furnon, 2019). The library provides good solutions fast using a combination of metaheuristics. We use default routing search parameters for our model which lets the software choose among many metaheuristics based on guided local search, simulated annealing and tabu search. The total time limit for solving all instances of the problem is set at 1200 seconds.

3.4 Numerical Experiments and Case Studies

We conduct extensive numerical analysis to gain crucial insights about the consolidated delivery proposal analyzed in this chapter. To account for different urban form, we build three separate case studies with data from three counties with varied population densities. For all three counties, the data about food desert tracts, grocery depots, convenience stores and customers is collected from various governmental and non-governmental sources. For each county, we create eight separate instances to evaluate the sensitivity of our model to densities of depot locations, store locations and the number of customers (orders). All the data instances are run with different values of model parameters for total delivery time T, delivery vehicle capacity P, walkable distance ω and the number of customer time windows q_c.

3.4.1 Data Collection

We limit the scope of our case study to three counties of varying population densities and sizes. We collect data for Hillsborough County in Florida, Hudson County in New Jersey and Henderson County in North Carolina. Hudson County and Henderson County have predominantly urban and rural characteristics, respectively, while Hillsborough has mixed urban rural characteristics.

We collect the data from four major sources. The Food Access Research Atlas Data by Economic Research Service at US Department of Agriculture (USDA, 2019) consists of various measures of food access at census tract level for the United States. For Hillsborough County in Florida, we use the USDA definition of 1 mile from the nearest grocery store for urban areas and 10 miles for rural areas. For Hudson and Henderson counties, we use a relatively liberal definition with distance measures of 0.5 miles for urban areas and 10 miles for rural areas to get enough number of representive food insecure tracts. Hillsborough County, for instance, has 43 food insecure census tracts out of a total of 320 tracts.

The second source of data is related to the cartographic boundary lines for various census tracts in our study areas. We use the 2015 TIGER data accessed from United States Census Bureau (Bureau, 2015) to get shapefiles for statewide census tracts. We then trim the data to our areas of study for respective counties.

The third source of data include the locations of depots, convenience stores, and potential customers. We consider Walmart and other large locations providing grocery delivery services. For instance, for Hillsborough County, 7 Walmart locations provide home delivery service (Walmart, 2020). In case no Walmart locations offer delivery in a county, we select locations which offer their own delivery services or Instacart delivery. The model chooses the optimal depot location for each order.

In order to identify the locations of convenience stores, we use SNAP retailer database (USDA, 2020). For instance, Hillsborough County has 1076 retailers in the database. Since we envisage business partnership involving deliverers and convenience stores, and also require refrigerated storage, independently owned convenience stores and chains with less than 3 stores are not considered in the current analysis. For Hillsborough County, for instance, we limit our selection to 13 largest chains of pharmacies, dollar stores and gas stations (stores). This reduces the number of stores to 442. Finally, only stores within 1 mile distance of a 'food desert' census tract are included in the analysis. We consider 217 convenience stores within 1-mile distance of a food desert in Hillsborough County. Stores are assumed to have refrigerated space for carrying groceries. There is no capacity limit for stores. The key data features for the three counties are given in Table 3.3. Figure 3.3 shows the census tracts designated as food deserts, the grocery depots (red) and the neighborhood store locations (green) considered for consolidation for the three counties.

The customers within the food insecure census tracts are created at random locations on the road network. The number of customers in each tract is proportional to the number of households without access to vehicles. We choose 30% of the number of such households as our potential customers. For food desert census tracts in Hillsborough County for instance,

Table 3.3 – Salient Data Features for Hillsborough, Hudson and Henderson Counties

County	Pop. Density (per sq. mi.)	# of Census Tracts	Food Desert Tracts	# of Delivery Points	# of Chain Stores	# of Total Customers
Hillsborough	702	320	43	7	217	1,619
Hudson	14,973	166	17	7	70	1,758
Henderson	286	27	6	5	48	372

(a) Hillsborough, Florida (b) Hudson, New Jersey (c) Henderson, North Carolina

Figure 3.3 – Food desert tracts, depot locations and neighborhood stores for Hillsborough, Hudson and Henderson counties

the number of 'potential' customers is 1619. The travel distances between road networks between points of interest including depots, stores, and customers are obtained using ArcGIS. The experimental setup consists of various instance sizes for each county. To understand the sensitivity of our model to the number of depot locations, number of convenience stores and number of customer orders, we vary these parameters to create different instances for all three case studies.

Customer orders are supposed to arrive at the beginning of the time horizon and the number of customer orders per planning period is varied as a model parameter. The total time limit for making deliveries is set to 4 hours (240 minutes) or 8 hours (480 minutes). The delivery time windows for customers and stores are also a model parameter. The time windows are evenly sized, e.g., if the total time $T = 240$, and $r = 40$ minutes, then q

Table 3.4 – Eight Instances with Different Densities for Depot Locations, Stores, and Customers for the Three Case Studies

	Hillsborough			Hudson			Henderson		
Instance	$\|\mathcal{V}_d\|$	$\|\mathcal{Q}\|$	$\|\mathcal{C}\|$	$\|\mathcal{V}_d\|$	$\|\mathcal{Q}\|$	$\|\mathcal{C}\|$	$\|\mathcal{V}_d\|$	$\|\mathcal{Q}\|$	$\|\mathcal{C}\|$
Instance 1	1	108	801	5	39	823	2	5	170
Instance 2	1	108	1619	5	39	1758	2	5	372
Instance 3	1	217	801	5	70	823	2	5	170
Instance 4	1	217	1619	5	70	1758	2	5	372
Instance 5	7	108	801	10	39	823	5	5	170
Instance 6	7	108	1619	10	39	1758	5	5	372
Instance 7	7	217	801	10	70	823	5	5	170
Instance 8	7	217	1619	10	70	1758	5	5	372

= 4 time windows of equal size are created. Customer orders are randomly assigned the delivery time window. Since time windows impact the total delivery time, this randomness translates into slightly different values of total travel time for every run of the instances. However, the difference does not considerably alter the fundamental insights of the model. For customers, we consider the following time windows sizes: 40 minutes, 80 minutes, 120 minutes, 240 minutes, and 480 minutes (only when $T = 480$ minutes). For stores, we consider the following time window size: 120 minutes (only when $T = 240$ minutes), 240 minutes and 480 minutes (only when $T = 480$ minutes). The capacity of delivery vehicles is measured in number of orders which can be delivered in a single run. We test the sensitivity of our model with capacity parameter of 5, 10, and 20 orders. Table 3.5 gives the details of experimental analysis and parameters for all three case studies.

3.5 Experimental Results

Some important managerial insights for delivery services will derive from measuring the extent of spatial and temporal consolidation (representing the delivery costs) and the percentage of accepted orders (representing the service level), under various operational circumstances. A delivery service may be interested in evaluating how different time window

Table 3.5 – Experimental Setup for the Study Involving Instances of Various Sizes and Sensitivity Analysis for Number and Size of Time Windows and other Parameters

Instances	County	Hillsborough, Hudson, Henderson
	# of Depots	{1,7}, {5,10}, {2, 5}
	# of Store Chains	{6,13}, {6,13}, {4, 8}
	Order Proportion	0.5, 1
Time Windows (TW)	Total Time	240 min, 480 min
	# of TWs (customers)	{6, 3, 2, 1}, {12, 6, 3, 2, 1}
	Size of TWs (customers)	{40, 80, 120, 240} , {40, 80, 120, 240, 480}
	# of TWs (stores)	{2, 1} , {2,1}
	Size of TWs (stores)	{120, 240} , {240, 480}
Parameters	Walkable Distance	600 m, 1,000 m
	Vehicle Capacity	5, 10, 20

sizes r, representing relatively strict or loose attended home delivery requirements, may impact the temporal consolidation. This may help determine the circumstances under which is it worthwhile to use neighborhood convenience stores for consolidated delivery. The extent of spatial consolidation is also impacted by various factors. The capacity of the delivery vehicle P may allow for in-vehicle pooling whereby using larger vehicles may reduce the delivery costs. The total number of stores a deliverer partners with, denoted as $\mathcal{Q}$, can also be an important determinant of percentage of accepted orders and the extent of spatial consolidation. Similarly, the walkable distance parameter ω can impact the percentage of accepted orders and also the number of convenience stores available for delivery.

In this section, we study the relationship between the total cost of delivery and all the aforementioned parameters of our model. Specifically, using our computational methods and the data from three counties representing different urban forms, we conduct an extensive numerical experiment by calculating the total delivery cost for a large number of instances for each county. We find that the biggest impact on delivery costs is due to time window requirements of attended home delivery. Besides the time windows, the vehicle capacity P, walkable distance parameter ω and, and number of partner convenience stores are important

determining factors for the extent of spatial consolidation achieved and the service level provided.

A template of results for a single instance of the model for Hudson County is provided in Table 3.6. For this instance, the number of orders served in a day is 1324. When served through the convenience stores, 57 store locations are utilized while 76 visits are made to the stores. Vehicle capacity is assumed to be 20 orders per trip. The table clearly shows the impact of spatial and temporal consolidation for the instance. If customer delivery time windows are narrow, and there are no time windows for store delivery, maximum improvement of more than 1,800% can be achieved through a combination of spatial and temporal consolidation. On the other hand, only spatial consolidation achieves an improvement of 234% for total delivery time. These results underscore the importance of convenience stores as points of temporal consolidation since store-delivery removes the time window constraints imposed by attended home delivery.

3.5.1 Sensitivity to Number and Size of Time Windows

A major issue with attended home delivery for groceries is relatively strict time windows. Due to threat of pilferage, and refrigeration requirements for fresh produce, customers do not prefer groceries to be left out in the open unattended. Therefore, the deliverers must adhere to strict time windows when making deliveries. We vary the parameter T representing the total time for delivery between 240 minutes (4 hours) and 480 minutes (8 hours). For each of these values, the number and size of time windows, denoted by q and r, respectively, are varied as a model parameter as given in Table 3.5. Since the experiments involve three separate case studies, and also eight instances for each case study, the total number of accepted (delivered) orders is different for all instances. Therefore, we calculate delivery time per order to normalize the total delivery time across instances.

Figure 3.4 gives the results for all three counties when $T = 240$ minutes and only one time window is considered for store delivery, i.e., $q_s = 1$. The thick black vertical

Table 3.6 – Experimental Results for a Single Instance (Instance 8) of the Problem for Hudson County when ω = 1,000 Meters. For this Instance, $|\mathcal{O}|$ = 1,324, $|\mathcal{N}_S|$ = 76, and P = 20

Total Time	(# of TWs, TW size) (customer)	(# of TWs, TW size) (store)	Delivery Time (customers)	Delivery Time (stores)	Percentage Improvement
240 min	(6, 40)	(1, 240)	7,035	500	1,307 %
	(6, 40)	(2, 120)	7,577	899	743 %
	(3, 80)	(1, 240)	6,343	500	1,168 %
	(3, 80)	(2, 120)	6,616	999	562 %
	(2, 120)	(1, 240)	4,859	500	872 %
	(2, 120)	(2, 120)	5,451	902	504 %
	(1, 240)	(1, 240)	1,670	500	234 %
	(1, 240)	(2, 120)	1,670	860	94 %
480 min	(12, 40)	(1, 480)	9,777	500	1,855 %
	(12, 40)	(2, 240)	9,577	881	987 %
	(6, 80)	(1, 480)	8,461	500	1,592 %
	(6, 80)	(2, 240)	7,512	959	683 %
	(4, 120)	(1, 480)	7,530	500	1,406 %
	(4, 120)	(2, 240)	7,866	799	884 %
	(2, 240)	(1, 480)	6,667	500	1,233 %
	(2, 240)	(2, 240)	6,782	940	621 %
	(1, 480)	(1, 480)	1,670	500	234 %
	(1, 480)	(2, 240)	1,670	861	94 %

lines separate the results for different P values representing vehicle capacity while green vertical lines separate the results for different number of customer time windows q_c. As the number of time windows increases, so does the difference between delivery costs for attended home delivery (blue) and store delivery (red) across all instances. When there is only one time window for customer delivery, i.e., $q_c = 1$, the difference in delivery costs is relatively insubstantial as shown in Table 3.7. This represents the situation when only spatial consolidation can be achieved.

When considering only spatial consolidation, the average improvement across all instances and vehicle capacity values for Hillsborough County is 24 %. For Hudson and Henderson counties the average improvement is 116% and 100 %, respectively. While the

Table 3.7 – The Percentage Difference between Delivery Costs for Store Delivery and Home Delivery for Different Values of Number of Customer Time Windows and Vehicle Capacity for the Three Case Studies when $T = 240$ and $q_s = 1$. The Percentage Difference is Averaged across the Eight Instances.

	P (Hillsborough)			P (Hudson)			P (Henderson)		
# of TWs (q_c)	5	10	20	5	10	20	5	10	20
1	12 %	23 %	37 %	48 %	104 %	198 %	66 %	92 %	142 %
2	112 %	179 %	210 %	269 %	587 %	855 %	511 %	657 %	825 %
3	122 %	207 %	288 %	336 %	627 %	976 %	539 %	819 %	1,073 %
6	153 %	272 %	382 %	428 %	829 %	1,291 %	722 %	1,023 %	1,377 %
Aggregate	100 %	170 %	229 %	270 %	536 %	830 %	460%	648 %	854 %

improvement is substantial, these averages are not commensurate with the number of vertices visited for store and home deliveries. For Hudson, the average number of vertices visited is 7 times less for store delivery compared to home delivery. Similarly for Hillsborough and Henderson counties, despite lesser number of vertices being visited, 4 times less on average, the delivery costs for store delivery do not improve proportional to the decrease in number of vertices visited. This is primarily due to stores being farther away from each other compared to homes. Besides, due to capacity limitations, the number of vehicle visits (trips) to deliver accepted orders is the same for both types of delivery.

3.5.2 Sensitivity to Vehicle Capacity

We also see that vehicle capacity plays an important role in determining the extent of consolidation. As shown in Figure 3.4, delivery costs per order decrease as vehicle capacity increases for both store and home delivery. When only spatial consolidation is considered, i.e, $q_s = q_c = 1$, increasing vehicle capacity brings substantial improvement to delivery costs. For Hudson County, on average, the costs for store delivery across instances, are 198% less than home delivery when $P = 20$ while the difference is only 48 % when $P = 5$. For Henderson, the numbers are 142 % versus 66 %, while for Hillsborough they are 37 % versus 12 %,

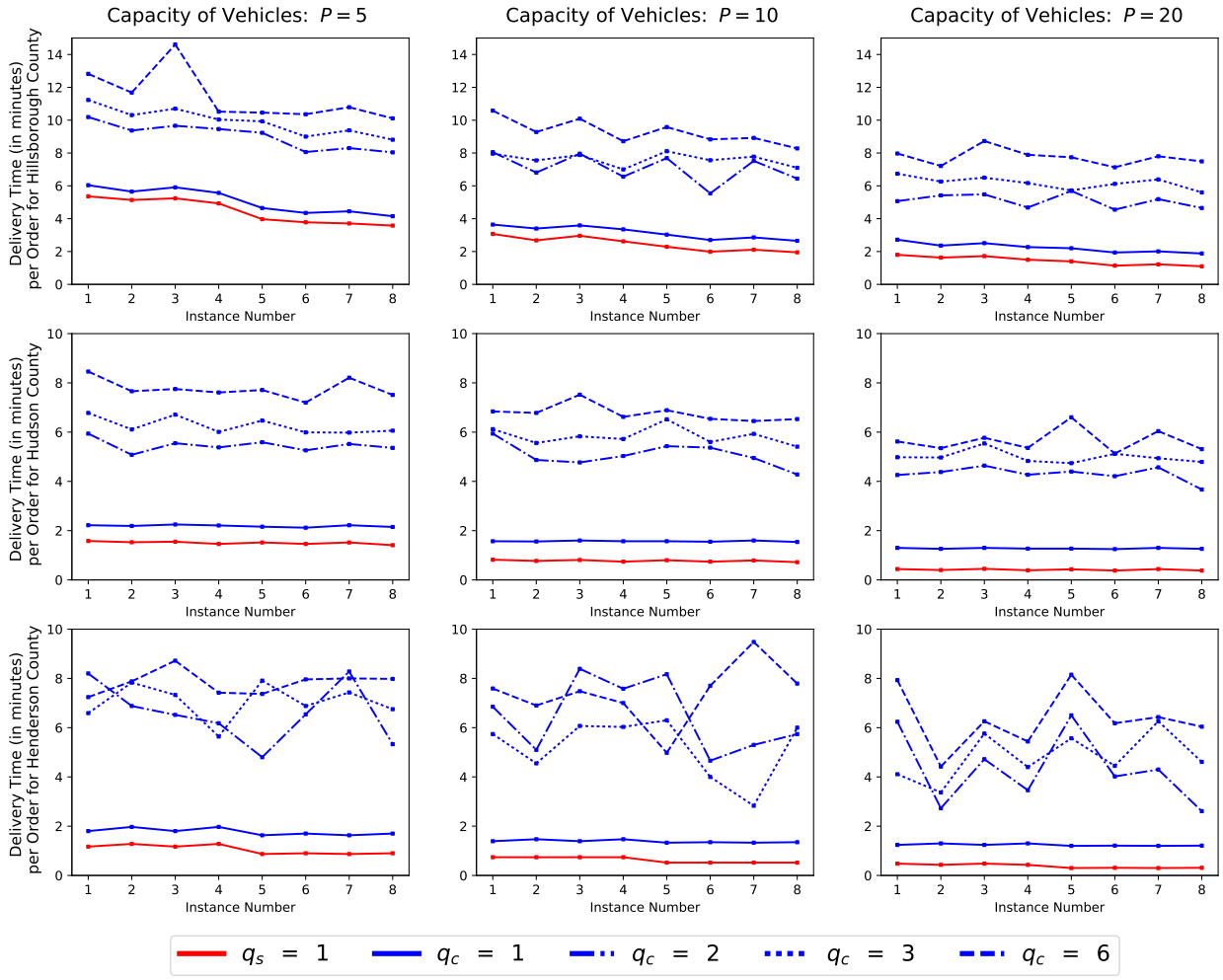

Figure 3.4 – Comparison of travel time per order for customers (blue) and stores (red) as a function of vehicle capacity and number of customer time windows (q_c) when $\omega = 1{,}000$ m, $T = 240$ mins, and $q_s = 1$

respectively, as shown in Table 3.7. Even for cases with temporal consolidation, i.e., when $q_s = 1$ and $q_c > 1$, larger vehicle capacity substantially improves the extent of consolidation and the total delivery costs for all three counties as evidenced by aggregate improvement values in Table 3.7.

3.5.3 Sensitivity to Walkable Distance and Urban Form

In addition to the cost of delivery, another important factor to consider for last mile consolidation is the service level the deliverer can provide to the customers. We define the

ratio of accepted orders $|\mathcal{O}|$ and total customers $|\mathcal{C}|$, i.e., $|\mathcal{O}|/|\mathcal{C}|$ as the service level. Since we envisage last mile consolidation of grocery deliveries at neighborhood convenience stores, the number of stores available for delivery, denoted by $|\mathcal{R}|$, is an important determinant of number of accepted orders $|\mathcal{O}|$. In turn, the number of walkable stores $|\mathcal{R}|$, depends on total number of stores $|\mathcal{Q}|$ and the walkable distance parameter ω. As shown in Figure 3.5, the service level improves significantly when ω is increased to 1000 meters (orange) from 600 meters (blue).

Another important factor is the urban form and built environment of the delivery neighborhood. Rural areas where customers and convenience stores are spread out may not provide sufficient service level if only chain stores are considered for consolidation. As can be seen in Figure 3.5, the service level for Henderson County is substantially lower than the other two case studies considered. This is because there are lesser number of possible convenience stores available for partnering and they are farther than walkable distance from most customers. In such cases, it is better to consider home delivery, and despite the cost advantages accrued due to store delivery, it may not be worthwhile due to very low service levels. Even for urban counties of Hillsborough and Hudson, the service level is lower than 50 % when $\omega = 600$ meters. Service level for Hudson County, the most urban of the three case studies considered, has the highest value across instances. This is despite the relatively lower number of available stores $|\mathcal{Q}|$ for Hudson County compared with Hillsborough County.

In this section, the service level is calculated considering all food desert neighborhoods in a county. However, not all food insecure neighborhoods have the same level of access to neighborhood convenience stores. For instance, as can be seen for Hillsborough County in Figure 3.3, the food desert tracts in the Southern (lower) and Western (right) half of the county have a relatively lower access to convenience stores. Similarly, for Hudson County, a large food insecure tract at the Western end, which is an industrial area, does not have any neighborhood convenience stores available. In such cases, it may be worthwhile for deliverer to evaluate the service level on tract by tract basis and serve the neighborhoods where most

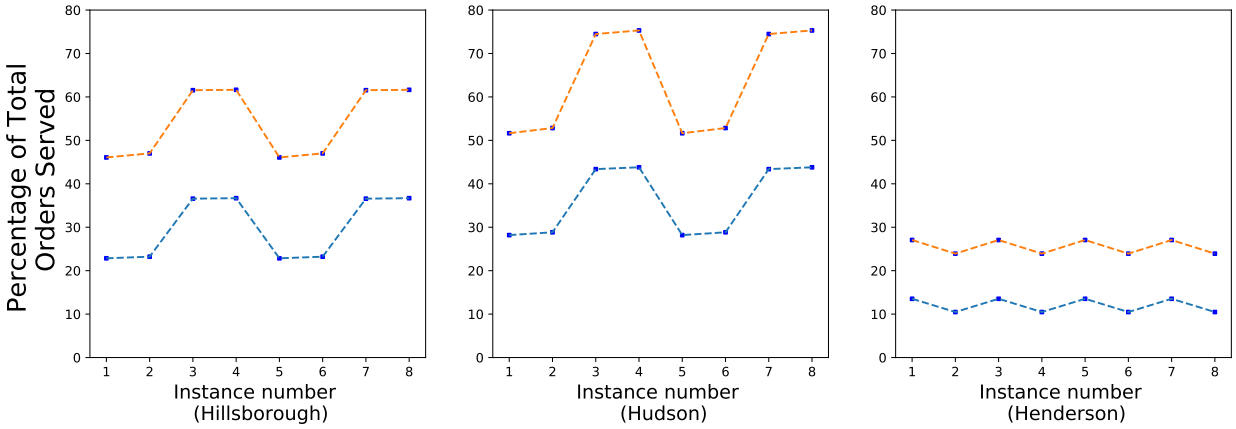

Figure 3.5 – Percentage of orders accepted for the three case studies when walkable distance (ω) = 1000 m (orange) and 600 m (blue)

orders can be delivered to consolidated locations within a walkable distance. Attended home delivery can still be an option for tracts and neighborhoods without any convenience stores.

3.5.4 Sensitivity to Number of Depot Locations, Number of Stores, and Number of Orders

The eight instances considered in our experiments for each of the three case studies signify different densities for depot locations, number of stores and the number of total customers as shown in Table 3.4. Having a larger number of depots (red bars) improves the delivery costs per order as shown in 3.6. The improvement is especially significant for Hillsborough and Henderson counties. This is expected since Hillsborough county is the largest in area while Henderson county is most rural. Having lesser number of depots increases the length of first and last legs of vehicle routes, therefore increasing the overall delivery costs.

We also evaluate the sensitivity of our model to the density of partner convenience stores by varying the number of store chains considered in our model as shown in Table 3.5. We find that although the number of partner stores significantly impacts the service level and the orders served (see Figure 3.5, instances 3, 4, 7, 8), it does not significantly improve the cost of delivery per order as can be seen in Figure 3.7. In this study, we only consider store chains in our analysis. For rural and less dense urban neighborhoods, partnerships

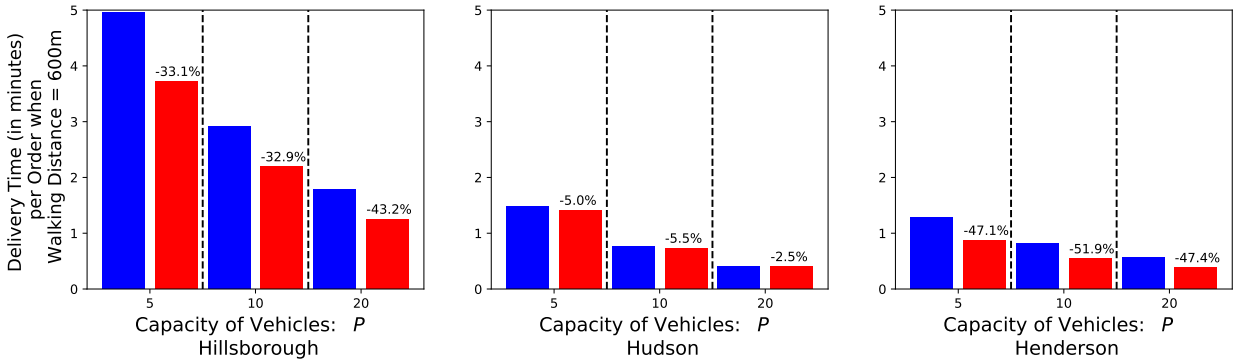

Figure 3.6 – Comparison of travel time per order for stores when the number of depots is less (blue) and more (red) for the three case studies

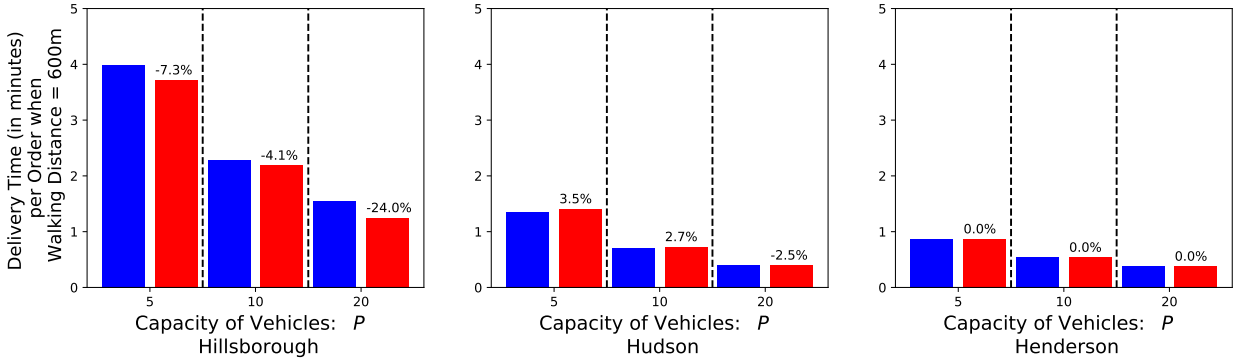

Figure 3.7 – Comparison of travel time per order for stores when store density = 0.5 (blue) and when store density = 1 (red) for the three case studies

with family owned corner stores can also be a viable option to increase the service level of store delivery.

Finally, we also alter customer density as a model parameter. It is of interest to deliverers to achieve scale in the delivery operations by having a larger customer base. Figure 3.8 shows the improvement in delivery cost per order when larger number of total customers $|\mathcal{Q}|$ or orders is available. This essentially signifies the scaling up of delivery operations. The results for all three case studies suggest a larger improvement in per unit delivery costs when vehicles of large capacity, $P = 20$, are utilized. This suggests that not only do large vehicles improve delivery costs significantly, the benefits of in-vehicle pooling especially accrue when larger number of orders are to be delivered.

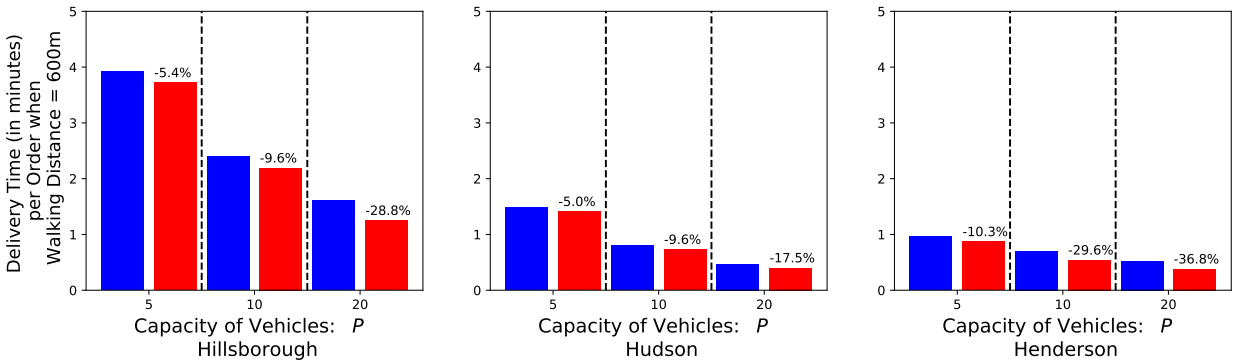

Figure 3.8 – Comparison of travel time per order for stores when customer density = 0.5 (blue) and when customer density = 1 (red) for the three case studies

Chapter 4: A Robust Optimization Approach for Solving Problems in Conservation Planning[3]

4.1 Introduction

Conservation Planning concerns itself with the issues related to maintaining and increasing biodiversity. Preserving biodiversity is crucial to human societies and the future of planet Earth. Hence its slow erosion constitutes a threat as consequential as that posed by the climate change (Billionnet, 2013). According the International Union for Conservation of Nature (2017), about 24,000 species out of the 91,000 listed are threatened with extinction. Two of the key issues, among others, resulting in the loss of biodiversity, as identified by the Convention on Biological Diversity (CBD), are land fragmentation and invasive predators. The alteration and loss of the habitats for many species is caused by rampant deforestation, overpopulation, agriculture and other economically beneficial land use alternatives (Polasky et al., 2008).

There is an abundant body of knowledge prescribing the creation of land reserves, geographic regions designated for the preservation of biodiversity, as a way to slow the process of habitat destruction and to protect threatened species from the processes that threaten their existence (Rodrigues et al., 2004). Due to limited monetary and land resources available for conservation and the difficulty of reversing land use decisions in the long term, it is imperative that the reserve selection decision to be based on sound scientific evidence. There is a long history of using optimization methods for reserve selection in assistance to the process of reserve selection (Haight et al., 2000; Polasky et al., 2000; Cabeza and Moilanen, 2001;

[3]This chapter was published in Ecological Modelling. Haider, Z., Charkhgard, H., & Kwon, C. (2018). A robust optimization approach for solving problems in conservation planning. *Ecological modelling*. https://doi.org/10.1016/j.ecolmodel.2017.12.006. Permission is included in Appendix A.

ReVelle et al., 2002; Arthur et al., 2002; Costello and Polasky, 2004). More recently there has been a growing interest in solving problems of reserve design, i.e., reserve selection with constraints on size, shape, connectivity, compactness and species complementarity (Jafari et al., 2017; Beyer et al., 2016; Haight and Snyder, 2009; Williams et al., 2005; Margules and Pressey, 2000). A brief review of the reserve selection literature and the issues therein is presented in Section 4.3.

Another major threat to biodiversity and other ecosystem services is the introduction of invasive species (Pejchar and Mooney, 2009). For example, Doherty et al. (2016) estimated that the invasions of mammalian species such as feral cats, rodents and pigs were responsible for massive extinctions (738 vertebrate species) and may have contributed to 58% of the cases of contemporary extinctions of birds, mammals and reptiles. Once established, it is very difficult and costly to fully eliminate an invasive species. Many mathematical optimization formulations have been presented to manage and control the spread of invasive species. We present a brief review of these formulations in Section 4.3.

Conservation planning also encompasses other problems besides the two we have mentioned above. Other authors have discussed the use of mathematical optimization to solve a variety of conservation problems (Billionnet, 2013). However, one crucial aspect that has not been sufficiently considered is the issue of noisy information, for example due to imperfect detection of species during surveys(Williams et al., 2005). In their seminal work on systematic conservation planning, Margules and Pressey (2000) point out that conservation planning is riddled with uncertainty. Uncertainty pervades the use of biodiversity surrogates, the setting of conservation targets, decisions about which kinds of land tenure can be expected to contribute to targets and for which features, and decisions about how best to locate, design, implement and manage new conservation areas in the face of limited resources, competition for other uses, and incursions from surrounding areas. New developments in all the planning stages will progressively reduce, but never eliminate, these uncertainties. They

recommend that planners, rather than proceeding as if certain, must learn to deal explicitly with uncertainty in ways that minimize the chances of serious mistakes.

Many problems in conservation planning require information about state variables (e.g., species abundance, occupancy), rates that pertain to the dynamic of ecological systems (e.g., population growth rate, movement rate), or conservation value of land parcels among other variables (Williams et al., 2005). Ignoring these potential sources of uncertainties may lead to bad decisions. Many studies have addressed these uncertainties with probabilistic and stochastic approaches. These approaches, although a big step up on the deterministic models, do not handle the uncertainty sufficiently. This is due to the fact that there are always certain inhibiting assumptions regarding the nature of the uncertainty in these methods. More precisely, due to sparsity of the data available, it is overly optimistic to try and over fit this data into certain probability distributions.

To deal with the issue of uncertainty and the lack of sufficient probabilistic information, there has long been a discussion of using robust optimization (see, for instance, Beyer et al. 2016). But we were not able to find any study that exploits this technique. In this chapter, we propose to use robust optimization for conservation planning and optimal control of invasive species.

Since robust optimization (Bertsimas and Sim, 2004; Ben-Tal et al., 2009) accounts for the worst case scenarios, it ensures that the problem is tractable and near optimal in the face of large uncertainty. When using the robust approach, the decision maker will know the quantum of parametric uncertainty they are protected against when they deploy the decisions and policies recommended by the robust counterpart of a formulation. In this chapter, we also show another crucial value of the robust optimization. For some conservation problems, if the uncertainty is very large it may be infeasible to find a solution that meets a budget constraint. A crucial question then arises; if we are unable to address all the uncertainty using the current resources, where can we best expend these resources for improving our data gathering efforts in order to reduce the quantum of uncertainty as much as possible.

We have developed a bi-objective optimization approach that addresses this question. Our approach gives managers the possibility to visualize how much uncertainty can be addressed for a given budget and provides a prescriptive set of recommendations about where to focus their data gathering efforts. As we show in Section 4.5, this knowledge can have profound policy implications. We come up with a novel bi-objective optimization formulation to model this approach and develop it further.

This chapter is organized as follows: In Section 4.2, we describe the robust optimization approach that we have used. In Section 4.3, we review existing basic optimization formulations developed for two fundamental problems in conservation planning. In Sections 4.4 and 4.5, we introduce a robust optimization approach for the invasive control problem and the reserve selection problem, respectively, and present some numerical experiments.

4.2 Preliminaries: Robust Optimization

Robust optimization is a principal method to address data uncertainty in mathematical programming formulations. This method has been successfully applied to solve many problems (under uncertainty) when the exact distribution for the data is unknown or difficult to determine or otherwise using stochastic optimization techniques is computationally impractical. In general, robust optimization is a conservative approach that seeks to protect the decision maker against the worst realizations of outcomes. The focus of this study is the robust optimization technique developed by Bertsimas and Sim (2004) since it allows for controlling the degree of conservatism of the solution.

Let $\boldsymbol{c}$ be an n-vector, $\boldsymbol{A}$ be an $m \times n$ matrix, and $\boldsymbol{b}$ be an m-vector. The deterministic optimization formulations in this study are in the form of mixed integer linear programs,

i.e.,

$$\min \boldsymbol{cx} \tag{4.1}$$

$$\text{s.t. } \boldsymbol{Ax} \leq \boldsymbol{b} \tag{4.2}$$

$$\boldsymbol{x} \geq \boldsymbol{0} \tag{4.3}$$

$$x_i \in \mathbb{Z} \qquad \text{for } i = 1, \ldots, n_1, \tag{4.4}$$

where $\boldsymbol{x}$ is the vector of variables containing n_1 number of integer variables, and n_2 number of continuous variables (note that $n = n_1 + n_2$). Also, all coefficients are rational, i.e., $\boldsymbol{A} \in \mathbb{Q}^{m \times n}$, $\boldsymbol{b} \in \mathbb{Q}^m$, and $\boldsymbol{c} \in \mathbb{Q}^n$. In all proposed formulations in this study, the data uncertainty affects only the elements of the matrix $\boldsymbol{A}$. To avoid any unnecessary confusion, we next explain a customized version of the robust optimization technique developed by Bertsimas and Sim (2004) that works on this specific class of optimization problems.

We do not make any assumption about the exact distribution of each entry a_{ij} of the matrix $\boldsymbol{A}$. However, it is assumed that reasonable estimates for the mean value of the coefficient $\bar{a}_{ij}$ and its range $\hat{a}_{ij}$ are available. In other words, we assume that each entry a_{ij} takes value in $[\bar{a}_{ij} - \hat{a}_{ij}, \bar{a}_{ij} + \hat{a}_{ij}]$. Note that $\hat{a}_{ij}$ can be equal to 0.

For each row $i \in \{1, \ldots, m\}$ of the matrix $\boldsymbol{A}$, we introduce a number Γ_i (defined by users) to adjust the the required level of conservatism in the proposed robust optimization formulation. This number simply imposes an upper bound on the number of entries of row i of the matrix $\boldsymbol{A}$ that can reach their worst-case values. Given that $\boldsymbol{Ax} \leq \boldsymbol{b}$ and all variables are non-negative, the worst-case value for the entry a_{ij} of the matrix $\boldsymbol{A}$ is $\bar{a}_{ij} + \hat{a}_{ij}$. So, higher the value of Γ_i, higher the degree of conservatism. The parameter Γ_i can only take values in the interval $[0, |J_i|]$ where $J_i = \{j : \hat{a}_{ij} > 0\}$. We assume that if $\Gamma_i \notin \mathbb{Z}$ then at most $\lfloor \Gamma_i \rfloor$ number of entries of row i of the matrix $\boldsymbol{A}$ can reach their worst-case values, i.e., $\bar{a}_{ij} + \hat{a}_{ij}$. One other entry r_i can reach the value of $\bar{a}_{ij} + (\Gamma_i - \lfloor \Gamma_i \rfloor)\hat{a}_{ij}$. In simpler terms, if there are one hundred entries in a row i of matrix $\boldsymbol{A}$, and the corresponding Γ_i value is 50.7, then

50 entries of row i of matrix $\boldsymbol{A}$ can reach their worst case values of $\bar{a}_{ij} + \hat{a}_{ij}$ and one other entry will reach the value of $\bar{a}_{ij} + 0.7\hat{a}_{ij}$. The robust optimization formulation that seeks to conduct the optimization against the worst-case scenario under these stated assumptions can be presented as follows:

$$\min \boldsymbol{cx} \tag{4.5}$$

$$\text{s.t.} \sum_{j=1}^{n} \bar{a}_{ij}x_j + \max_{\left\{S_i \cup \{r_i\}:\ S_i \subseteq J_i,\ |S_i| \leq \lfloor \Gamma_i \rfloor,\ r_i \in J_i \setminus S_i\right\}} \left\{ \sum_{j \in S_i} \hat{a}_{ij}x_j + (\Gamma_i - \lfloor \Gamma_i \rfloor)\hat{a}_{ir_i}x_{r_i} \right\} \leq b_i \qquad \text{for } i = 1, \ldots, m \tag{4.6}$$

$$\boldsymbol{x} \geq \boldsymbol{0} \tag{4.7}$$

$$x_i \in \mathbb{Z} \qquad \text{for } i = 1, \ldots, n_1. \tag{4.8}$$

It can be shown that this formulation has the following equivalent mixed integer linear programming formulation (Bertsimas and Sim, 2004):

$$\min \boldsymbol{cx} \tag{4.9}$$

$$\text{s.t.} \sum_{j=1}^{n} \bar{a}_{ij}x_j + z_i\Gamma_i + \sum_{j \in J_i} p_{ij} \leq b_i \qquad \text{for } i = 1, \ldots, m \tag{4.10}$$

$$z_i + p_{ij} \geq \hat{a}_{ij}x_j \qquad \text{for } i = 1, \ldots, m \text{ and } j \in J_i \tag{4.11}$$

$$p_{ij} \geq 0 \qquad \text{for } i = 1, \ldots, m \text{ and } j \in J_i \tag{4.12}$$

$$z_i \geq 0 \qquad \text{for } i = 1, \ldots, m \tag{4.13}$$

$$\boldsymbol{x} \geq \boldsymbol{0} \tag{4.14}$$

$$x_i \in \mathbb{Z} \qquad \text{for } i = 1, \ldots, n_1. \tag{4.15}$$

In this study, we call this formulation the *robust counterpart formulation.*

4.3 Optimization Models in Conservation Planning

As mentioned in the introduction, optimization methods have been used in conservation problems including reserve selection, reserve design, landscape fragmentation, forest management, control of invasive species, protection of genetic diversity and wildfire control (Billionnet, 2013). We illustrate the benefits of robust optimization methods for conservation with the two types of problems that we introduced earlier: reserve selection and control of invasive species.

4.3.1 Control of Invasive Species

Spatial and Temporal control of invasive species is an important problem in conservation planning. The simplest deterministic formulation for containing the spread of an alien invader was presented by Hof (1998). They divide the land under consideration into M identical square parcels. The invading species grows by a constant rate g every time period. Once a control action is implemented in a parcel i, the invader is supposed to be completely eliminated. There is also some diffusion or spread of the species to parcel i from parcel j. Table 4.1 shows the mathematical notation used in this basic deterministic formulation.

Table 4.1 – Mathematical Notation Used in the Basic Formulation for Invasive Species Control

Variables	
v_{it}	A non-negative variable that captures the population size of invasive species in parcel i at the beginning of time period t
x_{it}	A binary variable that is equal to 1 if parcel i is treated in time period t
Parameters	
T	The number of time periods in the planning horizon
M	The number of parcels in the land under consideration
p_{ji}	The proportion of population of parcel j that diffuses into parcel i between periods t and t+1
b_{it}	A sufficiently large value that provides an upper bound for the population of the invasive species in parcel i
g	The growth rate of the invasive species at any time period
U	The maximum number of parcels that can be treated at any time period
a_i	The initial population of invasive species in parcel i at the beginning of time period 0

The formulation presented by Hof (1998) can be represented as follows:

$$\text{(D1)} \qquad \min \quad \sum_{i=1}^{M}\sum_{t=1}^{T} v_{it} \tag{4.16}$$

$$\sum_{i=1}^{M} x_{it} \leq U \qquad \text{for } i = 1, \ldots, T \tag{4.17}$$

$$v_{i0} = a_i \qquad \text{for } i = 1, \ldots, M \tag{4.18}$$

$$v_{it} + b_{it}\sum_{t'=1}^{t} x_{ik} \geq \sum_{j=1}^{M} p_{ji}(1+g)v_{jt-1} \qquad \text{for } i = 1, \ldots, M \text{ and } t = 1, \ldots, T \tag{4.19}$$

$$v_{it} \geq 0 \qquad \text{for } i = 1, \ldots, M \text{ and } t = 1, \ldots, T \tag{4.20}$$

$$x_{it} \geq \{0, 1\} \qquad \text{for } i = 1, \ldots, M \text{ and } t = 1, \ldots, T \tag{4.21}$$

The objective function minimizes the population size of the invasive species on all parcels during a planning horizon with T time steps. Constraint (4.17) guarantees that the number of parcels treated in each time period is not greater than the imposed upper bound, i.e., U. Constraint (4.18) gives us the initial species population at each parcel at the beginning of first period. Finally, Constraint (4.19) simply captures the population size of invasive species in each parcel at the beginning of each time period. Given the previous period's population v_{jt-1} in all parcels, the growth rate g and the inter-parcel diffusion rates p_{ji}, the next period's population for a particular parcel i will be v_{it} when no control action is taken ($x_{it} = 0$). However, if a control action is taken ($x_{it} = 1$), then for a sufficiently large b_{it}, v_{it} becomes zero. We assume that b_{it} is sufficiently large, i.e., regardless of the value of $v_{jt-1}, \forall j$, we must have that $b_{it} \geq \sum_{j=1}^{M} p_{ji}(1+g)v_{jt-1}$. Therefore, the value of b_{it} can be computed recursively by using $b_{it} = \sum_{j=1}^{M} p_{ji}(1+g)b_{jt-1}$ and $b_{i0} = a_i$. In light of this observation, the objective function and constraint (4.19) together imply that $v_{it} = 0$ if parcel i is treated in or before time period t and $v_{it} = \sum_{j=1}^{M} p_{ji}(1+g)v_{jt-1}$ otherwise. Hence, implicitly, treating a parcel more than once is unnecessary in this formulation. In practice it is computationally advantageous to add the following valid inequalities to the formulation,

$$\sum_{t=1}^{T} x_{it} \leq 1 \qquad \text{for } i = 1, \ldots, M \tag{4.22}$$

Note that these valid inequalities are not part of the original formulation introduced by Hof (1998). However, we decide to use them since in practice we have observed that they can reduce the solution time by a factor of around two. Next, we briefly review some of the more advanced formulations.

The formulation we presented thus far is one of the oldest and most basic formulations. While we briefly describe some more sophisticated models here, it is important to note that robust optimization techniques presented in this chapter can be applied to any deterministic formulation in order to incorporate uncertainty. Our choice of the most basic

formulation does not imply an acceptance of all simplifying assumptions therein. Others have since come up with more realistic models of invasion control that consider a different set of assumptions on growth, diffusion and control of an invasive species. Büyüktahtakın et al. (2011, 2014, 2015) are examples of a series of more incrementally sophisticated models. As their objective, they attempt to reduce the damage to multiple resources in a single and multi objective setting. They also consider logistic growth as opposed to linear growth Hof (1998) has considered. Their formulation also considers different kill rates depending on the critical population density in a parcel, as opposed to 100% kill rate assumed by Hof (1998). In one of the models, they consider an age-structured approach to take into account the biological dynamics of the population. According to the authors, the large size of the dynamic problem and the nonlinearity make the application of direct optimization methods impossible. Instead, they analyze and compare the most frequently suggested strategies and their consequences.

Epanchin-Niell and Wilen (2012) present a temporally and spatially explicit formulation of the spread of invasive species. Their mixed integer linear programming (MILP) formulation considers binary decisions related to clearing of patches and controlling the spread of species across patch boundaries. They minimize the present value of the sum of control costs and invasion damages across space and time. Another simple linear programming based approach to invasion control is proposed by Hastings et al. (2006). They consider a linear, age or stage structured population of the invader. At different stages (age), the invader has different growth, survival rates, and fecundity.

The issue of uncertainty has also been considered in many recent studies. In summary, the formulations with uncertainty fall into two categories: Models that consider stochasticity in some parameters and formulations that consider lack of information about some parameters. The point of introduction, growth, diffusion, response to control and the harmful impacts of an invasion can all be stochastic processes. The data on these process for a new invader can be sparse and hence it is often difficult to construct representative probabil-

ity distributions although some recent work has been done in this area (Guisan et al., 2013; Elith, 2015; Uden et al., 2015). The optimization formulations also contain parameters whose values for a particular application are simply not known and their estimation remains difficult especially before or early in an invasion. Even during the invasion, accurate detection and measurement of invasions is difficult. These multiple uncertainties are an impediment to devising optimal control policies or evaluating their impacts. The approaches that have been tried so far include stochastic dynamic programming (Kotani et al., 2011), information gap theory (Carrasco et al., 2010), learning models (Eiswerth and Van Kooten, 2007), partially observable Markov decision processes (Haight and Polasky, 2010; Rout et al., 2014) and Bayesian analysis (Cook et al., 2007). For an exhaustive review of the work that considers uncertainty in invasion control we refer the readers to the review paper by Epanchin-Niell and Hastings (2010).

4.3.2 Reserve Selection Problem

The reserve selection problem is another well studied problem in conservation planning literature. The problem consists in selecting a proportion of a given geographic area for the purposes of conserving a given species or a set of species. It is oftentimes prohibitive to earmark a very large geographic area for species conservation because of opportunity costs associated with alternative, high economic value land use. Multiple variations on the basic reserve selection problem have been presented over the years. For a more exhaustive review of the science of reserve selection, readers can refer to Williams et al. (2005); Haight and Snyder (2009); Billionnet (2013); Beyer et al. (2016).

In this chapter, we use the basic reserve selection formulation presented in Beyer et al. (2016). There is a cost associated with the selection of each reserve, and each reserve contributes to the conservation of species of interest. The optimization procedure selects parcels of land so as to minimize the cost while achieving some explicit target conservation values for each species.

Table 4.2 – Mathematical Notation Used in the Basic Formulation for Reserve Selection

Variables	
x_i	A binary variable that is equal to 1 if parcel i is selected as reserve for species conservation
Parameters	
K	The number of species under consideration
M	The number of parcels in the land under consideration
c_i	The cost of selecting parcel i as a reserve
w_{ik}	The conservation value of parcel i for species k
W_k	The target conservation value that must be achieved for species k

Table 4.2 details the mathematical notation used in the basic deterministic reserve selection formulation. We divided the land under consideration into M parcels. If the conservation targets for species $k \in \{1, \ldots, K\}$ were achieved, the parcels were assumed to be conserved.

The formulation presented by Beyer et al. (2016) can be represented as follows:

$$\text{(D2)} \qquad \min \quad \sum_{i=1}^{M} c_i x_i \tag{4.23}$$

$$\sum_{i=1}^{M} w_{ik} x_i \geq W_k \qquad \text{for } k = 1, \ldots, K \tag{4.24}$$

$$x_i \in \{0, 1\} \qquad \text{for } i = 1, \ldots, M \tag{4.25}$$

The objective function minimizes the total cost of conservation. Constraint (4.24) ensures that the target conservation value for each species is achieved. Next, we explain some fundamental features of the reserve selection problem and the existing formulations for this problem in the literature.

- In all existing formulations, the area under consideration is divided into parcels of land. One or more species can be considered for conservation. The decision of reserve

selection can be single period or a multi-period dynamic decision (Costello and Polasky, 2004; Snyder et al., 2005; Tóth et al., 2011; Strange et al., 2006).

- In the basic deterministic version of the problem, there is a cost of selecting a parcel of land. More elaborate approaches to determine cost consider sophisticated economic models to get a more complete picture of these costs (Polasky et al., 2008; Tóth et al., 2011). Besides the cost or the number of reserves, other objectives like species or genetic diversity can also be considered (Cabeza and Moilanen, 2001). Some researchers have used multiobjective optimization to handle more than one objective functions together (Memtsas, 2003; Snyder et al., 2004).

- All existing formulations contain parameters related to the target value of conservation to be achieved for each species under consideration and the contribution of each parcel to the the species' conservation. In the more basic formulations, contribution was modeled through binary parameters representing presence/absence of the species for each parcel and the target was to make sure that each species is represented in the optimal choice of parcels (ReVelle et al., 2002). Other more advanced formulations use some geographical, ecological or biological surrogates and/or some survey or sightings data alongside statistical modeling (Margules and Pressey, 2000; Austin, 2002) to come up with estimates of spatial species distribution.

- Almost all formulations consider constraints to ensure some sort of spatial arrangement of parcels. This is done to achieve connectivity, contiguity, compactness, shape, size or certain boundary or buffer zone requirements for the reserve (Williams et al., 2005; Westphal et al., 2007; Jafari and Hearne, 2013; Wang and Önal, 2015; Beyer et al., 2016).

- Many existing formulations consider uncertainty related to one or more of the parameters described above. Probabilistic reserve selection formulations assign probabilities to species presence rather than using a binary variable (for presence (1) and absence

(0)). These formulations either maximize the expected coverage (expected coverage approach) (Polasky et al., 2000) or the number of species covered, where a species is considered covered if its cumulative presence probability exceeds a predetermined threshold (threshold approach). There are no formulations, however, that consider the parametric uncertainty related to value of each parcel to each species or the cost of acquiring a parcel of land in the formulation we have presented (Haight et al., 2000; Arthur et al., 2002).

Some recent review papers, for instance Billionnet (2013) and Beyer et al. (2016), emphasize the necessity of dealing with uncertainty related to these parameters, they recommend robust optimization approaches to account for this parametric uncertainty. Despite its great potential, robust optimization has been under utilized to address problems of conservation and natural resource management.

4.4 A Robust Optimization Approach for the Invasion Control Problem

In this section, we consider the basic deterministic formulation by Hof (1998), i.e., (D1), and incorporate uncertainty in some parameters through the robust optimization approach presented in Section 4.2. More precisely, we assume that all parameters of (D1) are known with certainty except the diffusion rate p_{ji}. We assume that $p_{ji} \in [\bar{p}_{ji} - \hat{p}_{ji}, \bar{p}_{ji} + \hat{p}_{ji}]$ and $\hat{p}_{ji} > 0$, i.e., we consider a range uncertainty in diffusion rates where the size of uncertainty is determined by $\hat{p}_{ji}$.

We denote the robust counterpart formulation of (D1) with (R1). This formulation can be easily constructed using the techniques developed in Section 4.2. Interested readers can find (R1) in Appendix 6.

4.4.1 Numerical Experiments and Findings

To compare the performance of (D1) and (R1), a random instance is generated by setting $M = 40$, $T = 5$, $U = 2$ and $r = 0.05$ in this section. We randomly chose a

geographical region in central Florida and divide it into M equal parcels. The value of a_i for each $i \in \{1, \ldots, M\}$ is generated randomly from $(-25, 25)$. We set negative values to zero. The value of diffusion rate p_{ji} is considered to be inversely proportional to the square of Euclidean distance between the parcels j and i, i.e., $\bar{p}_{ji} = 1/(d_{ji})^2$. Let $\alpha, \beta \geq 0$ be two user-defined parameters, we assume that $\hat{p}_{ji} = \beta \bar{p}_{ji}$ and $\Gamma_i^t = \alpha M$. Thus α and β control the level of uncertainty to be considered by modifying the range of uncertainty or the number of uncertain parameters. It is worth mentioning that to compare (R1) and (D1), we assume that $p_{ji} = \bar{p}_{ji}$ in (D1), i.e., the half value $\hat{p}_{ji}$ is zero. Next, we conduct a set of experiments on the generated instance by choosing different values for α and β. It is recognized that the Robust counterparts of the original deterministic formulations retain the benefit of LP (Linear Programming) and MILP (Mixed Integer Linear Programming) frameworks and are known to be computationally tractable and scalable if the original problem is also tractable and scalable. However, it is important to note that any Robust MILP model is only as good as the original deterministic MILP formulation that it originated from. The deterministic invasion control problem by Hof (1998) presented here is dynamic in time and contains a large number parameter b_{it} , as a big-M in a formulation. To prevent infeasibility, the value of b_{it} needs to be iteratively determined. As a result, the original formulation is very difficult to scale and has a huge room for improvement. We have added a valid inequality in (4.22) and also defined a method of determining b_{it} values iteratively in proposition 1 to prevent infeasibility. The basic deterministic model (D1) and the Robust model (R1) take a large amount of time to solve to optimality as the size of the problem increases. In Table 4.3 we report the time it takes to solve the problem instances of different sizes for D1 and R1. All the numerical experiments were done on a machine with 3.60 GHz CPU clock speed, 16 GB RAM and 64-bit Windows 8 operating system. The models D1 and R1 were solved using the Java API of CPLEX V12.4. Optimality gap was set at 2.5%.

We first note that solving (D1) and (R1) usually results in markedly different solutions and objective values. The objective function for both formulations is the total presence of

Table 4.3 – Time Required to Solve Problem Instances of Different Sizes for D1 and R1 when $T = 5$, $r = 0.2$, $\alpha = 0.5$ and $\beta = 0.5$

Total Number of Parcels	Parcels Per Period (U)	Time for D1 (sec)	Time for R1 (sec)
10	2	0.1	0.45
20	3	1.0	63
30	4	58	1589
40	5	2929	57,605

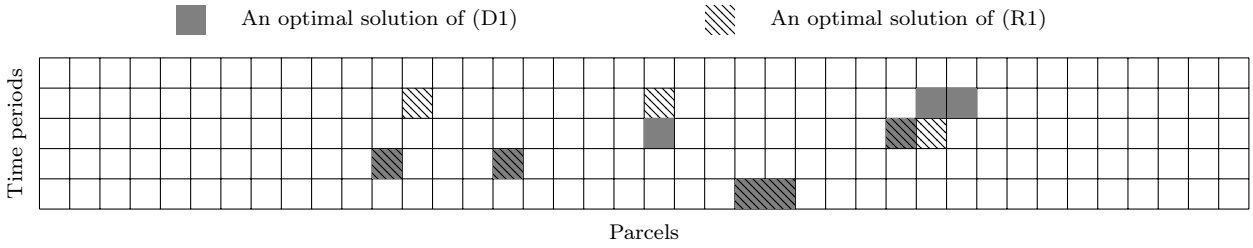

Figure 4.1 – Optimal values of x_{it} for $i = 1, \ldots, M$ and $t = 1, \ldots, T$ produced by (D1) and (R1) for an instance of invasion control problem.

the invasive species over all parcels of land and all time periods. However, the robust counterpart formulation (R1) cannot possibly achieve an objective value less than that of the deterministic formulation (D1) due to increased diffusion rates caused by considering uncertainty. Observe that the main decision variables of the problem are x_{it} for $i = 1, \ldots, M$ and $t = 1, \ldots, T$ and they indicate whether a parcel i is selected for treatment in a time period t or not. We can easily plot the optimal values of these variables produced by (D1) and (R1). An illustration of this observation when $\alpha = 0.3$ and $\beta = 0.05$ can be found in Figure 4.1 in which each cell represents x_{it}, and it is hatched/filled only if $x_{it} = 1$. As expected, the recommended values generated by (D1) and (R1) are different.

Since optimal solutions of (R1) and (D1) may differ significantly, and since their respective objective function values cannot be fairly compared due to increased diffusion rates in (R1), we introduce a few techniques to be able to compare the solutions and show the value of robust optimization. Since the main decision variables of the problem are x_{it}, let

$\boldsymbol{x}^d$ and $\boldsymbol{x}^r$ be the optimal value vectors of these decision variables produced by solving (D1) and (R1), respectively. Furthermore, for a given $\bar{\boldsymbol{x}}$, we define $D(\bar{\boldsymbol{x}})$ as the optimal objective value of (D1) when we set $x_{it} = \bar{x}_{it}$ in (D1). Similarly, for a given $\bar{\boldsymbol{x}}$, we define $R(\bar{\boldsymbol{x}})$ as the optimal objective value of (R1) when we set $x_{it} = \bar{x}_{it}$ in (R1). Using these definitions, four values can be computed:

- $D(\boldsymbol{x}^d)$: This is the the objective value that is reached when we implement the deterministic decision $\boldsymbol{x}^d$, made on assumptions of zero uncertainty, to a deterministic setting. If our assumption about zero uncertainty was indeed correct then implementing the deterministic decision represents the best case scenario for the decision maker.

- $D(\boldsymbol{x}^r)$: This is the objective value that is reached if we implement $\boldsymbol{x}^r$, i.e., the robust decision, made on assumptions of worst case scenario, to a deterministic setting. We may incur some extra cost in the process for being over prepared and making wrong assumptions about uncertainty.

- $R(\boldsymbol{x}^r)$: This is the objective value we get if we choose to implement $\boldsymbol{x}^r$, the robust decision, made on assumptions of worst case scenario, to a non-deterministic or uncertain setting. In this case, We are well equipped to handle this uncertainty since we prepared for it beforehand.

- $R(\boldsymbol{x}^d)$: This is the objective value we achieve if we use $\boldsymbol{x}^d$, i.e., the deterministic decision to a non-deterministic or uncertain setting. This situation represents the worst case scenario for the decision maker since they get penalized for being unprepared and making wrong assumptions about uncertainty.

It can be easily shown that $D(\boldsymbol{x}^d) \leq D(\boldsymbol{x}^r) \leq R(\boldsymbol{x}^r) \leq R(\boldsymbol{x}^d)$. In other words, using $\boldsymbol{x}^r$ results in less fluctuations in the objective value if realizations of data different than those anticipated arise in practice. To illustrate this observation, we assume that $\beta \in \{0.5, 1, 2\}$ and $\alpha \in \{0.25, 0.5, 0.75\}$, and run a small set of nine experiments by applying different

combinations for values of α and β. Larger values of α and β represent larger quantum of uncertainty. By varying these coefficients we are simply varying the quantum of uncertainty we consider. Experiments $1, 2, \ldots, 9$ are defined to be precisely $(\beta = 0.5, \alpha = 0.25), (\beta = 0.5, \alpha = 0.5), \ldots, (\beta = 2, \alpha = 0.75)$. The scaled results are reported in Figure 4.2 in which the vertical axis shows the ratio, i.e., $\frac{D(\boldsymbol{x}^d)}{R(\boldsymbol{x}^d)}$, $\frac{D(\boldsymbol{x}^r)}{R(\boldsymbol{x}^d)}$, $\frac{R(\boldsymbol{x}^r)}{R(\boldsymbol{x}^d)}$, and $\frac{R(\boldsymbol{x}^d)}{R(\boldsymbol{x}^d)}$, and the horizontal axis shows the experiment number. Observe that $\frac{D(\boldsymbol{x}^d)}{R(\boldsymbol{x}^d)} \approx \frac{D(\boldsymbol{x}^r)}{R(\boldsymbol{x}^d)}$ (in fact $\frac{D(\boldsymbol{x}^d)}{R(\boldsymbol{x}^d)}$ is slightly better/smaller than $\frac{D(\boldsymbol{x}^r)}{R(\boldsymbol{x}^d)}$ in all experiments). This implies that $\boldsymbol{x}^r$ is almost optimal for (D1). So, if we prepare for uncertainty by implementing the robust decision $\boldsymbol{x}^r$, but the worse case scenario (as defined by the robust optimization formulation) does not arise in reality, we almost lose nothing. Also observe that $\frac{R(\boldsymbol{x}^r)}{R(\boldsymbol{x}^d)}$ is up to 14% better/smaller than $\frac{R(\boldsymbol{x}^d)}{R(\boldsymbol{x}^d)}$. This implies that if the worse case scenario (as defined by the robust optimization formulation) arises then we are up to 14% better off by using $\boldsymbol{x}^r$. Simply put, we are better able to handle uncertainty if we have prepared for it beforehand. These two observations clearly illustrate the value of the proposed robust optimization, and the fact that $\boldsymbol{x}^r$ is a better choice in practice. Of course, these experiments can be repeated, with similar results, for any size of the problem and any set of parameters α and β. Finally, as enunciated earlier, the assumption of uncertainty and the robust formulation used to handle it, also impacts the gist of managerial decision making by prescribing to treat different parcels of land in different time periods, i.e., choosing different x_{it} variables to be 1, as compared with those suggested by the deterministic formulation.

4.5 A Robust Optimization Approach to the Reserve Selection Problem

In this section, the robust counterpart formulation of the basic reserve selection problem (Beyer et al., 2016), explained in Section 4.5, is developed. We assume that the cost coefficients for parcels, i.e., c_i for $i = 1, \ldots, M$, and the target values for species, W_k for $k = 1, \ldots, K$, are known with certainty. Note that this assumption may often be reasonable because the cost can be approximated using a range of values from alternative

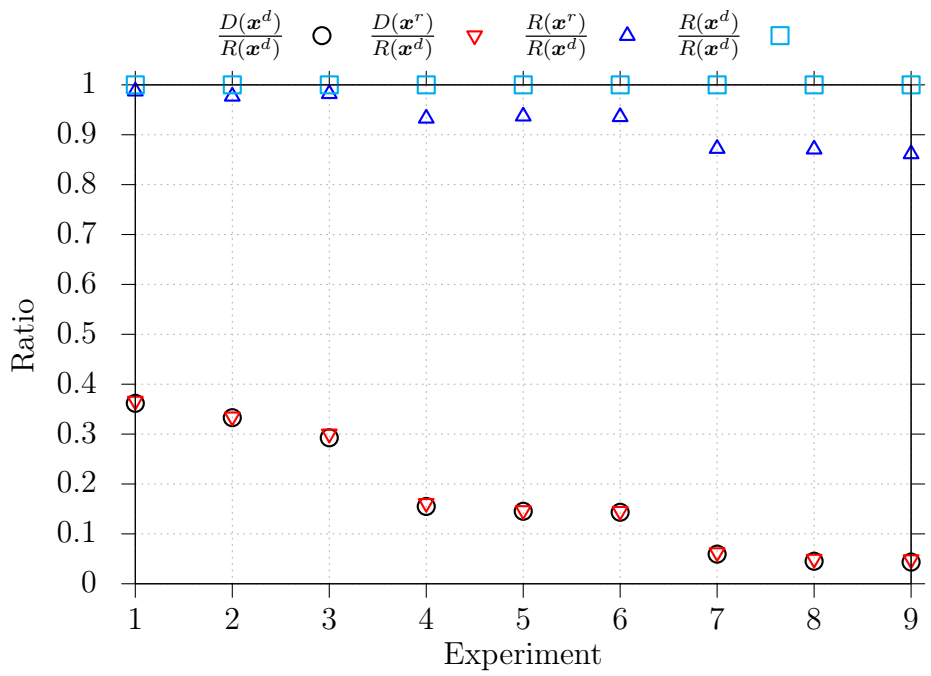

Figure 4.2 – Comparing the optimal solution generated by (D1) and (R1) in 9 different experiments.

economic models, and the species conservation target can be elicited from stakeholders. The parameters w_{ik} represent the contribution of parcel i to species k and are considered to be uncertain. These values often depend on a number of biological factors and therefore need thorough examination of the ecological characteristics of a certain parcel of land. The estimates for these biological factors are prone to estimation errors and changes over time. w More specifically, we assume that $w_{ik} \in [\bar{w}_{ik} - \hat{w}_{ik}, \bar{w}_{ik} + \hat{w}_{ik}]$ and $\hat{w}_{ik} > 0$; i.e., we consider a range uncertainty in contribution values where the size of uncertainty is determined by $\hat{w}_{ik}$. We denote the robust counterpart formulation of (D2) with (R2). This formulation can be easily constructed using the techniques developed in Section 4.2. Interested readers can find (R2) in Appendix 6.

4.5.1 Numerical Experiments and Findings

The goal of this section is to compare the performance of (D2) and (R2). We evaluated the performance of (D2) and (R2) with simulated data. The simulated data are generated by setting $M = 40$ and $K = 5$. Also, c_i for $i = 1, \ldots, M$ are randomly generated by using the discrete uniform distribution in the interval $[100, 1000]$. Furthermore, $\bar{w}_{ik}$ values are randomly drawn from the normal distribution with mean of 0 and standard deviation of 5. Values less than zero are truncated to zero. This implies that on average 50% of the parcels do not contribute to the conservation of a particular species. We also set $W_k = 0.5 \sum_{i=1}^{M} \bar{w}_{ik}$. Let $\alpha, \beta \geq 0$ be two user-defined parameters, we assume that $\hat{w}_{ik} = \beta \bar{w}_{ik}$ and $\Gamma_k = \alpha M$. It is worth mentioning that to compare (R2) and (D2), we assume that $w_{ik} = \bar{w}_{ik}$ in (D2). Next, we conduct some experiments on the simulated data by choosing different values for α and β. All the numerical experiments were done on a machine with 3.60 GHz CPU clock speed, 16 GB RAM and 64-bit Windows 8 operating system. The models D2, R2, and R3 were solved using the Java API of CPLEX V12.4. Optimality gap was set at 2.5%. Although, we present the results for 40 parcels for reader's convenience and consistency across the chapter, we ran a series of experiments with larger number of parcels to see how the deterministic and the robust models scale with the problem size. We ran our models with number of parcels equal to 100, 500, 1,000, 5,000 and 10,000 and reported and compared the run times for the deterministic and robust models D2 and R2, respectively. We also ran R3 with larger size of instances. We ran a set of experiments with number of parcels equal to 50, 100 and 200. As the model R3 contains linearization constraints to replace the bilinear terms, and also involves finding the full non-dominated frontier consisting of hundreds of points, we were unable to solve the problem with number of parcels larger than 200 in a reasonable amount of time. We report these run time results in Tables 4.4 and 4.5.

In rest of this section, we assume that (D2) is always feasible, but we make no such assumption about (R2). We first note that to compare (D2) and (R2), we cannot use the same technique developed in Section 4.4.1 because this problem has only one type of decision

Table 4.4 – Time Required to Solve Problem Instances of Different Sizes for D2, and R2 when $\alpha = 0.5$, $\beta = 0.5$

Total Number of Parcels	Time for D2 (sec)	Time for R2 (sec)
100	0.07	4.16
500	0.22	1.23
1,000	0.22	1.48
5,000	0.41	8.23
10,000	0.58	230.94

Table 4.5 – Number of Nondominated Points, Corresponding Number of Single-Objective MILPs Solved and the Time Required to Solve Problem Instances of Different Sizes for R3 when $\alpha = 0.5$, $\beta = 0.5$

Total Number of Parcels	Time for R3 (sec)	# of Non-dominated points	# of MILPs solved
25	5	53	106
50	41	137	274
100	576	228	456
200	35,908	329	458

variables, and so the solution corresponding to (D2) is unlikely to be feasible for (R2). This implies that using the solution of the deterministic formulation would be a poor choice because under the worst case scenario (as defined by the robust optimization formulation), the deterministic solution fails to satisfy the target values for species of interest.

Based on this observation, one may be tempted to make the determination to always use the robust optimization formulation (R2), because it is always feasible. However, as we subsequently explain, that is not necessarily the case. In general, the structure of (R2) is such that it is quite possible to increase the degree of uncertainty in (R2) to such an extent so as to render the problem infeasible.

Although, using the optimal solution obtained by (D2) does not seem to be a good choice. At the same time, however, employing (R2) as currently defined may not be a good

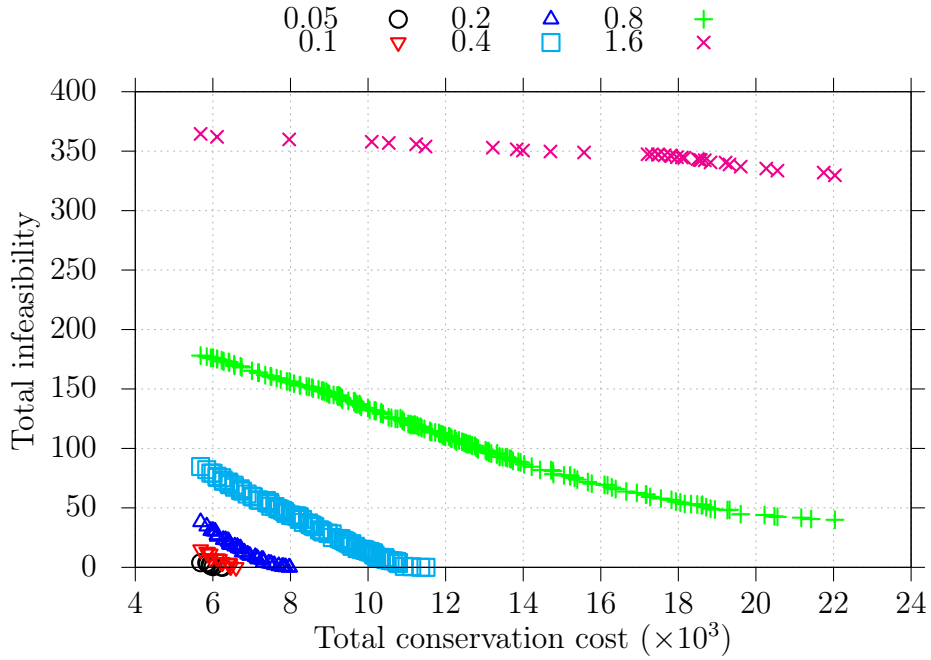

Figure 4.3 – The nondominated frontier of (R3) for different values of β when $\alpha = 0.25$. Each curve represents the nondominated frontier for a different value of β. The axes represent the values of the respective objective functions.

option either as the issue of possible infeasibility persists. Consequently, we need to revise (R2) in order to ensure that the revised formulation is always feasible (if (D2) is feasible).

We revised (R2) by adding a second objective to the problem (in addition to the total conservation cost) to measure the total infeasibility of the robust formulation. It is worth mentioning that the total infeasibility can be interpreted as the amount of decrease in the uncertainty ranges in order to make the robust counterpart formulation feasible. We denote the revised formulation by (R3). It is worth mentioning that (R3) can be easily written as a bi-objective mixed integer linear program (BOMILP) by using a few linearization techniques. In bi-objective optimization the goal is to compute the nondominated frontier or simply the set of all nondominated points. These points are the projection (image) of Pareto-optimal solutions in the objective space. Interested readers can find (R3) and its linearization process in Appendix 6.

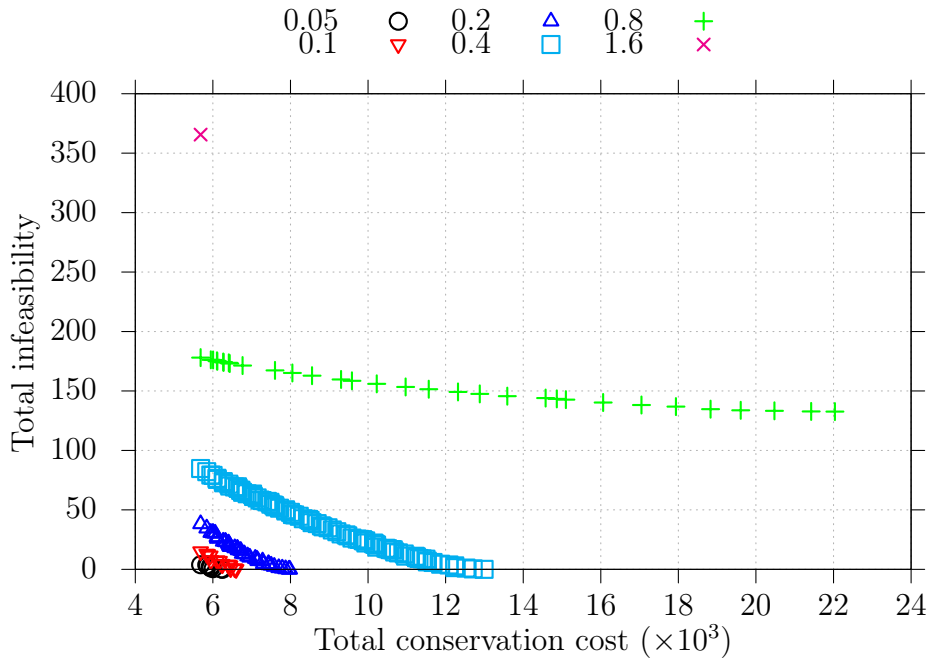

Figure 4.4 – The nondominated frontier of (R3) for different values of β when $\alpha = 0.5$. Each curve represents the nondominated frontier for a different value of β. The axes represent the values of the respective objective functions.

We use the ϵ-constraint method to solve the BOMILP corresponding to (R3) for

$$\beta = \{0.05, 0.1, 0.2, 0.4, 0.8, 1.6\}$$

and $\alpha \in \{0.25, 0.5\}$. Figures 4.3 and 4.4 show the (exact) nondominated frontier of the problem for different values of β when $\alpha = 0.25$ and $\alpha = 0.5$, respectively. We next make a few observations about these figures.

- Intuitively, it can be seen that the upper left and lower right endpoints of each nondominated frontier provide information about (D2) and (R2), respectively. More specifically, the upper left point shows the infeasibility of the optimal solution obtained with (D2) under the worst case scenario. For this solution all the uncertainty is unaddressed and total infeasibility is maximum possible. It also shows the optimal cost of conservation by allowing (R3) to handle this amount of infeasibility when the worst case scenario

arises. Similarly, the lower right endpoint shows the total infeasibility of (R2), and the optimal cost of conservation by allowing (R3) to handle this amount of infeasibility.

- For a fixed α and β, the decision maker(s) can visualize the nondominated frontier and choose a desirable point. Obviously, choosing a point closer to the lower right corner indicates that the decision makers adopt a more conservative or risk averse approach since the lower right point represents the total infeasibility of (R2).

- For a fixed α, the nondominated frontier shifts upward, i.e., the value of infeasibility increases, as β increases, and it converges towards a plateau. This is not surprising because as β increases, the uncertainty goes up. Indeed, increasing β adds more uncertainty to the problem. We observe that it is possible that the nondominated frontier becomes so flat that eventually reduces to a single point, see for instance $\beta = 1.6$ and $\alpha = 0.5$. Note that this is also true for the other extreme case representing very small or no uncertainty. If the uncertainty is very small then it is expected that the nondominated frontier would become so steep that it would eventually reduce to a single point.

These observations imply that (for the formulation of the reserve selection problem explored in this study), the decision makers would not gain much by trying to handle a large amount of uncertainty using the proposed robust optimization technique. At higher values of assumed uncertainty, the nondominated frontier may become so flat that to improve the infeasibility by small amount, we need to increase the conservation cost significantly. Similarly, if the assumed uncertainty is very small the robust optimization technique is almost equivalent to the deterministic formulation. Even in this extreme case, using the robust optimization approach is not particularly helpful. Nevertheless, for a reasonable amount of uncertainty using the proposed robust optimization approach seems to be quite helpful. For instance, the nondominated frontiers of the problem when $\beta = 0.2$, $\beta = 0.4$ or $\beta = 0.8$ and when $\alpha = 0.25$ or $\alpha = 0.5$ in Figures 4.3 and 4.4 seem very promising since the lower right endpoint of these

nondominated frontiers has the total infeasibility value of zero, but the upper left point has a significant total infeasibility value. Also observe that since these curves are generally steeper, i.e., we have significant gains on infeasibility without losing much on the conservation cost, the decision maker can genuinely achieve a trade-off between his competing objectives by choosing a suitable point on these nondominated frontiers.

Another crucial information that (R3) can provide us is the optimal values of variables ϵ_{ik}. These values represent the portion of $\hat{w}_{ik}$ that remained unaddressed. These values can indicate to a decision maker where to concentrate their data gathering efforts in order to minimize the unaddressed uncertainty as defined by the second objective function in (R3) especially in a situation when the budget for such efforts is limited.

Chapter 5: Conclusions and Future Research Directions

5.1 Conclusion Chapter 2

The second chapter presents a mathematical model to solve the problem of nightly repositioning and recharging of electric vehicles in a FFEVS system. Since in many such systems, EVs are moved by a crew of shuttles and drivers, we propose that the relocation decision be made in synchronization with shuttle routing decision to minimize the cost of relocation operation. In contrast, most current approaches make the relocation and shuttle routing decisions sequentially. Our unique path based formulation can solve problems of moderate size. For system sized instances, we propose an exchange based neighborhood search method which draws from the mathematical model and solves all the instances within 10 minutes. A comparison of synchronized approach with sequential approach shows that the former improves the total length of shuttle routes and in turn the cost of relocation operation by 15% on average. FFEVS systems require an elaborate relocation operation and improving the cost of such an operation improves the bottom line of these systems. Moreover, our model achieves complete system-wide repositioning and recharging, therefore improving the distribution of EVs and directly addressing the issues of demand imbalance and range anxiety in FFEVS systems.

The data for our experiments comes from a real life FFCS operator and the instances used in this chapter represent the complexities of an actual relocation operation. This chapter presents EBNSM which uses cluster-relocate-route approach to solve the system-sized relocation instances for relocating and recharging. For the largest instance solved in this chapter, we relocate 155 EVs while increasing the system-wide average charging levels from 42 % to 90 %. The model is also flexible to changes in system status, initial battery

levels, and desired demand configuration. It allows for partial recharging of EVs and their relocation close to the actual demand points.

We conduct a variety of experiments with different numbers of shuttles and drivers per shuttle, a proxy for shuttle size, to find out the most cost-effective human resource allocation. The results suggest that given certain number of personnel, it is more cost-effective to increase the number of shuttles rather than number of drivers on each shuttle, especially when the service area is large. This trend may be reversed for small service areas and small number of EV relocations per shuttle. In these cases, adding extra shuttles only adds to wait times, and increasing the number of drivers may be beneficial. This implies that although increasing the number of drivers on shuttles improves the route length, the improvement is not justified due to extra cost. Therefore, systems with relatively high labor cost should consider single person mobility options like foldable bicycles or scooters as this will relieve the cost of an extra car and driver.

5.1.1 Limitations and Future Directions

One fundamental limitation of the decision models presented in this chapter is their inability to include the new incoming demand for EVs in the relocation and routing decisions. It is worth noting that since we model the nighty static relocation, we assume that no new demand arrives during the night. This ensures that the current EV locations and the desired inventory in each neighborhood stay unchanged throughout the relocation operation. This assumption is justified since many FFEVS systems close their operations at night. Even when a system stays operational, the demand levels are insignificant. For instance, in the case study we consider, the demand is only 6% of the peak demand. The algorithms presented in this chapter can be extended to include the newly arriving demand. As EV's become unavailable due to new demand, the old EV paths chosen for relocation can be replaced with new EV paths by solving the relocation problem again. This can be done either by resolving the model SEQ-A or by using heuristic approaches. Once the new EV paths are selected, the

`updatedRoutes` and `RouteImprovement` procedures of the EBNSM algorithm can be used to update the shuttle routes accordingly.

A second related limitation is related to the deterministic assumption for next day's demand and the simple demand prediction model used in this chapter. The current model considers the demand for the next morning to be known in advance. We use historical averages of the demand to predict the desired EV locations for the next morning. While the deterministic assumption can work accurately if sufficient data and sophisticated prediction algorithms are available, the inherent uncertainty in future demand makes all relocation models insufficient to address the incoming demand. As future research into the relocation operations, it may be worthwhile to quantify the reduction in service level due to inaccurate demand prediction or assumptions of known demand. A more sophisticated demand prediction model, although outside the purview of this paper, can also increase the applicability of our work.

The second source of limitations in our model is the underlying assumptions of our modeling approach. This may limit the applicability of this approach in some niche situations. For instance, we only allow a charging station to be used once during the process of relocation. This implies that in situations where the charging infrastructure is limited, the number of EV relocations is also limited by the charging stations available. While this assumption is justified for systems with large charging infrastructure, like those in many European and North American cities, it may not be applicable for cities with scarce infrastructure. Future research in EV relocation operations can allow for reusing the same charging point multiple times.

The relocation decision in our problem considers the charging process as part of the optimal EV path selection. Our model for the charging process assumes that charging time has a linear relationship with charging levels. Others have considered non-linear charging process and used piece-wise linearization to model different charging speeds (Pelletier et al., 2018). However, a linear charging process sufficiently models the reality for our case when

the focus is on the operational problem and the total time spent on recharging rather than the non-linearities of the charging process itself. This assumption, however, may impact the managerial decision of selecting the desired charging levels especially when charging infrastructure is scarce and there is a pressure for EVs to be made available for fast arriving demand.

By design, the relocation model in this chapter only allows for single vehicle per cluster. As a consequence, each EV path is serviced by a single vehicle. In reality, however, each cluster can have multiple vehicles and even a single EV path can be serviced partially by multiple vehicles. A corollary to this assumption is that only exchanges within clusters are allowed which is why as the number of clusters increases, the neighborhood becomes smaller, and potential for improvement also decreases as can be seen in Figrue 2.6. Currently these static clusters are created by solving the optimization model NCA. Dynamic clusters could be created by allowing inter-cluster node exchange as future improvement to the algorithm.

The third source of limitations in our model relates to the parametric assumptions. In deriving the managerial insights in Section 2.6, we have considered β_1 and β_2 values of 2.5 and 0.4, respectively. The parameter value of β_1 represents the vehicle's charge depletion rate while β_2 represents a vehicle's charging rate and given in percentage gain in charging per minute. Similarly, personnel cost is assumed to be \$40/hr and the shuttle operating cost is set at \$24/hr. Although we have considered the sensitivity of our model to the parameter values, some of the insights in this chapter may be limited to the context considered in the chapter.

Future research in EV relocation and routing problems can extend the neighborhood search approaches discussed in this chapter to the dynamic relocation problem throughout the day. Further research can also explore the decomposition-based approaches to get information about the solution bounds. Due to the large size of solved instances in this chapter, solution time was an important consideration. The operational nature of the problem necessitates solution methods that provide "reasonably good" solutions within a few

minutes. In some cases, customized decomposition-based approaches have previously been used for similar integrated models in other industries. However, the instances solved were either small (Luo et al., 2019) or took many hours to achieve sufficient convergence (Cordeau et al., 2001). The structure of our problem combined with the large size of our instances and the need for quick solutions makes our problem less suitable for decomposition-based approaches. However, exploring the problem formulations more suitable for such approaches can be an interesting research direction. Finally, we only explore the deterministic setting in this chapter. To handle uncertainty in arriving demand, or travel and charging times, simulation-based approaches could also be explored for smaller instances of the problem.

5.2 Conclusion Chapter 3

Low income, lack of viable transportation options and unavailability of proximate supermarkets make access to fresh and healthy food an urgent issue in many neighborhoods. This chapter proposes using last-mile grocery delivery services as a solution to the food insecurity problem for these low income and low access neighborhoods, the so called food deserts.' Due to various issues with attended home delivery and the minimum order size requirements, the cost of home delivery for groceries can be prohibitively expensive for low-income households. To resolve these problems, we propose using the neighborhood convenience stores as consolidation pickup points where the grocery delivery services can deliver orders and the customers can pick them up. Oftentimes, these neighborhood stores are the only source of food but carry more expensive and unhealthy food items. The solution we propose converts these locations to hubs of healthy food.

The main focus of this research is to quantify the consolidation benefits achieved due to this arrangement. To this end, we compare the cost of delivering customer orders to customer homes with store delivery. A set cover problem is solved to find the minimal number of stores required to serve all customers within a predefined walkable distance to one of the stores. Subsequently, we solve a customized vehicle routing problem with time

windows twice: first to deliver the accepted orders direct to customers and second to deliver the same orders through pick up convenience stores. The time windows of customer delivery are changed as a model parameter to see how the narrowness of delivery windows impacts the temporal aspect of consolidation. The total cost of delivery for the two situations is compared to answer the main research question. We also evaluate the operational circumstances under which this solution may or may not be worthwhile in real neighborhoods by comparing the service level, i.e., the percentage of accepted orders for store delivery, across many operational situations. Our experimental analysis uses real-life data from three counties with different urban forms. We also evaluate the sensitivity of our model to the capacity of delivery vehicles, the number of partner convenience stores, the number of depot locations, and the number of orders.

The results suggest that the consolidation benefits of store delivery across instances are substantial. In the best case instance (with narrowest customer time windows considered), the delivery cost reduction of up to 1800% can be achieved compared to home delivery. However, spatial consolidation alone does not reduce the delivery costs sufficiently to justify store delivery. We find that most of the improvement in delivery costs comes from temporal consolidation which is higher when customer time windows are narrow. The capacity of delivery vehicles is an important factor in determining the extent of consolidation. The difference in delivery costs between two schemes is larger for larger capacity vehicles due to in-vehicle pooling. The number of available partner stores positively impacts the service level, while a higher number of depot locations and customer orders reduces the cost of delivery. We also find that the consolidated delivery to only chain stores for rural and less dense urban neighborhoods provides insufficient service level and therefore a wider set of potential partnerships needs to be explored.

5.2.1 Limitations and Future Directions

One key limitation of this study is in terms of its applicability to all customers inside food deserts. The three dimensions of food insecurity related to income, location, and mobility impact each individual to a different extent. Food insecurity is a cross-sectorial and multiscale problem and no solution can address it in all its complexities. Current efforts to address food insecurity address one or more of these dimensions. In the US, these efforts include federal nutritional assistance programs, subsidiesm and incentives provided to retailers to locate in food insecure neighborhoods, and non-for-profit initiatives by community organizations, e.g., food banks, community kitchens etc. Despite these efforts, the issue of food insecurity is still present and relevant. Like all other approaches, the consolidated delivery services alone cannot be the solution for all customers inside food deserts. Qualitative studies can further inform how this solution can be achieved while fulfilling customer expectations.

The second source of limitations is related to customer arrival and customer acceptance mechanisms considered in the model. In the case studies considered in this chapter, the total number of orders is assumed to be 30 % of the number of households without vehicles inside a census tract. This assumption is based on each household ordering groceries twice a week. However, when the solution is initially rolled out, the number of customers may be much smaller. A customer is assigned a pick up store which is within walkable distance to their home. Our model therefore cannot service all customers and only those within a walkable distance are accepted for service. Information about all customer orders is assumed to be available at the beginning of the planning horizon and the orders must be delivered on the same day. This assumption models the reality in situations where people plan their grocery orders in advance and orders taken the previous day are to be delivered the next day. If same day delivery is to be considered, then the orders can arrive throughout the day and a mechanism for accepting the new orders may need to be put in place. Similarly, in reality, customers may be given multiple choices with cost options for home delivery or

delivery at multiple stores in the neighborhood. These modifications can take into account the heterogeneity of customers inside food deserts.

Some limitations relate to the modeling approach employed in this chapter. We assume all customers within walking distance of a convenience store will accept the offer to pick their order at the store. In reality, only a proportion of such offers will actually be accepted by customers. Qualitative data collection based on neighborhood specific surveys in this lieu could help determine the number of people interested in the service. We also do not consider capacity limits on the number of orders each store location can handle. This may inflate the service level since orders which would be otherwise unfulfilled are assigned to the store. The capacity available at a store for receiving grocery orders in fact depends on the nature of the partnership between delivery services and convenience stores, the size of the store, the space available, and other store specific factors. The requirement for refrigerated space may further limit the capacity available. Pick up points can have limited capacity, especially if they are a standalone kiosk rather than a store. However, since we only consider convenience stores with refrigerated storage, we assume these points to have unlimited capacity to serve customer orders.

We only consider large convenience stores and gas stations which are associated with big store chains. This limits the number of neighborhood stores available for consolidation. In Hudson County, the number of chain stores was much smaller compared to Hillsborough despite a higher population and population density. Similarly, in Hendeson County, the number of chain stores within walkable distance to customers was very small. Therefore, the resultant service level is too small. However, if other locations are considered as pickup points, our findings could change considerably.

We also assume the depot locations to have unlimited capacity. This assumption is justified since the retail locations of large grocery retailers are used as depots in this study and there is no limit for shelf and storage space. Similarly, the delivery routes available are also assumed to be unlimited in number since we must deliver all the accepted orders. The

delivery vehicles are assumed to be homogenous and are assumed not to have a refrigerated compartment for the delivery of refrigerated/frozen groceries. The size of delivery time windows is also assumed to be the same for all customers. Finally, although we conduct sensitivity analysis for the number of customers, depots, and stores, we only consider two possible values for these parameters. A more detailed sensitivity analysis can further inform how changing these affects consolidation.

This chapter is an important step in enabling the use of consolidated grocery delivery to substantially address the problem of food insecurity in socioeconomically disadvantaged neighborhoods. Further research, both qualitative and quantitative, is required to resolve what Besiou and Van Wassenhove (2015) call the problem of an unfamiliar context. A holistic approach using in depth field research based on interviews and focus groups can engage the stakeholders, including convenience stores and neighborhood residents to enable the proposed solution. Further research can be conducted in designing a market to enable consolidated delivery operations. A market design approach can further inform how the costs and benefits of the consolidated delivery can be divided between stakeholders, and how targeted government subsidies, if required, can make this model financially viable for all parties including food delivery service, convenience stores and customers.

5.3 Conclusion Chapter 4

Many conservation problems involve a lot of uncertainty, which may not always be captured with probability distributions. In this study, we explored the idea of applying robust optimization techniques for solving conservation problems while accounting for high levels of uncertainty. To the best of our knowledge, this is the first study in applying a robust optimization approach in conservation planning problems. We illustrated our proposed approach with two types of problems: the invasion control problem and the reserve selection problem. More importantly, we developed novel techniques to compare the results obtained by the proposed robust optimization approach and the corresponding deterministic formula-

tion. We hope that the applicability, versatility, and performance of our approach encourages practitioners and researchers to implement it to address important issues in natural resource management and conservation.

References

Adams, S.A., 2020. Coronavirus causing more issues for people in food deserts. *The Weirton Daily Times*

Agatz, N., Campbell, A., Fleischmann, M., Savelsbergh, M., 2011. Time slot management in attended home delivery. *Transportation Science* 45, 3, 435–449.

Akobundu, U.O., Cohen, N.L., Laus, M.J., Schulte, M.J., Soussloff, M.N., 2004. Vitamins a and c, calcium, fruit, and dairy products are limited in food pantries. *Journal of the American Dietetic Association* 104, 5, 811–813.

de Almeida Correia, G.H., Antunes, A.P., 2012. Optimization approach to depot location and trip selection in one-way carsharing systems. *Transportation Research Part E: Logistics and Transportation Review* 48, 1, 233–247.

Arthur, J.L., Haight, R.G., Montgomery, C.A., Polasky, S., 2002. Analysis of the threshold and expected coverage approaches to the probabilistic reserve site selection problem. *Environmental Modeling and Assessment* 7, 2, 81–89.

Asdemir, K., Jacob, V.S., Krishnan, R., 2009. Dynamic pricing of multiple home delivery options. *European Journal of Operational Research* 196, 1, 246–257.

Aussenberg, R.A., 2014. *SNAP and related nutrition provisions of the 2014 Farm Bill (PL 113-79)*. Congressional Research Service.

Austin, M., 2002. Spatial prediction of species distribution: an interface between ecological theory and statistical modelling. *Ecological Modelling* 157, 2, 101–118.

Balakrishnan, A., Ward, J.E., Wong, R.T., 1987. Integrated facility location and vehicle routing models: Recent work and future prospects. *American Journal of Mathematical and Management Sciences* 7, 1-2, 35–61.

Bellan, R., 2018. The grim state of electric vehicle adoption in the u.s.

Ben-Tal, A., El Ghaoui, L., Nemirovski, A., 2009. *Robust optimization*. Princeton University Press.

Bert, J., Collie, B., Gerrits, M., Xu, G., 2016. What's ahead for car sharing?: The new mobility and its impact on vehicle sales,

Bertsimas, D., Sim, M., 2004. The price of robustness. *Operations Research* 52, 1, 35–53.

Besiou, M., Van Wassenhove, L.N., 2015. Addressing the challenge of modeling for decision-making in socially responsible operations. *Production and Operations Management* 24, 9, 1390–1401.

Beyer, H.L., Dujardin, Y., Watts, M.E., Possingham, H.P., 2016. Solving conservation planning problems with integer linear programming. *Ecological Modelling* 328, 14–22.

Bhatt, J., 2020. More than a disease, COVID-19 exposes health risk of food insecurity: OPINION. *ABC News*

Bhattarai, G.R., Duffy, P.A., Raymond, J., 2005. Use of food pantries and food stamps in low-income households in the united states. *Journal of Consumer Affairs* 39, 2, 276–298.

Billionnet, A., 2013. Mathematical optimization ideas for biodiversity conservation. *European Journal of Operational Research* 231, 3, 514–534.

Boscoe, F.P., Henry, K.A., Zdeb, M.S., 2012. A nationwide comparison of driving distance versus straight-line distance to hospitals. *The Professional Geographer* 64, 2, 188–196.

Bruglieri, M., Colorni, A., Luè, A., 2014. The vehicle relocation problem for the one-way electric vehicle sharing: an application to the milan case. *Procedia-Social and Behavioral Sciences* 111, 18–27.

Bureau, C., 2015. Census Bureau Cartographic Boundary Files.

Büyüktahtakın, İ.E., Feng, Z., Frisvold, G., Szidarovszky, F., Olsson, A., 2011. A dynamic model of controlling invasive species. *Computers & Mathematics with Applications* 62, 9, 3326–3333.

Büyüktahtakın, İ.E., Feng, Z., Szidarovszky, F., 2014. A multi-objective optimization approach for invasive species control. *Journal of the Operational Research Society* 65, 11, 1625–1635.

Büyüktahtakın, İ.E., Kıbış, E.Y., Cobuloglu, H.I., Houseman, G.R., Lampe, J.T., 2015. An age-structured bio-economic model of invasive species management: insights and strategies for optimal control. *Biological Invasions* 17, 9, 2545–2563.

Cabeza, M., Moilanen, A., 2001. Design of reserve networks and the persistence of biodiversity. *Trends in Ecology & Evolution* 16, 5, 242–248.

Caggiani, L., Camporeale, R., Ottomanelli, M., 2017. A dynamic clustering method for relocation process in free-floating vehicle sharing systems. *Transportation Research Procedia* 27, 278–285.

Campbell, A.M., Savelsbergh, M., 2006. Incentive schemes for attended home delivery services. *Transportation Science* 40, 3, 327–341.

Campbell, A.M., Savelsbergh, M.W.P., 2005. Decision support for consumer direct grocery initiatives. *Transportation Science* 39, 3, 313–327.

Cannuscio, C.C., Tappe, K., Hillier, A., Buttenheim, A., Karpyn, A., Glanz, K., 2013. Urban food environments and residents' shopping behaviors. *American Journal of Preventive Medicine* 45, 5, 606–614.

Caramaschi, S., 2016. Counteracting food deserts. the potential for mobile food vending in regenerating contemporary cities. *Urban Regeneration & Sustainability* p. 384.

Carman, T., 2018. D.c. has never had more food delivery options. unless you live across the anacostia river. *Washington Post*

Carrasco, L.R., Baker, R., MacLeod, A., Knight, J., Mumford, J., 2010. Optimal and robust control of invasive alien species spreading in homogeneous landscapes. *Journal of the Royal Society Interface* 7, 44, 529–540.

Castillo, V.E., Bell, J.E., Rose, W.J., Rodrigues, A.M., 2018. Crowdsourcing last mile delivery: strategic implications and future research directions. *Journal of Business Logistics* 39, 1, 7–25.

Chianese, Y., Avenali, A., Gambuti, R., Palagi, L., 2017. One-way free floating car-sharing: applying vehicle-generated data to assess the market demand potential of urban zones. In *Computer Software and Applications Conference (COMPSAC), 2017 IEEE 41st Annual*, Vol. 2, IEEE, pp. 777–782.

Conway, A., Fatisson, P.E., Eickemeyer, P., Cheng, J., Peters, D., 2012. Urban micro-consolidation and last mile goods delivery by freight-tricycle in manhattan: Opportunities and challenges.

Cook, A., Marion, G., Butler, A., Gibson, G., 2007. Bayesian inference for the spatio-temporal invasion of alien species. *Bulletin of mathematical biology* 69, 6, 2005–2025.

Cordeau, J.F., Stojković, G., Soumis, F., Desrosiers, J., 2001. Benders decomposition for simultaneous aircraft routing and crew scheduling. *Transportation science* 35, 4, 375–388.

Costello, C., Polasky, S., 2004. Dynamic reserve site selection. *Resource and Energy Economics* 26, 2, 157–174.

Council, N.R., 2009. *The public health effects of food deserts: workshop summary*. National Academies Press.

Cummins, S., Flint, E., Matthews, S.A., 2014. New neighborhood grocery store increased awareness of food access but did not alter dietary habits or obesity. *Health Affairs* 33, 2, 283–291.

Dai, D., Wang, F., 2011. Geographic disparities in accessibility to food stores in southwest mississippi. *Environment and Planning B: Planning and Design* 38, 4, 659–677.

Daponte, B.O., 2000. Private versus public relief: use of food pantries versus food stamps among poor households. *Journal of Nutrition Education* 32, 2, 72–83.

Davis, L.B., Sengul, I., Ivy, J.S., Brock III, L.G., Miles, L., 2014. Scheduling food bank collections and deliveries to ensure food safety and improve access. *Socio-Economic Planning Sciences* 48, 3, 175–188.

Dayarian, I., Savelsbergh, M., Clarke, J.P., 2020. Same-day delivery with drone resupply. *Transportation Science*

De Marco, M., Thorburn, S., 2009. The relationship between income and food insecurity among oregon residents: does social support matter? *Public Health Nutrition* 12, 11, 2104–2112.

Desaulniers, G., Madsen, O.B.G., Ropke, S., 2014. Chapter 5: The vehicle routing problem with time windows. In *Vehicle Routing: Problems, Methods, and Applications, Second Edition*. SIAM, pp. 119–159.

Deutsch, Y., Golany, B., 2018. A parcel locker network as a solution to the logistics last mile problem. *International Journal of Production Research* 56, 1-2, 251–261.

Dillahunt, T.R., Simioni, S., Xu, X., 2019. Online grocery delivery services: An opportunity to address food disparities in transportation-scarce areas. In *Proceedings of the 2019 CHI Conference on Human Factors in Computing Systems*, pp. 1–15.

Doherty, T.S., Glen, A.S., Nimmo, D.G., Ritchie, E.G., Dickman, C.R., 2016. Invasive predators and global biodiversity loss. *Proceedings of the National Academy of Sciences* 113, 40, 11261–11265.

Durand, B., Mahjoub, S., Senkel, M.P., 2013. Delivering to urban online shoppers: the gains from "last-mile" pooling. *Supply Chain Forum: An International Journal* 14, 4, 22–31.

Echeverría, C., Coomes, D., Salas, J., Rey-Benayas, J.M., Lara, A., Newton, A., 2006. Rapid deforestation and fragmentation of chilean temperate forests. *Biological conservation* 130, 4, 481–494.

Egbue, O., Long, S., Samaranayake, V.A., 2017. Mass deployment of sustainable transportation: evaluation of factors that influence electric vehicle adoption. *Clean Technologies and Environmental Policy* 19, 7, 1927–1939.

Ehmke, J.F., Campbell, A.M., 2014. Customer acceptance mechanisms for home deliveries in metropolitan areas. *European Journal of Operational Research* 233, 1, 193–207.

Eiswerth, M.E., Van Kooten, G.C., 2007. Dynamic programming and learning models for management of a nonnative species. *Canadian Journal of Agricultural Economics/Revue canadienne d'agroeconomie* 55, 4, 485–498.

Elith, J., 2015. Predicting distributions of invasive species.

Elkington, J., Rowlands, I.H., 1999. Cannibals with forks: the triple bottom line of 21st century business. *Alternatives Journal* 25, 4, 42.

Emeç, U., Çatay, B., Bozkaya, B., 2016. An adaptive large neighborhood search for an e-grocery delivery routing problem. *Computers & Operations Research* 69, 109–125.

Epanchin-Niell, R.S., Hastings, A., 2010. Controlling established invaders: integrating economics and spread dynamics to determine optimal management. *Ecology Letters* 13, 4, 528–541.

Epanchin-Niell, R.S., Wilen, J.E., 2012. Optimal spatial control of biological invasions. *Journal of Environmental Economics and Management* 63, 2, 260–270.

Faugere, L., Montreuil, B., 2016. Hyperconnected city logistics: Smart lockers terminals & last mile delivery networks. In *Proceedings of the 3rd International Physical Internet Conference, Atlanta, GA, USA*, Vol. 29.

Firnkorn, J., Müller, M., 2011. What will be the environmental effects of new free-floating car-sharing systems? the case of car2go in ulm. *Ecological Economics* 70, 8, 1519–1528.

Folkestad, C.A., Hansen, N., Fagerholt, K., Andersson, H., Pantuso, G., 2020. Optimal charging and repositioning of electric vehicles in a free-floating carsharing system. *Computers & Operations Research* 113, 104771.

Formentin, S., Bianchessi, A.G., Savaresi, S.M., 2015. On the prediction of future vehicle locations in free-floating car sharing systems. In *Intelligent Vehicles Symposium (IV), 2015 IEEE*, IEEE, pp. 1006–1011.

Fricker, C., Gast, N., 2016. Incentives and redistribution in homogeneous bike-sharing systems with stations of finite capacity. *Euro Journal on Transportation and Logistics* 5, 3, 261–291.

Gambella, C., Malaguti, E., Masini, F., Vigo, D., 2018. Optimizing relocation operations in electric car-sharing. *Omega* 81, 234–245.

Garfinkel, R.S., Nemhauser, G.L., 1969. The set-partitioning problem: set covering with equality constraints. *Operations Research* 17, 5, 848–856.

Garrick, D., 2016. Car2go ceases san diego operations.

Ghosh-Dastidar, B., Cohen, D., Hunter, G., Zenk, S.N., Huang, C., Beckman, R., Dubowitz, T., 2014. Distance to store, food prices, and obesity in urban food deserts. *American Journal of Preventive Medicine* 47, 5, 587–595.

Ghosh-Dastidar, M., Hunter, G., Collins, R.L., Zenk, S.N., Cummins, S., Beckman, R., Nugroho, A.K., Sloan, J.C., Dubowitz, T., 2017. Does opening a supermarket in a food desert change the food environment? *Health & Place* 46, 249–256.

Gottlieb, R., Fisher, A., 1996. Food access for the transit-dependent. *ACCESS Magazine* 1, 9, 18–20.

Guisan, A., Tingley, R., Baumgartner, J.B., Naujokaitis-Lewis, I., Sutcliffe, P.R., Tulloch, A.I., Regan, T.J., Brotons, L., McDonald-Madden, E., Mantyka-Pringle, C., et al., 2013. Predicting species distributions for conservation decisions. *Ecology letters* 16, 12, 1424–1435.

Haider, Z., Nikolaev, A., Kang, J.E., Kwon, C., 2018. Inventory rebalancing through pricing in public bike sharing systems. *European Journal of Operational Research* 270, 1, 103–117.

Haight, R.G., Polasky, S., 2010. Optimal control of an invasive species with imperfect information about the level of infestation. *Resource and Energy Economics* 32, 4, 519–533.

Haight, R.G., Revelle, C.S., Snyder, S.A., 2000. An integer optimization approach to a probabilistic reserve site selection problem. *Operations Research* 48, 5, 697–708.

Haight, R.G., Snyder, S.A., 2009. Integer programming methods for reserve selection and design. *Spatial conservation prioritization: quantitative methods and computational tools.(A Moilanen, KA Wilson, HP Possingham, eds.). Oxford University Press, New York, NY* pp. 43–57.

Hastings, A., Hall, R.J., Taylor, C.M., 2006. A simple approach to optimal control of invasive species. *Theoretical Population Biology* 70, 4, 431–435.

He, L., Hu, Z., Zhang, M., 2019a. Robust repositioning for vehicle sharing. *Manufacturing & Service Operations Management* in print.

He, L., Ma, G., Qi, W., Wang, X., 2019b. Charging electric vehicle sharing fleet. *Manufacturing and Service Operations Management* forthcoming.

He, L., Mak, H.Y., Rong, Y., Shen, Z.J.M., 2017. Service region design for urban electric vehicle sharing systems. *Manufacturing & Service Operations Management* 19, 2, 309–327.

Herrmann, S., Schulte, F., Voß, S., 2014. Increasing acceptance of free-floating car sharing systems using smart relocation strategies: a survey based study of car2go hamburg. In *International Conference on Computational Logistics*, Springer, pp. 151–162.

Hobbs, J.E., 2020. Food supply chains during the covid-19 pandemic. *Canadian Journal of Agricultural Economics/Revue canadienne d'agroeconomie*

Hof, J., 1998. Optimizing spatial and dynamic population-based control strategies for invading forest pests. *Natural Resource Modeling* 11, 3, 197–216.

Hungerländer, P., Rendl, A., Truden, C., 2017. On the slot optimization problem in on-line vehicle routing. *Transportation Research Procedia* 27, 492–499.

International Union for Conservation of Nature, 2017. The IUCN Red List of Threatened Species.

Jafari, N., Hearne, J., 2013. A new method to solve the fully connected reserve network design problem. *European Journal of Operational Research* 231, 1, 202–209.

Jafari, N., Nuse, B.L., Moore, C.T., Dilkina, B., Hepinstall-Cymerman, J., 2017. Achieving full connectivity of sites in the multiperiod reserve network design problem. *Computers & Operations Research* 81, 119–127.

Jian, S., Rey, D., Dixit, V., 2016. Dynamic optimal vehicle relocation in carshare systems. *Transportation Research Record: Journal of the Transportation Research Board* , 2567, 1–9.

Kalkanci, B., Rahmani, M., Toktay, L.B., 2019. The role of inclusive innovation in promoting social sustainability. *Production and Operations Management* 28, 12, 2960–2982.

Kek, A.G., Cheu, R.L., Meng, Q., Fung, C.H., 2009. A decision support system for vehicle relocation operations in carsharing systems. *Transportation Research Part E: Logistics and Transportation Review* 45, 1, 149–158.

Khan, M., Kar, N.C., 2009. Hybrid electric vehicles for sustainable transportation: A canadian perspective. *World electric vehicle journal* 3, 3, 551–562.

Kim, S.W., Mak, H.Y., Olivares, M., Rong, Y., 2019. Empirical investigation on the range anxiety for electric vehicles. *Working Paper*

Klapp, M.A., Erera, A.L., Toriello, A., 2019. Order acceptance in same-day delivery,

Klein, R., Neugebauer, M., Ratkovitch, D., Steinhardt, C., 2019. Differentiated time slot pricing under routing considerations in attended home delivery. *Transportation Science* 53, 1, 236–255.

Kodransky, M., Lewenstein, G., 2014. Connecting Low-Income People to Opportunity with Shared Mobility. *Report produced for Living Cities. New York, NY: Institute for Transportation & Development Policy*

Köhler, C., Ehmke, J.F., Campbell, A.M., 2020. Flexible time window management for attended home deliveries. *Omega* 91, 102023.

Köhler, C., Haferkamp, J., 2019. Evaluation of delivery cost approximation for attended home deliveries. *Transportation Research Procedia* 37, 67–74.

Kotani, K., Kakinaka, M., Matsuda, H., 2011. Optimal invasive species management under multiple uncertainties. *Mathematical Biosciences* 233, 1, 32–46.

Kypriadis, D., Pantziou, G., Konstantopoulos, C., Gavalas, D., 2018. Minimum walking static repositioning in free-floating electric car-sharing systems. IEEE, pp. 1540–1545.

Lang, T., Barling, D., 2012. Food security and food sustainability: reformulating the debate. *The Geographical Journal* 178, 4, 313–326.

Laporte, G., Meunier, F., Calvo, R.W., 2015. Shared mobility systems. *4OR* 13, 4, 341–360.

Le Vine, S., Polak, J., 2017. The impact of free-floating carsharing on car ownership: Early-stage findings from london. *Transport Policy*

Levinson, R.S., West, T.H., 2018. Impact of public electric vehicle charging infrastructure. *Transportation Research Part D: Transport and Environment* 64, 158–177.

Lim, M.K., Mak, H.Y., Rong, Y., 2015. Toward mass adoption of electric vehicles: Impact of the range and resale anxieties. *Manufacturing & Service Operations Management* 17, 1, 101–119.

Lin, J., Chen, Q., Kawamura, K., 2013. Environmental and energy benefits of freight delivery consolidation in urban area. Technical report.

Lin, S., 1965. Computer solutions of the traveling salesman problem. *Bell System Technical Journal* 44, 10, 2245–2269.

Loose, W., 2010. The state of european car-sharing. *Project Momo Final Report D* 2.

Luo, Z., Liu, M., Lim, A., 2019. A two-phase branch-and-price-and-cut for a dial-a-ride problem in patient transportation. *Transportation Science* 53, 1, 113–130.

Lyft, 2019. Lyft launches grocery access program in select markets.

Magana, G., 2020. Online grocery shopping report 2020: Market stats and delivery trends for ecommerce groceries. *Business Insider*

Margules, C.R., Pressey, R.L., 2000. Systematic conservation planning. *Nature* 405, 6783, 243–253.

Mark, S., Lambert, M., O'Loughlin, J., Gray-Donald, K., 2012. Household income, food insecurity and nutrition in canadian youth. *Canadian Journal of Public Health* 103, 2, 94–99.

Martin, E., Shaheen, S., Lidicker, J., 2010. Impact of carsharing on household vehicle holdings: Results from north american shared-use vehicle survey. *Transportation Research Record: Journal of the Transportation Research Board* , 2143, 150–158.

Megiddo, N., Supowit, K.J., 1984. On the complexity of some common geometric location problems. *SIAM Journal on Computing* 13, 1, 182–196.

Memtsas, D.P., 2003. Multiobjective programming methods in the reserve selection problem. *European Journal of Operational Research* 150, 3, 640–652.

MonitorDeloitte., 2017. Car sharing in europe: Business models, national variations and upcoming variations.

Morganti, E., Dablanc, L., Fortin, F., 2014a. Final deliveries for online shopping: The deployment of pickup point networks in urban and suburban areas. *Research in Transportation Business & Management* 11, 23–31.

Morganti, E., Seidel, S., Blanquart, C., Dablanc, L., Lenz, B., 2014b. The impact of e-commerce on final deliveries: alternative parcel delivery services in france and germany. *Transportation Research Procedia* 4, 0, 178–190.

Nair, D.J., Grzybowska, H., Fu, Y., Dixit, V.V., 2018. Scheduling and routing models for food rescue and delivery operations. *Socio-Economic Planning Sciences* 63, 18–32.

Nair, D.J., Rey, D., Dixit, V.V., 2017. Fair allocation and cost-effective routing models for food rescue and redistribution. *IISE Transactions* 49, 12, 1172–1188.

National Center for Chronic Disease Prevention and Health Promotion, 2011. State initiatives supporting healthier food retail: An overview of the national landscape,

Netzer, T., Krause, J., Hausmann, L., Bauer, F., Ecker, T., 2017. The urban delivery bet: Usd 5 billion in venture capital at risk. *McKinsey & Company, Travel, Transport and Logistics, Market report*

Obama, F.L.M., 2012. Let's move! raising a healthier generation of kids. *Childhood Obesity* 8, 1, 1.

Olsson, E.G.A., 2018. Urban food systems as vehicles for sustainability transitions. *Bulletin of Geography. Socio-economic Series* 40, 40, 133–144.

Parnell, S., Schewenius, M., Sendstad, M., Seto, K.C., Wilkinson, C., 2013. *Urbanization, biodiversity and ecosystem services: challenges and opportunities*. Springer, Dordrecht.

PBS, 2014. Why it takes more than a grocery store to eliminate a 'food desert'. *PBS NewsHour*

Pejchar, L., Mooney, H.A., 2009. Invasive species, ecosystem services and human well-being. *Trends in Ecology & Evolution* 24, 9, 497–504.

Pelletier, S., Jabali, O., Laporte, G., 2018. Charge scheduling for electric freight vehicles. *Transportation Research Part B: Methodological* 115, 246–269.

Pendall, R., Blumenberg, E., Dawkins, C., 2016. What if cities combined car-based solutions with transit to improve access to opportunity? *The Urban Institute*

Perron, L., Furnon, V., 2019. Google OR-Tools.

Pfrommer, J., Warrington, J., Schildbach, G., Morari, M., 2014. Dynamic vehicle redistribution and online price incentives in shared mobility systems. *Intelligent Transportation Systems, IEEE Transactions on* 15, 4, 1567–1578.

Plesník, J., 1987. A heuristic for the p-center problems in graphs. *Discrete Applied Mathematics* 17, 3, 263–268.

Polasky, S., Camm, J.D., Solow, A.R., Csuti, B., White, D., Ding, R., 2000. Choosing reserve networks with incomplete species information. *Biological Conservation* 94, 1, 1–10.

Polasky, S., Nelson, E., Camm, J., Csuti, B., Fackler, P., Lonsdorf, E., Montgomery, C., White, D., Arthur, J., Garber-Yonts, B., et al., 2008. Where to put things? spatial land management to sustain biodiversity and economic returns. *Biological Conservation* 141, 6, 1505–1524.

Prieto, M., Baltas, G., Stan, V., 2017. Car sharing adoption intention in urban areas: What are the key sociodemographic drivers? *Transportation Research Part A: Policy and Practice* 101, 218–227.

Psaraftis, H.N., 1983. k-interchange procedures for local search in a precedence-constrained routing problem. *European Journal of Operational Research* 13, 4, 391–402.

Raviv, T., Tzur, M., Forma, I.A., 2013. Static repositioning in a bike-sharing system: models and solution approaches. *EURO Journal on Transportation and Logistics* 2, 3, 187–229.

ReVelle, C.S., Williams, J.C., Boland, J.J., 2002. Counterpart models in facility location science and reserve selection science. *Environmental Modeling and Assessment* 7, 2, 71–80.

Rockett, D., 2020. In Chicago-area food deserts, it's getting even harder for residents to find fresh, healthy groceries because of the coronavirus. *Chicago Tribune*

Rodrigues, A.S., Andelman, S.J., Bakarr, M.I., Boitani, L., Brooks, T.M., Cowling, R.M., Fishpool, L.D., Da Fonseca, G.A., Gaston, K.J., Hoffmann, M., et al., 2004. Effectiveness of the global protected area network in representing species diversity. *Nature* 428, 6983, 640–643.

Rout, T.M., Moore, J.L., McCarthy, M.A., 2014. Prevent, search or destroy? a partially observable model for invasive species management. *Journal of applied ecology* 51, 3, 804–813.

Sanchez, A.B.T., 2016. Car sharing as an alternative to car ownership: opportunities for carsharing organizations and low-income communities. Ph.D. thesis.

Santos, A.G., Cândido, P.G., Balardino, A.F., Herbawi, W., 2017. Vehicle relocation problem in free floating carsharing using multiple shuttles. In *Evolutionary Computation (CEC), 2017 IEEE Congress on*, IEEE, pp. 2544–2551.

Savelsbergh, M., Van Woensel, T., 2016. 50th anniversary invited article–city logistics: Challenges and opportunities. *Transportation Science* 50, 2, 579–590.

Schulte, F., Voß, S., 2015. Decision support for environmental-friendly vehicle relocations in free-floating car sharing systems: The case of car2go. *Procedia CIRP* 30, 275–280.

Shaheen, S., Cohen, A., 2007. Growth in worldwide carsharing: An international comparison. *Transportation Research Record: Journal of the Transportation Research Board* , 1992, 81–89.

Simoni, M.D., Bujanovic, P., Boyles, S.D., Kutanoglu, E., 2018. Urban consolidation solutions for parcel delivery considering location, fleet and route choice. *Case Studies on Transport Policy* 6, 1, 112–124.

Snyder, S., ReVelle, C., Haight, R., 2004. One-and two-objective approaches to an area-constrained habitat reserve site selection problem. *Biological Conservation* 119, 4, 565–574.

Snyder, S.A., Haight, R.G., ReVelle, C.S., 2005. A scenario optimization model for dynamic reserve site selection. *Environmental Modeling and Assessment* 9, 3, 179–187.

Southey, F., 2020. Food insecurity: How covid-19 is exacerbating a crisis already on a 'knife-edge'.

Starr, M.K., Van Wassenhove, L.N., 2014. Introduction to the special issue on humanitarian operations and crisis management. *Production and Operations Management* 23, 6, 925–937.

Strange, N., Thorsen, B.J., Bladt, J., 2006. Optimal reserve selection in a dynamic world. *Biological Conservation* 131, 1, 33–41.

Syed, S.T., Gerber, B.S., Sharp, L.K., 2013. Traveling towards disease: transportation barriers to health care access. *Journal of Community Health* 38, 5, 976–993.

Tang, C.S., Zhou, S., 2012. Research advances in environmentally and socially sustainable operations. *European Journal of Operational Research* 223, 3, 585–594.

Tarasuk, V., Reynolds, R., 1999. A qualitative study of community kitchens as a response to income-related food insecurity. *Canadian Journal of Dietetic Practice and Research* 60, 1, 11.

Thomas, L., 2019. Walmart is expanding its 'unlimited' grocery delivery service nationwide. *CNBC*

Toth, P., Vigo, D., 2002. Models, relaxations and exact approaches for the capacitated vehicle routing problem. *Discrete Applied Mathematics* 123, 1-3, 487–512.

Tóth, S.F., Haight, R.G., Rogers, L.W., 2011. Dynamic reserve selection: Optimal land retention with land-price feedbacks. *Operations Research* 59, 5, 1059–1078.

Tyndall, J., 2017. Where no cars go: Free-floating carshare and inequality of access. *International journal of sustainable transportation* 11, 6, 433–442.

Uden, D.R., Allen, C.R., Angeler, D.G., Corral, L., Fricke, K.A., 2015. Adaptive invasive species distribution models: a framework for modeling incipient invasions. *Biological invasions* 17, 10, 2831–2850.

USDA, 2019. USDA ERS - documentation.

USDA, 2020. FNS launches the online purchasing pilot.

Varney, V., 2019. The solution to food deserts isn't more supermarkets - it's better transport.

Ver Ploeg, M., Breneman, V., Dutko, P., Williams, R., Snyder, S., Dicken, C., Kaufman, P., 2012. Access to affordable and nutritious food: Updated estimates of distance to supermarkets using 2010 data. Technical report.

Voccia, S.A., Campbell, A.M., Thomas, B.W., 2019. The same-day delivery problem for online purchases. *Transportation Science* 53, 1, 167–184.

Walker, R.E., Keane, C.R., Burke, J.G., 2010. Disparities and access to healthy food in the United States: A review of food deserts literature. *Health & place* 16, 5, 876–884.

Walmart, 2020. Find a store near you | walmart. com.

Wang, Y., Önal, H., 2015. Optimal design of compact and connected nature reserves for multiple species. *Conservation Biology*

Wang, Y., Ong, T., Lee, L.H., Chew, E.P., 2017. Capacitated competitive facility location problem of self-collection lockers by using public big data. IEEE, pp. 1344–1344.

Wegener, M., 2013. The future of mobility in cities: Challenges for urban modelling. *Transport Policy* 29, 275–282.

Weikl, S., Bogenberger, K., 2013. Relocation strategies and algorithms for free-floating car sharing systems. *IEEE Intelligent Transportation Systems Magazine* 5, 4, 100–111.

Weikl, S., Bogenberger, K., 2015. A practice-ready relocation model for free-floating carsharing systems with electric vehicles–mesoscopic approach and field trial results. *Transportation Research Part C: Emerging Technologies* 57, 206–223.

Westphal, M.I., Field, S.A., Possingham, H.P., 2007. Optimizing landscape configuration: a case study of woodland birds in the mount lofty ranges, south australia. *Landscape and Urban Planning* 81, 1, 56–66.

Widener, M.J., 2018. Spatial access to food: Retiring the food desert metaphor. *Physiology & Behavior* 193, 257–260.

Williams, J.C., ReVelle, C.S., Levin, S.A., 2005. Spatial attributes and reserve design models: a review. *Environmental Modeling and Assessment* 10, 3, 163–181.

Yang, X., Strauss, A.K., Currie, C.S.M., Eglese, R., 2016. Choice-based demand management and vehicle routing in e-fulfillment. *Transportation Science* 50, 2, 473–488.

Zorbas, C., McCartan, J., De Mel, R., Narendra, K., Tassone, E.C., Yin, E., Palermo, C., 2018. Engaging a disadvantaged community with a fruit and vegetable box scheme. *Health Promotion Journal of Australia* 29, 1, 108–110.

Appendix A: Copyright Permissions

Appendix A1: Reprint Permission for Chapter 4

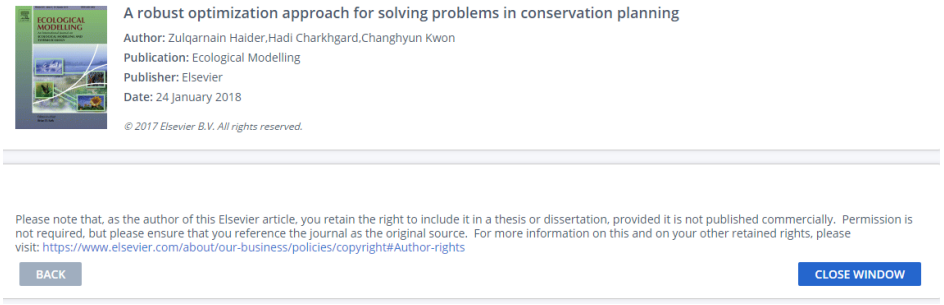

Reprint Permission for Chapter 4

Appendix B: Proofs of Chapter 2

B1: Two-Interchange Algorithm for Multiple Precedence Constraints

We present a customised 2-interchange algorithm which draws from a 2-interchange procedure for Dial-A-Ride Problem (DARP) presented in Psaraftis (1983). A DARP involves a vehicle picking up and dropping off multiple customers. A DARP tour, unlike that of a Travelling Salesman Problem (TSP) (Lin, 1965), must satisfy precedence constraints since origin of each customer must precede his/her destination on the route. In our problem, the EVs are equivalent to customers in DARP. Contrary to a customer in DARP, each EV moves multiple times through the nodes on its route. Therefore, a shuttle must satisfy multiple precedence constraints for each EV. We borrow and extend the notation used in Psaraftis (1983).

A given shuttle route r of length $M = \text{length}(r)$ can be described as a sequence $\left(\hat{\mathcal{S}}_1, \hat{\mathcal{S}}_2, \ldots, \hat{\mathcal{S}}_i, \ldots, \hat{\mathcal{S}}_M\right)$ where i represents the i-th stop of the route and $\hat{\mathcal{S}}_i$ is defined using the following symbolic values:

$$\hat{\mathcal{S}}_i = \begin{cases} 0 & \text{if } i = 1 \text{ or } i = M \text{ (Depots)} \\ n^{+} & \text{if shuttle visits supplier node of EV } n \text{ at node } i \\ n^{>} & \text{if shuttle visits charger node of EV } n \text{ at node } i \\ n^{<} & \text{if shuttle visits dummy charger node of EV } n \text{ at node } i \\ n^{-} & \text{if shuttle visits demander node of EV } n \text{ at node } i \end{cases}$$

$\forall \; i = 1, 2, \ldots, M$

Alternativelty, the shuttle route can be represented through matrix $[m(n,i)]$ where $m(n,i)$ is the status of EV n at the i-th stop of the shuttle tour.

$$m(n,i) = \begin{cases} 5 & \text{if supplier for EV } n \text{ has not been visited so far.} \\ 4 & \text{if charger for EV } n \text{ has not been visited so far.} \\ 3 & \text{if dummy charger for EV } n \text{ has not been visited so far.} \\ 2 & \text{if demander for EV } n \text{ has not been visited so far.} \\ 1 & \text{if route for EV } n \text{ has been completed.} \end{cases}$$

$(n = \text{EV number},\ i = 1, 2, \ldots, M)$.

Given an initial route r, a 2-interchange swapping algorithm works by interchanging two links in the route with two other links. For a given route r and a proposed swap (i, j), a new route r_{new} can be constructed by substituting two links. Link $i \to i+1$ is substituted with $i \to j$, while $j \to j+1$ is substituted with $i+1 \to j+1$. Since direction of segment $(i+1 \to \cdots \to j)$ is now reversed, it is necessary to check precedence feasibility. The shuttle also picks up and drops off the drivers at each node it visits. Therefore, a proposed 2-interchange must also be feasible in terms of number of drivers on the shuttle. Furthermore, a proposed 2-interchange must also improve (decrease) the length of the shuttle route.

Given a route r and a proposed interchange (i, j), we next describe the steps for `PrecedenceFeasibilityCheck(`r_{new}`)`, `CapacityFeasibilityCheck(`r_{new}`)` and `RouteImprovement(`r, r_{new}`)`. Let us also consider a small example to illustrate the steps of the 2-interchange procedure. We consider 4 EVs with the following paths: $11 \to 2$, $40 \to 15$, $23 \to 16 \to 47 \to 4$ and $24 \to 13 \to 46 \to 12$. EVs 1 and 2 have direct paths while EVs 3 and 4 visit interdmediate charging stations.

Algorithm 4: A customized 2-interchange procedure for finding 2-optimal shuttle route

Input: q; set of EV paths $\mathcal{X}$; Iter = number of 2-interchange iterations
Output: **z**

Given $\mathcal{X}$, use `GreedyProcedure(`$\mathcal{X}$`)`to obtain an initial route r as an array $r[1], r[2], \cdots, r[\text{end}]$;
for $k \leftarrow 1$ **to** Iter **do**
    $\Delta \leftarrow 0$;
    for $i \leftarrow 1$ **to** length$(r) - 3$ **do**
        for $j \leftarrow i + 2$ **to** length$(r) - 1$ **do**
            `// Swapping nodes` $i+1$ `and` j `and reversing nodes between them`
            $r_{\text{new}} \leftarrow \text{copy}(r)$;
            $r_{\text{new}}[i+1 : j] \leftarrow r_{\text{new}}[j : i+1]$;
            if ¬`PrecedenceFeasibilityCheck(`r_{new}`)` **then** `// for synchronization`
                continue ;
            if ¬`CapacityFeasibilityCheck(`r_{new}`)` **then** `// for driver availability`
                continue ;
            $\Delta_{ij} \leftarrow$ `RouteImprovement(`r, r_{new}`)`;
            if $\Delta_{ij} > \Delta$ **then**
                $\Delta \leftarrow \Delta_{ij}$, $r_{\text{best}} \leftarrow r_{\text{new}}$;
    $r \leftarrow r_{\text{best}}$;
Given route r, generate a vector **z**.

B1.1: GreedyProcedure($\mathcal{X}$)

Given a set of EV paths, we use the procedure described in Algorithm 5 to construct an initial route r. The initial shuttle route for the example with 4 EV routes is shown in Table B.1.

Algorithm 5: `GreedyProcedure(`$\mathcal{X}$`)`: Greedy algorithm for finding initial shuttle route

Input: $\mathcal{X}$ = set of EV routes, q, y = current number of drivers, $\mathcal{V} \leftarrow \{\}$
Output: $r = [r[1], r[2], \cdots, r[\text{end}]]$

$j \leftarrow 1$;
$r[j] \leftarrow 0, y \leftarrow q$;
$j \leftarrow j + 1$;
foreach $x \in \mathcal{X}$ **do**
    while $y \geq 1$ **do**
        $r[j] \leftarrow \{\mathcal{S}(x)\}$;
        $y \leftarrow y - 1$;
        $j \leftarrow j + 1$;
    while $y \leq q - 1$ **do**
        $r[j] \leftarrow \{\mathcal{C}(x)\}$;
        $y \leftarrow y + 1$;
        $j \leftarrow j + 1$;
foreach $x \in \mathcal{X}$ **do**
    while $y \geq 1$ **do**
        $r[j] \leftarrow \{\mathcal{C}^d(x)\}$;
        $y \leftarrow y - 1$;
        $j \leftarrow j + 1$;
    while $y \leq q - 1$ **do**
        $r[j] \leftarrow \{\mathcal{D}(x)\}$;
        $y \leftarrow y + 1$;
        $j \leftarrow j + 1$;
end $\leftarrow j$;
$r[\text{end}] \leftarrow 0$;

B1.2: PrecedenceFeasibilityCheck(r_{new})

For a given shuttle route to be precedence feasible, the supplier of each EV route must be visited before the charger, which in turn must be visited before the dummy charger and finally the dummy charger must be visited before the demander. Therefore, for each EV n, there are three precedence constraints. We can use the matrix $m(n, i)$ to ensure the feasibility of all three precedence constraints. Given a proposed 2-interchange (i, j), assume that for an EV n, $m(n, i) = 5$ and $m(n, j) = 3$. This implies that the supplier for EV n has not been visited at node i but the charger has already been visited before node j. It follows then that the supplier and charger nodes for EV n lie within the shuttle route segment $(i + 1 \rightarrow \cdots \rightarrow j)$.

Since performing the 2-interchange (i, j) will reverse the direction of traversal on segment $(i+1 \rightarrow \cdots \rightarrow j)$, the charger node will be visited before the supplier node. This will violate the first precedence constraint for EV n. Similarly, if $m(n, i) = 4$ and $m(n, j) = 2$, the proposed 2-interchange (i, j) will result in the dummy charger node being visited before the charger node of an EV n, violating the second precedence feasibility constraint.

Normally, performing the feasibility check will require $O(N^3)$ time since we must perform $O(N)$ checks for each 2-interchange. However, the computational complexity can be reduced to $O(N^2)$ by performing a customized version of *screening* procedure described in Psaraftis (1983). For a given tour r and a given stop i $(1 \leq i \leq M-2)$, we define FIRSTSTOP(i) to be the position of the first stop (charger) beyond node $(i+1)$ for which the corresponding EV supplier has not been visited including and up to node i. If no such stop exists, FIRSTSTOP(i) $= M$. Similarly, we define SECONDSTOP(i) to be the position of the second stop (dummy charger) beyond node $(i+1)$ for which the corresponding EV charger has not been visited including and up to node i. If no such stop exists, SECONDSTOP(i) $= M$.

Finally, we define THIRDSTOP(i) to be the position of the third stop (demander) beyound node $(i+1)$ for which the corresponding EV dummy-charger has not been visited including and up to node i. If no such stop exists, THIRDSTOP(i) $= M$. Mathematically, FIRSTSTOP(i) $= h$ if h is the smallest number above $(i+1)$ for which there exists an EV n so that $m(n, i) = 5$ and $m(n, h) = 3$. If no such EV exists, the $h = M$. Similarly, SECONDSTOP(i) $= h$ if h is the smallest number above $(i+1)$ for which there exists an EV n so that $m(n, i) = 4$ and $m(n, h) = 2$. If no such EV exists, the $h = M$. Finally, THIRDSTOP(i) $= h$ if h is the smallest number above $(i+1)$ for which there exists an EV n so that $m(n, i) = 3$ and $m(n, h) = 1$. If no such EV exists, the $h = M$. Theorem 1 describes the test for precedence feasibility check for a proposed 2-interchange (i, j).

Theorem 1. The exchange (i, j) is precedence feasible if and only if $j <$ FIRSTSTOP(i) and $j <$ SECONDSTOP(i) and $j <$ THIRDSTOP(i).

Proof. Proof. This theorem is similar to the result of (Psaraftis, 1983). The proof is obvious and hence omitted. □

The screening part of the 2-interchange algorithm can be summarized as follows:

Algorithm 6: Screening Procedure for Prercedence Feasibility Check for a Proposed 2-Interchange

Input: FIRSTSTOP(i), SECONDSTOP(i), THIRDSTOP(i)
Output: TF(i, j)

```
1 for i ← 1 to M − 2 do
2     for j ← i + 1 to M do
3         if j < FIRSTSTOP(i) and j < SECONDSTOP(i) and j < THIRDSTOP(i)
           then
4             TF(i, j) ← 'true' ;
5         else
6             TF(i, j) ← 'false' ;
```

The values for $m(n, i)$, $\hat{\mathcal{S}}_i$, FIRSTSTOP(i), SECONDSTOP(i), THIRDSTOP(i), and the matrix TF(i, j) for the small example are calculated in Table B.1.

We use a depth first procedure to select the best interchange. The TF(i, j) matrix checks for precedence feasibility for all possible (i, j) swaps given an initial route r. The precedence feasible swaps are shown as T in the table. We next apply capacity feasibility check and improvement check on this set of routes.

Table B.1 – An Example Illustrating the Screening Procedure for Precedence Feasibility Check

i	1	2	3	4	5	6	7	8	9	10	11	12	13	14
Type	**	S	S	S	S	C	C	DC	DC	D	D	D	D	**
Node, $r[i]$	0	11	40	23	24	16	13	47	46	2	15	4	12	0
$\hat{\mathcal{S}}_i$	0	1^+	2^+	3^+	4^+	$3^>$	$4^>$	$3^<$	$4^<$	1^-	2^-	3^-	4^-	0
$m(1,i)$	5	4	4	4	4	4	4	4	4	3	3	3	3	3
$m(2,i)$	5	5	4	4	4	4	4	4	4	4	3	3	3	3
$m(3,i)$	5	5	5	4	4	3	3	2	2	2	2	1	1	1
$m(4,i)$	5	5	5	5	4	4	3	3	2	2	2	2	1	1
FIRSTSTOP[i]	6	6	6	7	14	14	14	14	14	14	14	14	14	14
SECONDSTOP[i]	14	14	14	8	8	9	14	14	14	14	14	14	14	14
THIRDSTOP[i]	14	14	14	14	14	12	12	13	14	14	14	14	14	14

i|j			**3**	**4**	**5**	**6**	**7**	**8**	**9**	**10**	**11**	**12**	**13**	**14**
1			T	T	T	F	F	F	F	F	F	F	F	F
2				T	T	F	F	F	F	F	F	F	F	F
3					T	F	F	F	F	F	F	F	F	F
4						T	F	F	F	F	F	F	F	F
5							T	F	F	F	F	F	F	F
6								T	F	F	F	F	F	F
7									T	T	T	F	F	F
8										T	T	T	F	F
9											T	T	T	F
10												T	T	F
11													T	F
12														F

Table B.2 – An Example Illustrating the Capacity Feasibility Check for Interchange (7, 10)
.

i	1	2	3	4	5	6	7	8	9	10	11	12	13	14
Node, $r[i]$	0	11	40	23	24	16	13	47	46	2	15	4	12	0
Type	**	S	S	S	S	C	C	DC	DC	D	D	D	D	**
y_i^{old}	4	3	2	1	0	1	2	1	0	1	2	3	4	4
i	1	2	3	4	5	6	7	10	9	8	11	12	13	14
Node, $r_{\text{new}}[i]$	0	11	40	23	24	16	13	2	46	47	15	4	12	0
Type	**	S	S	S	S	C	C	D	DC	DC	D	D	D	**
y_i^{new}	4	3	2	1	0	1	2	3	2	1	2	3	4	3

B1.3: CapacityFeasibilityCheck(r_{new})

The capacity feasibility check is done to ensure that the proposed 2-interchange does not cause the number of drivers to drop below zero or jump above the capacity q. A given shuttle route r begins at the depot with q drivers. A driver is dropped at each supplier and dummy charger node and one is picked from each charger and demander node. Given a proposed 2-interchange (i, j), and the new route r_{new}, the capacity only changes for the route segment $(j \to \cdots \to i + 1)$. Given y_i^{old}, i.e., the number of drivers at node i on the current shuttle route r, one can easily determine y_i^{new}, i.e., the number of drivers at node i for new shuttle route r_{new}.

If for a given node i on shuttle route, y_i^{new} falls below 0 or above capacity q, the proposed interchange (i, j) is deemed infeasible. For example, the proposed interchange $(7, 10)$ is capacity feasible as shown in Table B.2.

B1.4: RouteImprovement(r, r_{new})

A proposed two interchange (i, j) involves sustitution of two links $(i, i+1)$ and $(j, j+1)$ with two new links (i, j) and $(i+1, j+1)$. In traditional TSP and DARP problems, an interchange is considered to be improving or favorable if $t_{i,i+1}+t_{j,j+1} > t_{i,j}+t_{i+1,j+1}$. The improvement for an interchange (i, j) can simply be calculated as $t_{i,i+1}+t_{j,j+1}-(t_{i,j}+t_{i+1,j+1})$. The updated arrival times τ_j for the new route can be calculated by iteratively adding the link traversal times, i.e., $\tau_1 = 0$, $\tau_j = \tau_i + t_{ij}, \forall (i, j)$. In case of the synchronized EV relocation and shuttle routing problem presented in this paper, the improvement check is computationally more challenging. The arrival time of a shuttle at a demander node on an EV path $p \in \mathcal{X}$ depends on both the EV path length (l_p) and the shuttle arrival time on corresponding supplier node. This dependency is given by Equations (2.17) and (2.18). Therefore for a shuttle moving on link (i, j) the arrival time τ_j at node j is calculated as:

$$\tau_j = \begin{cases} \max(\tau_i + t_{ij}, \tau_l + l_p) & \text{if } \ p \in \mathcal{X}, l = \mathcal{S}(p), j = \mathcal{D}(p) \\ \tau_i + t_{ij} & \text{otherwise.} \end{cases}$$

Since a proposed interchange (i, j) reverses the shuttle traversal on segment $(i+1 \rightarrow \cdots \rightarrow j)$, a demander node contained in the segment may have its arrival time changed from $\tau_{i'} + t_{ij}$ to $\tau_{l'} + l_p$ or vice versa, owing to the change in its position. Similarly, a supplier node l' contained in the segment may have its arrival time changed due to change in its position on the route. If the supplier node belongs to path $p \in \mathcal{X}$, this change in τ'_l can also nonlinearly impact the shuttle arrival at the downstream demander node $j' = \mathcal{D}(p)$ and at any nodes after j' on the route. Therefore, improvement after a proposed 2-interchange can only be checked by fully calculating the shuttle arrival times at all nodes using the expression for τ_j given above. Let τ_M^{old} be the total route time for a given route r. Let τ_M^{new} be the total route time for the route r_{new}. The improvement Δ_{ij} can be calculated as: $\Delta_{ij} = \tau_M^{\text{new}} - \tau_M^{\text{old}}$.

Appendix C: Proofs of Chapter 4

C1: Robust Formulation of (D1)

Based on our discussion in Section 4.2, it is easy to show that the robust counterpart formulation of (D1) can be stated as:

$$\text{(R1)} \qquad \min \quad \sum_{i=1}^{M}\sum_{t=1}^{T} v_{it} \tag{1}$$

$$\sum_{i=1}^{M} x_{it} \le U \qquad \text{for } i = 1,\dots,T \tag{2}$$

$$v_{i0} = a_i \qquad \text{for } i = 1,\dots,M \tag{3}$$

$$v_{it} + b_{it}\sum_{t'=1}^{t} x_{ik} \ge \sum_{j=1}^{M} \bar{p}_{ji}(1+g)v_{jt-1} + z_{it}\Gamma_i^t + \sum_{j=1}^{M} q_{jit}$$

$$\text{for } i = 1,\dots,M \text{ and } t = 1,\dots,T \tag{4}$$

$$z_{it} + q_{jit} \ge \hat{p}_{ji}(1+g)v_{jt-1}$$

$$\text{for } i = 1,\dots,M \text{ and } j = 1,\dots,M \text{ and } t = 1,\dots,T \tag{5}$$

$$q_{jit} \ge 0 \qquad \text{for } i = 1,\dots,M \text{ and } j = 1,\dots,M \text{ and } t = 1,\dots,T \tag{6}$$

$$z_{it} \ge 0 \qquad \text{for } i = 1,\dots,M \text{ and } t = 1,\dots,T \tag{7}$$

$$v_{it} \ge 0 \qquad \text{for } i = 1,\dots,M \text{ and } t = 1,\dots,T \tag{8}$$

$$x_{it} \ge \{0,1\} \qquad \text{for } i = 1,\dots,M \text{ and } t = 1,\dots,T, \tag{9}$$

where Γ_i^t for $i = 1,\dots,M$ and $t = 1,\dots,T$ is a user-defined parameter showing the level of conservatism in constraint (4).

Note that we assume that b_{it} is sufficiently large, i.e., regardless of the value of v_{jt-1}, z_{it}, and q_{ijt} for $j = 1, \ldots, M$, $j = 1, \ldots, M$ and $t = 1, \ldots, T$, we must have that

$$b_{it} \geq \sum_{j=1}^{M} \bar{p}_{ji}(1+g)v_{jt-1} + z_{it}\Gamma_i^t + \sum_{j=1}^{M} q_{jit}.$$

Therefore, the value of b_{it} should be computed differently in (R1). This can be done using the following proposition.

Proposition 1. *Let* $\boldsymbol{u_{i,t-1}} := (u_{i,t-1}^1, u_{i,t-1}^2, \ldots, u_{i,t-1}^M)$ *such that* $u_{i,t-1}^j := \hat{p}_{ji}(1+g)b_{j,t-1}$ *for* $i = 1, \ldots, M$ *and* $t = 1, \ldots, T$. *Also, let* $u_{i,t-1}^{(j)}$ *be the* j*-th largest component of* $\boldsymbol{u_{i,t-1}}$. *For each,* $i \in \{1, \ldots, M\}$ *and* $t \in \{1, \ldots, T\}$, b_{it} *can be computed recursively by using*

$$b_{it} = \sum_{j=1}^{M} \bar{p}_{ji}(1+g)b_{jt-1} + \sum_{j=1}^{\Gamma_i^t} u_{it-1}^{(j)} + (\Gamma_i^t - \Gamma_i^t)u_{i,t-1}^{(\Gamma_i^t)},$$

and $b_{i0} = a_i$.

Proof. We first note that based on the discussion given in Section 4.2, (R1) is equivalent to

$$\min \quad \sum_{i=1}^{M}\sum_{t=1}^{T} v_{it} \tag{10}$$

$$\sum_{i=1}^{M} x_{it} \leq U \qquad \text{for } i = 1, \ldots, T \tag{11}$$

$$v_{i0} = a_i \qquad \text{for } i = 1, \ldots, M \tag{12}$$

$$v_{it} + b_{it}\sum_{t'=1}^{t} x_{ik} \geq \sum_{j=1}^{M} \bar{p}_{ji}(1+g)v_{jt-1} + \max_{\left\{S_i^t \cup \{r_{it}\}:\ S_i^t \subseteq J_i^t,\ |S_i^t| \leq \lfloor \Gamma_i^t \rfloor,\ r_{it} \in J_i^t \setminus S_i^t\right\}} \left\{ \sum_{j \in S_i^t} \hat{p}_{ji}(1+g)v_{jt-1} + (\Gamma_i^t - \lfloor \Gamma_i^t \rfloor)\hat{p}_{r_{it},i}(1+g)v_{r_{it},t-1} \right\}$$

$$\text{for } i = 1, \ldots, M \text{ and } t = 1, \ldots, T \tag{13}$$

$$v_{it} \geq 0 \qquad \text{for } i = 1, \ldots, M \text{ and } t = 1, \ldots, T \tag{14}$$

$$x_{it} \geq \{0, 1\} \qquad \text{for } i = 1, \ldots, M \text{ and } t = 1, \ldots, T. \tag{15}$$

Based on Constraints (13), b_{it} where $i \in \{1,\ldots,M\}$ and $t \in \{1,\ldots,T\}$ is sufficiently large if regardless of the value of v_{jt-1} for $j = 1,\ldots,M$, we have that

$$b_{it} \geq \sum_{j=1}^{M} \bar{p}_{ji}(1+g)v_{jt-1} + \max_{\left\{S_i^t \cup \{r_{it}\}:\ S_i^t \subseteq J_i^t,\ |S_i^t| \leq \lfloor \Gamma_i^t \rfloor,\ r_{it} \in J_i^t \setminus S_i^t\right\}} \left\{ \sum_{j \in S_i^t} \hat{p}_{ji}(1+g)v_{jt-1} + (\Gamma_i^t - \lfloor \Gamma_i^t \rfloor)\hat{p}_{r_{it},i}(1+g)v_{r_{it},t-1} \right\}.$$

It is evident that

$$\max_{\left\{S_i^t \cup \{r_{it}\}:\ S_i^t \subseteq J_i^t,\ |S_i^t| \leq \lfloor \Gamma_i^t \rfloor,\ r_{it} \in J_i^t \setminus S_i^t\right\}} \left\{ \sum_{j \in S_i^t} \hat{p}_{ji}(1+g)v_{jt-1} + (\Gamma_i^t - \lfloor \Gamma_i^t \rfloor)\hat{p}_{r_{it},i}(1+g)v_{r_{it},t-1} \right\} \leq \sum_{j=1}^{\Gamma_i^t} u_{it-1}^{(j)} + (\Gamma_i^t - \Gamma_i^t)u_{i,t-1}^{(\Gamma_i^t)},$$

for $i = 1,\ldots,M$ and $t = 1,\ldots,T$. So, the result follows. □

C2: Robust Formulation of (D2)

Based on our discussion in Section 4.2, it is easy to show that the robust counterpart formulation of (D2) can be stated as:

$$\text{(R2)} \qquad \min \quad \sum_{i=1}^{M} c_i x_i \tag{16}$$

$$\sum_{i=1}^{M} \bar{w}_{ik} x_i - z_k \Gamma_k - \sum_{i=1}^{M} q_{ik} \geq W_k \quad \text{for } k = 1,\ldots,K \tag{17}$$

$$z_k + q_{ik} \geq \hat{w}_{ik} x_i \quad \text{for } i = 1,\ldots,M \text{ and } k = 1,\ldots,K \tag{18}$$

$$q_{ik} \geq 0 \quad \text{for } i = 1,\ldots,M \text{ and } k = 1,\ldots,K \tag{19}$$

$$z_k \geq 0 \quad \text{for } k = 1,\ldots,K \tag{20}$$

$$x_i \in \{0,1\} \quad \text{for } i = 1,\ldots,M, \tag{21}$$

where Γ_k for $k = 1, \ldots, K$ is a user-defined parameter showing the level of conservatism in Constraint (17).

C3: Revised Robust Formulation of (D2)

It is evident from Constraint (17) that the term $-z_k\Gamma_k - \sum_{i=1}^{M} q_{ik}$ cannot take a positive value and so it can force more x_i to take the value of 1 (in comparison to (D2)). However, this in itself can force the value of $-z_k\Gamma_k - \sum_{i=1}^{M} q_{ik}$ to become even more negative due to Constraint (18). Thus, it is possible for (R2) to be infeasible. The higher the degree of uncertainty in (R2), i.e., larger the values of $\hat{w}_{ik}$ and Γ_k for $i = 1, \ldots, M$ and $k = 1, \ldots, K$, larger the probability of this outcome arising.

So, to deal with infeasibility of (R2), we propose a revised formulation as follows:

$$\text{(R3)} \qquad \min \quad \sum_{i=1}^{M} c_i x_i \tag{22}$$

$$\min \quad \sum_{i=1}^{M} \sum_{k=1}^{K} \epsilon_{ik} \tag{23}$$

$$\sum_{i=1}^{M} \bar{w}_{ik} x_i - z_k\Gamma_k - \sum_{i=1}^{M} q_{ik} \geq W_k \quad \text{for } k = 1, \ldots, K \tag{24}$$

$$z_k + q_{ik} \geq (\hat{w}_{ik} - \epsilon_{ik}) x_i \quad \text{for } i = 1, \ldots, M \text{ and } k = 1, \ldots, K \tag{25}$$

$$0 \leq \epsilon_{ik} \leq \hat{w}_{ik} \quad \text{for } i = 1, \ldots, M \text{ and } k = 1, \ldots, K \tag{26}$$

$$q_{ik} \geq 0 \quad \text{for } i = 1, \ldots, M \text{ and } k = 1, \ldots, K \tag{27}$$

$$z_k \geq 0 \quad \text{for } k = 1, \ldots, K \tag{28}$$

$$x_i \in \{0, 1\} \quad \text{for } i = 1, \ldots, M, \tag{29}$$

where ϵ_{ik} is a new continuous variable that is introduced in order to revise/reduce the value of $\hat{w}_{ik}$ for $i = 1, \ldots, M$ and $k = 1, \ldots, K$. This can be observed from Constraints (25) and (26). In consequence, the new objective function, $\sum_{i=1}^{M} \sum_{k=1}^{K} \epsilon_{ik}$, simply measures the infeasibility of (R2) with respect to the value of $\hat{w}_{ik}$ for $i = 1, \ldots, M$ and $k = 1, \ldots, K$. To understand the formulation better, we now explore two extreme cases. In the first case we suppose that $\epsilon_{ik} = 0$ for $i = 1, \ldots, M$ and $k = 1, \ldots, K$. In such a scenario, (R3) is precisely equivalent to (R2). Now, in the second case, let us suppose that $\epsilon_{ik} = w_{ik}$ for $i = 1, \ldots, M$ and $k = 1, \ldots, K$. In this case, the optimal solution of (D2) is also optimal for (R3) because we now have the option to set $z_k = 0$ and $q_{ik} = 0$ for $i = 1, \ldots, M$ and $k = 1, \ldots, K$. So, this formulation captures the essence of both (D2) and (R2), and it is guaranteed to be feasible (since we assume that (D2) is feasible).

Note that solving this bi-objective optimization problem returns the trade-off between the total cost of conservation, i.e., the first objective function, and the total infeasibility, i.e., the second objective function. However, the proposed formulation is not linear. In order to linearize it, a new non-negative variable $\hat{\epsilon}_{ik}$ can be introduced to capture the value of the bilinear term $\epsilon_{ik} x_j$ for $i = 1, \ldots, M$ and $k = 1, \ldots, K$, and then Constraint (25) can be replaced by the following constraints:

$$z_k + q_{ik} \geq \hat{w}_{ik} x_i - \hat{\epsilon}_{ik} \qquad \text{for } i = 1, \ldots, M \text{ and } k = 1, \ldots, K \tag{30}$$

$$\hat{\epsilon}_{ik} \leq \epsilon_{ik} \qquad \text{for } i = 1, \ldots, M \text{ and } k = 1, \ldots, K \tag{31}$$

$$\hat{\epsilon}_{ik} \leq \hat{w}_{ik} x_i \qquad \text{for } i = 1, \ldots, M \text{ and } k = 1, \ldots, K \tag{32}$$

$$\hat{\epsilon}_{ik} \geq \epsilon_{ik} - \hat{w}_{ik} x_i - \hat{w}_{ik} \qquad \text{for } i = 1, \ldots, M \text{ and } k = 1, \ldots, K \tag{33}$$

$$\hat{\epsilon}_{ik} \geq 0 \qquad \text{for } i = 1, \ldots, M \text{ and } k = 1, \ldots, K. \tag{34}$$

This linearization is valid since if $x_i = 1$ then $\hat{\epsilon}_{ik} = \epsilon_{ik}$ and if $x_i = 0$ then $\hat{\epsilon}_{ik} = 0$ for $i = 1, \ldots, M$ and $k = 1, \ldots, K$.